

TECHNISCHE UNIVERSITÄT MÜNCHEN

Lehrstuhl für Entwicklungsgenetik

The MENX syndrome: an animal model
to study the role of p27 in tumor predisposition and the response of
neuroendocrine tumors to therapeutic agents

Mi Su Lee

Vollständiger Abdruck der von der Fakultät Wissenschaftszentrum Weihenstephan für
Ernährung, Landnutzung und Umwelt der Technischen Universität München zur Erlangung
des akademischen Grades eines

Doktors der Naturwissenschaften
genehmigten Dissertation.

Vorsitzender: Univ.-Prof. Dr. S. Scherer

Prüfer der Dissertation:

1. apl.Prof. Dr. J. Graw
2. Uni.-Prof. A. Schnieke, Ph.D
3. Priv.-Doz. Dr. N. S. Pellegata

Die Dissertation wurde am 28.02.2011 bei der Technischen Universität München eingereicht
und durch die Fakultät Wissenschaftszentrum Weihenstephan für Ernährung, Landnutzung und
Umwelt am 29.06.2011 angenommen.

Erklärung

Ich erkläre hiermit an Eides statt, dass ich die vorliegende Arbeit selbständig ohne unzulässige fremde Hilfe angefertigt habe.

Die verwendeten Literaturquellen sind im Literaturverzeuchnis vollständig zitiert.

München, den

Mi Su Lee

Acknowledgements

I would like to thank all of my colleagues in the Pathology department at the Helmholtz Zentrum Muenchen for their support. Special thanks go to Dr. Natalia. S. Pellegata and Prof. Dr. J. Graw for their support, advice and patience not just as my supervisors, but as mentors. I would also like to express my gratitude to my graduate committee: Prof. Dr. A. Schnieke and Prof. Dr. S. Scherer for their valuable criticism and suggestions during the course of my research. I thank all members of Dr. Pellegatas' lab for their help and advices. I would also like to thank E. Samson for helping me to take care of my rats.

Finally, I would like to dedicate this dissertation to my family, whose love and support made all these possible.

Table of contents

ABBREVIATIONS	1
SUMMARY	3
ZUSAMMENFASSUNG	5
1. INTRODUCTION	7
1.1. Multiple endocrine neoplasia (MEN).....	7
1.1.1. MEN syndrome	7
1.1.2. MEN1-like syndrome (MEN4)	8
1.1.3. MEN-like syndrome in the rat.....	11
1.2. Cyclin-dependent kinase inhibitor	12
1.3. Pituitary	15
1.3.1. Anatomy of the pituitary gland	15
1.3.2. Pituitary development	17
1.3.3. Pituitary adenoma.....	18
1.3.4. Current treatment of pituitary adenomas.....	19
1.3.5. PI3K/AKT/mTOR pathway as a therapeutic target	21
1.3.6. Animal models of pituitary adenoma	23
2. AIMS	25
3. MATERIALS	26
3.1. Equipments.....	26
3.2. Consumable materials	28
3.3. Chemicals and reagents	29
3.4. Buffers and solutions.....	31
3.5. Commercially available kits	33
3.6. Constructs	33
3.7. Software	33
4. METHODS	34
4.1. Mutagenesis.....	34
4.1.1. Primer design.....	34
4.1.2. PCR reaction	35
4.1.3. Digestion by <i>DpnI</i>	35
4.1.4. Transformation & DNA extraction	36
4.2. Dye-terminator sequencing	36
4.3. Animals	38
4.4. Histology	38
4.5. Cell culture	40
4.6. Cell viability	41
4.7. RNA interference	42
4.8. Transient transfection	42
4.9. Protein extraction and western blotting	43
4.10. RNA isolation.....	44
4.11. Reverse transcription.....	44

4.12. Quantitative (q) RT-PCR	45
4.13. Immunofluorescence	47
4.14. Glutathione-S-transferase (GST) pull down assay.....	47
4.15. Apoptosis assay	47
4.16. Clonogenic assay and growth curve.....	48
4.17. Statistical analysis	49
5. RESULTS.....	50
5.1. Germline <i>Cdkn1b</i> (p27^{Kip1}) mutation in the MENX rat syndrome.....	50
5.1.1. The MENX mutation in <i>Cdkn1b</i> affects p27 stability.....	50
5.1.2. Proteasome-mediated degradation of p27fs177 <i>in vitro</i>	53
5.1.3. Instability of p27fs177 in primary rat cells	58
5.2. Characterization of MENX-associated pituitary tumors	60
5.2.1. Macroscopic and histological analysis.....	60
5.2.2. Immunophenotype of the pituitary tumors.....	62
5.2.3. Proliferative index of rat pituitary tumors.....	64
5.3. MENX as a preclinical model to evaluate compounds with therapeutic activity against neuroendocrine tumors.....	65
5.3.1. Establishing a protocol to obtain single pituitary primary cells from MENX	65
5.3.2. Receptor profiling of pituitary primary cells from MENX	66
5.3.3. Effect of somatostatin-related drugs on the viability of rat primary pituitary cells	68
5.3.4. Correlation of response to SSA with somatostatin receptor expression	72
5.3.5. Overactivation of the PI3K/mTOR/AKT pathway in rat pituitary tumor cells.....	74
5.3.6. Effect of RAD001 and NVP-BEZ235 in rat pituitary tumor cells	76
5.3.7. p27 expression sensitizes to NVP-BEZ235 treatment	80
5.3.8. The proteasome inhibitor improves the response to NVP-BEZ235.....	83
5.4. Germline <i>CDKN1B</i> mutations in human neuroendocrine tumor patients	88
5.4.1. Germline genetic changes and clinical presentation	88
5.4.2. Functional characterization of the p27 variants	89
5.4.3. Stability and protein binding ability of p27P69L and p27W76X	91
5.4.4. p27W76X fails to inhibit cell growth.....	93
5.4.5. Stability of p27K96Q and p27I119T and their ability to inhibit cell growth.....	94
5.4.6. p27K96Q has reduced Grb2 binding ability	96
5.4.7. The size-shift of p27I119T does not depend on abnormal phosphorylation.....	96
6. DISCUSSION	99
7. REFERENCES	107
LEBENSLAUF	120

ABBREVIATIONS

αSU	Glycoprotein hormone alpha-subunit
ACTH	Adrenocorticotropic hormone
AP	Anterior pituitary
ATP	Adenosine triphosphate
CDK	Cyclin-dependent kinase
cDNA	Complementary deoxyribonucleic acid
CHX	Cycloheximide
DA	Dopamine agonist
DR	Dopamine receptor
DRD2	Dopamine receptor type 2
DMSO	Dimethyl sulfoxide
ERK	Extracellular-signal-regulated kinases
<i>E. coli</i>	<i>Escherichia coli</i>
ELISA	Enzyme-linked immunosorbent assay
FSHβ	Follicle-stimulating hormone β-subunit
GFP	Green fluorescent protein
GH	Growth hormone
GPCR	G-protein coupled receptors
H&E	Hematoxylin and eosin
IHC	Immunohistochemistry
IL	Intermediate lobe
IP	Immunoprecipitation
KPC	Kip1 ubiquitylation-promoting complex
LB	Lysogeny broth (Luria-Bertani medium)
LHβ	Luteinising hormone β-subunit
MEN	Multiple endocrine neoplasia
MENX	Multiple endocrine neoplasia-like syndrome
mTOR	Mammalian target of rapamycin
MAPK	Mitogen-activated protein kinases
NFA	Nonfunctioning pituitary adenoma
PDK1	Phosphatidylinositol-dependent kinase 1
PIP3	Phosphatidylinositol 3,4,5-trisphosphate
PRL	Prolactin

Rb	Retinoblastoma protein
RT-PCR	Reverse transcription polymerase chain reaction
SDS-PAGE	Sodium dodecyl sulfate poly-acrylamide gel electrophoresis
SF1	Steroidogenic factor 1
siRNA	Small interfering ribonucleic acid
SKP2	S-phase kinase-associated protein 2
SSA	Somatostatin analogue
SSTR	Somatostatin receptor
SRIF	Somatostatin
TRH	Thyrotropin-releasing hormone
TSH	Thyroid-stimulating hormone
YFP	Yellow fluorescent protein

SUMMARY

p27^{Kip1} (p27) is an important negative regulator of the cell cycle and a putative tumor suppressor. A spontaneous germline frameshift mutation in *Cdkn1b* (encoding p27fs177) causes the MENX multiple endocrine neoplasia syndrome in the rat. Germline mutations in p27 were later found to be responsible for a novel MEN syndrome in human patients. To better understand the role of p27 in tumor predisposition we decided to characterize these new germline p27 mutations found in human patients. We first studied the molecular properties of the rat mutant p27 protein, p27fs177. At the molecular level, p27fs177 retains some properties of the wild-type p27 (p27wt) protein: it localizes to the nucleus; it interacts with cyclin-dependent kinases and, to a lower extent, with cyclins. In contrast to p27wt, p27fs177 is highly unstable and rapidly degraded in every phase of the cell-cycle, including quiescence. It is in part degraded by S-phase kinase-associated protein 2 (Skp2)-dependent proteasomal proteolysis, similarly to p27wt.

We also performed the functional *in vitro* analysis of novel human *CDKN1B* mutations found in patients with multiple endocrine tumors (p27P69L, p27W76X, p27K96Q and p27I119T) in order to identify the critical functions of p27 which are associated to tumor predisposition. We show that p27P69L is expressed at reduced level similar to the p27fs177 and is impaired in both binding to Cdk2 and inhibiting cell growth. p27W76X, which is mislocalized to the cytoplasm, can no longer efficiently bind Cyclins-Cdks, nor inhibit cell growth or induce apoptosis. p27K96Q seems to have a reduced affinity for Grb2 binding. In contrast to the other mutations, p27I119T has no molecular phenotype we could identify except slower migration in SDS-PAGE. Based on *in vitro* analysis and comparison of *Cdkn1b/CDKN1B* mutations, we show that most likely reduced p27 levels, not newly acquired properties, trigger tumor formation in rats and also in several human patients.

Besides the opportunity to expand the current knowledge about p27 functions, MENX rats might be used as a model system to study the response of neuroendocrine tumor cells to novel therapeutic approaches. Due to the scarcity of animal models of neuroendocrine tumors, so far preclinical therapy-response studies have been difficult to carry out. Although MENX rats develop a variety of neuroendocrine tumors (bilateral pheochromocytoma, anterior pituitary adenoma, multifocal thyroid C-cell hyperplasia, and parathyroid hyperplasia), here we focus on only the pituitary tumors they develop because of the lack of a reliable animal model of this tumor type for preclinical drug testing.

A prerequisite for *in vivo* drug screening is the characterization of the rat tumors. Through careful evaluation of histo-morphology, hormone immunophenotype and proliferation rate we have shown that the MENX-associated pituitary tumors resemble atypical gonadotroph tumors, which are part of the group of non-functioning pituitary adenoma (NFA), meaning tumors that do not produce hormones. To determine whether the pituitary tumors in MENX rats are a good model of human NFA, we treated dispersed rat primary NFA cells grown *in vitro* with different antitumor compounds. Then we compared the data with existing literature on the treatment of human pituitary tumor cells. Cell survival was the treatment readout. Being somatostatin analogs (SSA) and dopamine agonists (DA) the main-stay therapy of human pituitary adenomas, we treated rat NFA cells with octreotide, SOM230 or BIM-23A760, a chimeric SSA/DA. We also evaluated the effects of RAD001 (mTOR inhibitor) and NVP-BEZ235 (dual PI3K/mTOR inhibitor) on rat tumor cells. We observed that rat NFA cells partially responded to SSA and RAD001, like human primary NFA cells. In contrast, NVP-BEZ235 inhibited the survival of all rat primary cultures. At the molecular level, NVP-BEZ235 treatment was associated with PI3K pathway blockade and induction of apoptosis. NVP-BEZ235 was shown to require high p27 levels for best antiproliferative activity. In conclusion, MENX rats seem to be a faithful model of NFA and can be used in preclinical therapy-response studies.

ZUSAMMENFASSUNG

p27^{Kip1} (p27) ist ein wichtiger negativer Regulator des Zellzyklus und ein putativer Tumorsuppressor. Eine spontane Keimbahnmutation in *Cdkn1b* (kodiert für p27fs177) führt zu einer Verschiebung des Leserasters und löst in der Ratte das multiple endokrine Syndrom MENX aus. Später wurde in Patienten festgestellt, dass Keimbahnmutationen in p27 für ein neuartiges MEN-Syndrom verantwortlich sind. Um die Rolle von p27 in der Tumorprädisposition besser verstehen zu können, beschlossen wir diese neu entdeckten p27 Keimbahnmutationen näher zu charakterisieren.

Zunächst untersuchten wir die molekularen Eigenschaften des mutierten p27 Proteins (p27fs177) in der Ratte. Auf molekularer Ebene behält p27fs177 einige Eigenschaften des p27 Wildtyp-Proteins (p27wt) bei: Es ist nuklear lokalisiert; es interagiert mit Cyclin-abhängigen Kinasen und, in geringerem Maße, mit Cyclinen. Im Gegensatz zu p27wt, ist p27fs177 in hohem Maße instabil und wird in jeder Phase des Zellzyklus, auch im Ruhezustand (Quieszenz), rasch degradiert. Ähnlich wie p27wt wird es teilweise durch Skp2-abhängige proteasomale Proteolyse degradiert. Außerdem führten wir funktionelle *in vitro* Analysen für neuartige *CDKN1B* Mutationen durch, die in Patienten mit multiplen endokrinen Tumoren gefunden wurden (p27P69L, p27W76X, p27K96Q und p27I119T). Dies diente dazu individuelle mit Tumorprädisposition assoziierte Funktionen von p27 genauer zu verstehen. Wir konnten zeigen, dass p27P69L, ähnlich wie p27fs177, in reduziertem Maße exprimiert wird und hinsichtlich der Bindung an Cdk2 und der Zellzyklusinhibition beeinträchtigt ist. p27W76X, das falsch lokalisiert im Zytoplasma vorliegt, kann weder Cyclin-Cdks effizient binden, noch das Zellwachstum inhibieren oder Apoptose induzieren. p27K96Q scheint eine reduzierte Bindungsaffinität für Grb2-Bindung zu besitzen. Im Gegensatz zu den anderen Mutationen konnten wir, abgesehen von einem verlangsamtem Migrationsverhalten in der SDS-PAGE, keinen molekularen Phänotyp für p27I119T identifizieren.

Basierend auf *in vitro* Analysen und Vergleich von *Cdkn1b/CDKN1B* Mutationen, konnten wir zeigen, dass höchstwahrscheinlich reduzierte p27-Mengen und nicht neu erworbene Eigenschaften des Proteins die Bildung von Tumoren in der Ratte sowie in etlichen Patienten auslösen.

Neben der Möglichkeit den derzeitigen Wissensstand über Funktionen von p27 zu erweitern, könnten MENX-Ratten ein nützliches Modellsystem zur Untersuchung des Ansprechens neuroendokriner Tumorzellen auf neuartige therapeutische Ansätze darstellen. Aufgrund des Mangels an Tiermodellen für neuroendokrine Tumoren war es bislang schwierig, solche

präklinischen Untersuchungen durchzuführen. Obwohl MENX-Ratten eine Vielfalt neuroendokriner Tumoren entwickeln (bilaterale Phäochromozytome, Adenome des Hypophysenvorderlappens, multifokale C-Zell-Hyperplasie der Schilddrüse und Hyperplasie der Nebenschilddrüse), konzentrieren wir uns hier nur auf die auftretenden Hypophysentumoren, da für diese Tumorart verlässliche Tiermodelle für präklinische Arzneimitteltests fehlen.

Eine Grundvoraussetzung für *in vivo* „Arzneimittel-Screenings“ ist die genaue Charakterisierung der Rattentumoren. Durch sorgfältige Evaluierung der Histologie, des Immunphänotyps bezüglich Hormonproduktion und der Proliferationsrate zeigen wir, dass MENX-assoziierte Hypophysentumoren atypischen gonadotrophen Tumoren gleichen, welche zu den nicht-funktionellen Hypophysenadenomen (NFPA: *non-functioning pituitary adenoma*) zählen. Diese Tumoren produzieren keine Hormone. Um zu untersuchen, ob Hypophysentumoren in MENX-Ratten ein gutes Modell für humane NFPA sind, behandelten wir *in vitro* NFPA-Primärzellen aus Ratten mit verschiedenen Anti-Tumor-Wirkstoffen. Die daraus gewonnenen Daten verglichen wir mit existierender Literatur zur Behandlung menschlicher Hypophysentumorzellen. Da zur Therapie humaner Hypophysentumoren hauptsächlich Somatostatin-Analoga (SSA) und Dopaminrezeptor-Agonisten (DA) verwendet werden, behandelten wir Ratten NFPA-Zellen mit Octreotid, SOM320 oder BIM-23A760 (=chimerer SSA/DA). Zudem testeten wir RAD001 (mTOR Inhibitor) und NVP-BEZ235 (dualer PI3K/mTOR Inhibitor) in Ratten Tumorzellen. Wir beobachteten, dass Ratten NFPA-Zellen, vergleichbar mit primären humanen NFPA-Zellen, teilweise auf SSA und RAD001 ansprachen. Im Gegensatz dazu reduzierte NVP-BEZ235 das Überleben aller primären Rattenzellkulturen. Auf molekularer Ebene blockierte die Behandlung mit NVP-BEZ235 den PI3K-Signalweg und induzierte Apoptose. Wir konnten zeigen, dass NVP-BEZ235 für die höchstmögliche antiproliferative Aktivität große Mengen an p27 benötigt. Zusammenfassend lässt sich sagen, dass MENX-Ratten ein zuverlässiges NFPA-Modell darstellen und in präklinischen Untersuchungen zum Therapieansprechen eingesetzt werden können.

1. INTRODUCTION

1.1. Multiple endocrine neoplasia (MEN)

1.1.1. MEN syndrome

Multiple Endocrine Neoplasias (MEN) are autosomal dominant disorders characterized by tumor involving two or more endocrine glands, although tumors can also develop in non-endocrine organs other than these glands. Two main MEN syndrome have been known since long: MEN type 1 (MEN1) and type 2 (MEN2). The MEN1 syndrome affects approximately 1 in 30,000 people with an equal sex distribution, and no racial predilection (Lairmore et al., 2004). This syndrome is caused by loss-of-function mutations of the *MEN1* gene, which is considered a tumor suppressor gene, meaning that it functions as a negative regulator of cell proliferation (Chandrasekharappa et al., 1997). *MEN1* is mutated in the germline of MEN1 patients, but it is also often found somatically mutated in sporadic MEN1-associated tumors. More than 500 different germline and somatic mutations have been identified: they occur mostly in coding exons, but also in intronic sequences and are composed of all types of changes, with a relatively high incidence of frameshift mutations (Lemos and Thakker, 2008). The protein encoded by *MEN1* is called Menin. The physiological functions of Menin and its role in tumorigenesis are actively investigated. Menin has many interacting partners, which include transcription factors member of the AP-1 family, such as c-Jun and JunD, the nuclear factor (NF)- κ B, the Smad family of transcription factors, cell cycle regulators and a variety of other transcription factors and cell structural elements (Agarwal et al., 1999; Agarwal et al., 2005). Menin also interacts with proteins involved in DNA damage-dependent cell cycle arrest or in DNA repair after damage (Yang and Hua, 2007). Through these interactions Menin plays a role in transcriptional regulation, cell proliferation and DNA repair. The earliest and most common phenotypic feature of MEN1 syndrome is hyperparathyroidism. Primary hyperparathyroidism causes excessive release of parathyroid hormone (PTH) and alters the normal balance of calcium concentration in the blood, leading to kidney stones or kidney damage, bone thinning, high blood pressure (hypertension), weakness and fatigue. In contrast to the sporadic cases of primary hyperparathyroidism present as single-gland adenomas, MEN1-associated cases often present as diffuse hyperplasia or multiple adenomas. Pancreatic islet cell tumors occur in 60-70% of MEN1 patients and are mostly multi-centric. Anterior pituitary tumors occur in 15-42% of MEN1 patients and are in general larger, are

often multi-focal and behave more aggressively than their sporadic counterpart. The most common type of pituitary adenoma occurring in MEN1 patients is prolactinoma, which overproduce the hormone prolactin, followed by tumors secreting growth hormone (GH) or GH together with prolactin, thereby causing acromegaly (Brandi et al., 2001). A small percentage of pituitary tumors secrete the adrenocorticotropic hormone (ACTH), causing Cushing's disease (Verges et al., 2002).

MEN2 is a rare familial cancer syndrome, frequency is 1 case per 30,000-50,000 persons. This syndrome has several variants depending on the clinical presentation of the patients, specially MEN2 type A (MEN2A), MEN2 type B (MEN2B) and familial medullary thyroid carcinoma (FMTC). MEN2A is the most common variant, presenting with medullary thyroid carcinoma (MTC) and pheochromocytoma in about 20-50% of cases, and with MTC and primary hyperparathyroidism (parathyroid adenoma) in 5-20% of cases (Brandi et al., 2001). MEN2B develops MTC, pheochromocytoma (in 50% of cases), marfanoid habitus and mucosal and digestive ganglioneuromatosis (Koch, 2005). MEN2B is the most aggressive variant, but occurs in only 5% of all MEN2 cases. Other rare variants of MEN2 include familial medullary thyroid cancer (FMTC) without other associated endocrinopathies and FMTC with Hirschsprung's disease (Marini et al., 2006). MEN2 is caused by mutations of the *RET* proto-oncogene (Mulligan et al., 1993). The *RET* proto-oncogene encodes a putative tyrosine kinase receptor. Its endogenous ligand is the glial cell line-derived neurotrophic factor (GDNF). GDNF plays a crucial role in the development, function and maintenance of the nervous system, by regulating cell proliferation and survival, migration and axon growth. Ligand-induced activation of *RET* proto-oncogene results in transduction of multiple signals that induce cell growth, cell motility, survival and differentiation through different downstream pathways, including the mitogen-activated protein (MAP) kinases, extracellular-signal-regulated (ERK) kinases and phosphatidylinositol 3 kinases (PI3K)/Akt pathways (Arighi et al., 2005; de Groot et al., 2006). The MEN2-associated mutation in *RET* proto-oncogene are gain-of-function mutations and trigger the activation of the tyrosine kinase activity, without the presence of the physiological ligands. This condition results in the constitutive activation of the downstream signal transduction pathways.

1.1.2. MEN1-like syndrome (MEN4)

Approximately 30% of the clinically suspected MEN1 patients do not exhibit *MEN1* mutations, suggesting that other predisposing genes may play a role in this phenotype. In the

last few years, germline mutations in the human *CDKN1B* gene, encoding p27^{kip1} (p27) were identified in few patients with multiple endocrine tumors, but without germline mutations in *MEN1* or *RET* (Table.1). These findings lead to the identification of a novel MEN syndrome named MEN4 (OMIM No.610755).

The first *CDKN1B* mutation was identified in a 48-year-old Caucasian female affected by a GH-secreting pituitary tumor (acromegaly) and primary hyperparathyroidism. The mutation is a germline heterozygous TGG-TAG nonsense mutation at codon 76 which determines the premature truncation of the protein at this residue (W76X). A sister of the mutation-positive proband carries the same mutation and has been diagnosed with renal angiomyolipoma (a MEN1-associated tumor) indicating that this change is inherited together with tumor predisposition (Pellegata et al., 2006). A second germline *CDKN1B* mutation was later identified in a Dutch patient diagnosed with three lesions compatible with MEN1: small-cell neuroendocrine cervical carcinoma, ACTH-secreting pituitary adenoma (Cushing's disease) and hyperparathyroidism. This mutation is a 19-bp duplication which results in a truncated p27 protein due to a premature stop at codon 69. The cervical carcinoma of the patient showed loss of the wild-type allele of *CDKN1B* and very little p27 protein expression (Georgitsi et al., 2007).

In a study of American patients showing a MEN1-like phenotype or familial primary hyperparathyroidism (1°HPT) but no *MEN1* and *RET* mutations, three new potentially pathogenic *CDKN1B* mutations were discovered. A mutation at the -7 position in the Kozak sequence (ATG-7G>C) was found in a patient with a parathyroid tumor, bilateral adrenal masses and uterine fibroids. No loss of heterozygosity was found in the tumor but protein expression could not be assessed. A second individual affected by primary hyperparathyroidism (1°HPT) and displaying masses in both duodenum and pancreas was found to carry a CCC>TCC missense mutation at codon 95, leading to an amino acid change from Pro to Ser (P95S). The third variant changes the stop codon to glutamine (TAA>CAA; stop>Q), and leads to a protein predicted to be 60 amino acids longer than the wild-type one. This mutation was found in a patient with a family history of 1°HPT. The stop>Q variant *in vitro* associates with a reduction of the encoded p27 protein amount (Agarwal et al., 2009).

Recently, we have identified a CCC>CTC mutation at position 678 leading to an exchange of Pro by Leu (P69L) in a patient. This patient presents multiple typical bronchial carcinoids, 1°HPT, papillary thyroid carcinoma with neck lymph node metastasis, microadenoma in the pituitary gland and bilateral multiple lung metastasis (Molatore et al., 2010a).

Table 1 Clinical and molecular characteristics of the identified *CDKN1B/p27* variants

Data source: (Molatore and Pellegata, 2010b).

<i>CDKN1B</i> mutation	Clinical phenotype of proband	Relatives affected	Mutation description	<i>CDKN1B</i> status in the tumor	Reference
W76X	1° HPT, GH-pituitary tumor	2	Truncated protein.	No LOH	Pellegata et al, 2006
K25fs	1° HPT, ACTH-pituitary tumor, carcinoid tumor of uterine cervix	0	Frameshift longer protein	LOH	Georgitsi et al, 2007
	1° HPT (1 parathyroid tumor), bilateral adrenal mass nonfunctioning	0	Reduction in protein expression <i>in vitro</i>	No LOH	
ATG-7G>C					Agarwal et al, 2009
P95S	1° HPT (2 parathyroid tumors), ZES	0	Reduced binding of the mutant protein with Grb2	Nd	Agarwal et al, 2009
Stop>Q	1° HPT (3 parathyroid tumors)	3	Longer protein, very unstable.	Nd	Agarwal et al, 2009
P69L	1° HPT, bronchial carcinoids, papillary thyroid carcinoma with neck lymphnode metastasis, microadenoma in the pituitary gland and bilateral multiple lung metastasis		Unstable protein, impaired CDK2 binding.	Nd	Molatore et al, 2010
		nd			

1 °HPT = Primary hyperparathyroidism; ZES = Zollinger-Ellison syndrome; LOH = loss of heterozygosity; ND = not determined.

1.1.3. MEN-like syndrome in the rat

We recently discovered a variant of the MEN syndromes that spontaneously developed in a Sprague-Dawley rat colony. Affected animals develop multiple neuroendocrine tumors, showing phenotypic compatible with both the MEN1 and MEN2 syndromes; bilateral pheochromocytoma (incidence: 100%), anterior pituitary adenoma (100%), multifocal thyroid C-cell hyperplasia (78%), parathyroid hyperplasia (65%) as well as extra-adrenal pheochromocytoma (paragangliomas, incidence: 10%) (Fritz et al., 2002). Due to the unique combination of affected organs of this multi-tumor syndrome, we named it MENX. The average life span of MENX is 10±2 months which is significantly shorter than 24-30 months of wild type littermates' life. Adrenal medullary hyperplasia in MENX presents at 3-4 months and progress to tumor pheochromocytoma at 6-8 months. Similarly, anterior pituitary hyperplasia are developed around at 4 months and become adenoma by 8-12 months. Therefore, these malignancies show a clear progression from hyperplasia to tumor with time. Specially, affected animals develop macroscopically visible bilateral cataracts in the first few weeks of life (Pellegata et al., 2006).

Among several candidates' genes, *Cdkn1b*, encoding the cyclin-dependent kinase-inhibitor p27^{Kip1} (p27) was indentified as the gene responsible for this disease in MENX by classical linkage studies. Upon sequencing of the *Cdkn1b* gene a tandem duplication of 8 nucleotides in exon 2 of *Cdkn1b* was identified only in affected rats, but not in unaffected littermates. This mutation results in a frameshift after codon 176, predicting a novel C-terminal domain containing forty-two p27-unrelated amino-acid residues. As a consequence of this mutation, the encoded mutant p27 protein is not expressed in adrenals, pituitary, lung, kidney, liver, and testis of affected rats. In thyroid, thymus, parathyroid, and brain have normal expression level of p27 compare to wild-type rats. The amount of *Cdkn1b* mRNA shows no significant difference between affected and unaffected rats (Pellegata et al., 2006).

1.2. Cyclin-dependent kinase inhibitor

The cell cycle is the process by which cells divide into daughter cells. The basic regulation of the cell cycle has been studied in yeasts; *Schizosaccharomyces pombe* and *Saccharomyces cerevisiae*. In these organisms, cell cycle is controlled by a single cyclin-dependent kinase (CDK) (Morgan, 1997). However, in mammalian cells this process is regulated by many different CDKs (Fig.1). These kinases are activated by binding to regulatory cyclin protein. For instance, during G1 phase CDK4/CDK6 become complex with D-type cyclins (cyclin D1, D2 and D3) to prepare to initiate DNA synthesis (Sherr, 1994). CDKs also negatively regulated by CDK inhibitors (CKIs). There are two families of CKIs, the INK4 family and the CIP/KIP family. The INK4 family ($p16^{INK4a}$, $p15^{INK4b}$, $p18^{INK4c}$ and $p19^{INK4d}$) inhibits cell cycle progression at G1 to S phase by binding CDK4 and CDK6. In contrast, members of the Cip/Kip family ($p21^{Cip1}$, $p27^{Kip1}$, and $p57^{Kip2}$) have different roles depending on the binding to various CDK/Cyclin complexes (Sherr and Roberts, 1995).

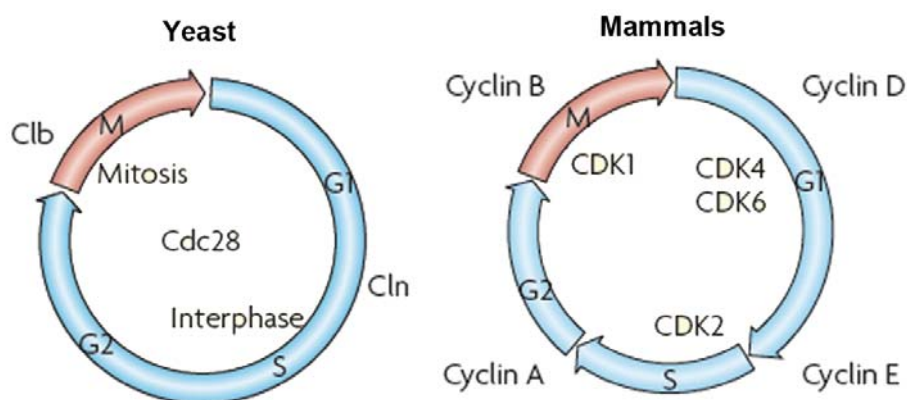


Fig.1 Cell cycle of yeast (*Saccharomyces cerevisiae*) and mammals. The cell cycle is controlled by Cdc28 in *S.cerevisiae*. In contrast, the eukaryotic cell cycle is driven by unique cyclin-dependent kinases (CDKs) binding with specific cyclins. The entry into the G1 phase is determined by assembly and activation of cyclinD/CDK4 or cyclinD/CDK6 complexes. The subsequent progression through G1/S transition and S phase is dependent on cyclinD/CDK2 and cyclinA/CDK2 complexes. Data source: (Malumbres and Barbacid, 2009).

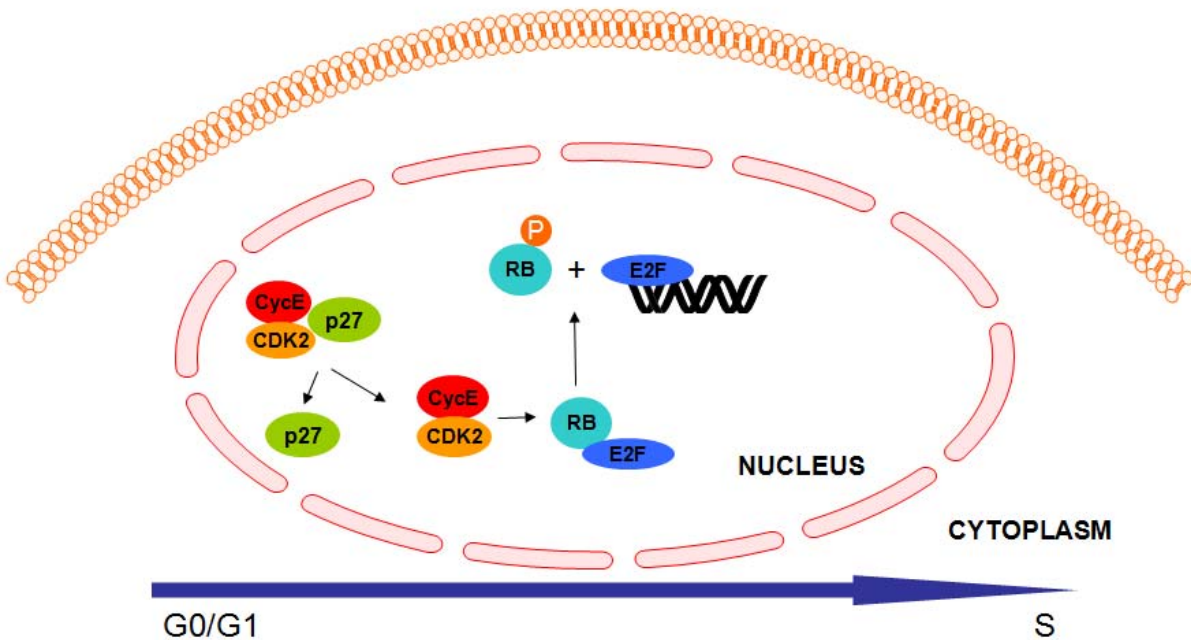


Fig.2 Graphic representation of the pathways involved in p27. Upon mitogenic stimulation, p27 is released from the cyclin E/Cdk2 complex and the dissociation from p27 activates Cdk2, which in turn phosphorylates the Rb protein. Phosphorylated Rb releases the transcription factor E2F which induces the expression of genes required for the G1 to S phase progression. Data source: (Marinoni and Pellegata, 2010).

p27^{Kip1} (p27), a member of CKI is a nuclear protein that regulates cell cycle progression G1/S by inactivating cyclin E/CDK2 complexes (Sheaff et al., 1997). The substrate of CDK2 is the retinoblastoma protein (pRb). Upon phosphorylation by CDK2, pRb release members of the E2F family of transcription factors which in turn activate the transcription of genes required for the G1 to S progression (Fig.2). The intracellular level of p27 is tightly regulated at different levels: transcriptional, mRNA translational (Dijkers et al., 2000; Millard et al., 1997; Servant et al., 2000), but the best known mechanism is post-translational and regulates its abundance: proteolysis via ubiquitin-mediated proteasome pathway (Pagano et al., 1995).

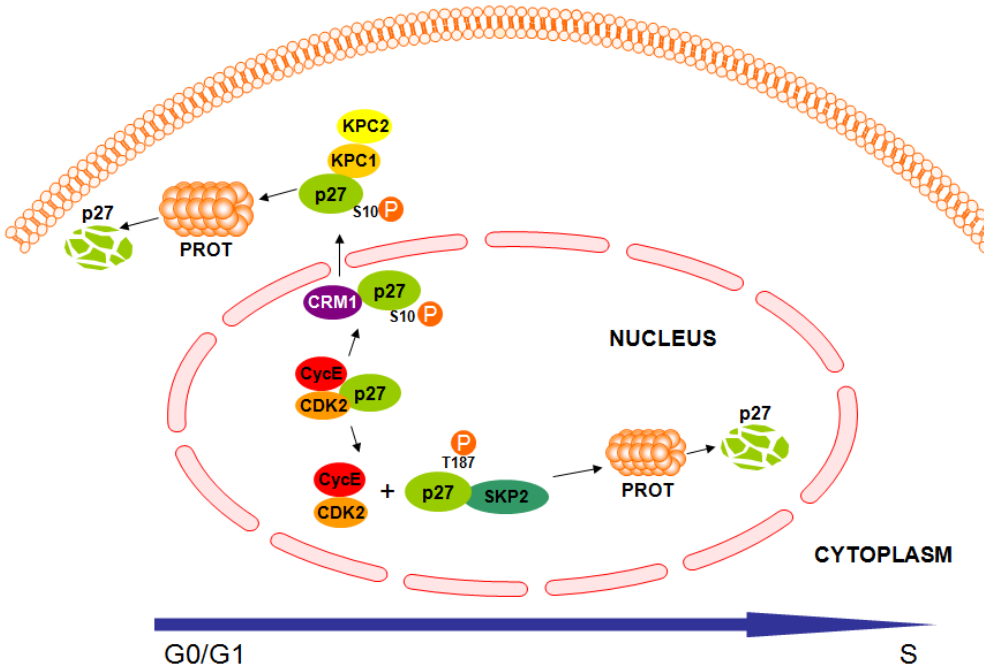


Fig.3 Diagram of p27 degradation pathway. After the dissociation of p27 from the cyclin E/Cdk2 complex in early G1, a portion of p27 is phosphorylated on Ser10 and interacts with CRM1 (exportin) which exports p27 into the cytoplasm. Once in the cytoplasm, p27 interacts with the KPC1/KPC2 complex that promotes p27 ubiquitylation and degradation by the proteasome (PROT). Upon mitogenic stimulation, p27 becomes a substrate of the cyclin E/Cdk2 complex which phosphorylates the protein at the Thr187 residue. Phosphorylation on T187 allows the interaction with Skp2 and the subsequent ubiquitylation-mediated degradation by the proteasome (PROT) in the S phase. Data source: (Marinoni and Pellegata, 2010).

Two main pathways involved in p27 degradation have been identified (Fig.3). The first pathway is mediated by the Skp2-dependent SCF (Skp1-cullin-f-box protein) E3 ligase: phosphorylation of p27 by cyclinE/Cdk2 at conserved threonine (Thr187). The phosphorylation at Thr187 creates a recognition site for the Skp2 ubiquitin ligase, which allows polyubiquitylation and subsequent proteasomal degradation of p27. This degradation pathway is active in the nucleus of G1-S and G2 phase cells (Carrano et al., 1999).

The second degradation pathway involves the ubiquitylation-promoting complex KPC1 (Kip1 ubiquitylation-promoting complex 1) and is responsible for the degradation of p27 in the cytoplasm. At the G0-G1 transition, after dissociation from the cyclin E/Cdk2 complex, p27 is phosphorylated at Serin 10 (Ser10), which results in an increased binding affinity of p27 for CRM1 (exportin 1) (Ishida et al., 2002). This triggers the export of p27 from the cell nucleus to the cytoplasm upon mitogenic stimuli, thereby allowing the protein's degradation by the KPC ubiquitin ligase (Kamura et al., 2004).

1.3. Pituitary

The second part of this thesis work deals with the characterization of the pituitary tumors that develop in MENX-affected rats. Therefore, this part gives an introduction about the pituitary gland and its pathophysiology.

1.3.1. Anatomy of the pituitary gland

The pituitary gland, or hypophysis, is considered to be the ‘master gland’ which regulates physiological functions such as growth, reproduction and metabolic homeostasis. It is a bean-shaped gland located in the sella turcica (Turkish saddle) of the sphenoid bone at the base of the brain, and is connected with the hypothalamus by the infundibulum, a stalk containing nerve fibers and small blood vessels. The pituitary gland is composed of three anatomically and functionally distinct lobes: the posterior pituitary (neurohypophysis), the anterior pituitary (adenohypophysis) and the intermediate lobe (Fig.4). The intermediate lobe is found between the anterior and posterior lobe, but is normally very small or absent in the adulthood. The posterior pituitary is derived from the infundibulum and is neural tissue extending from hypothalamus, whereas the anterior and intermediate lobes originated from the oral ectoderm (Kouki et al., 2001; Osumi-Yamashita et al., 1994). The posterior pituitary releases two hormones, oxytocin and vasopressin (antidiuretic hormone), which are synthesized in the hypothalamus, specifically in the cell bodies of the hypothalamic neurons whose axons pass down the infundibulum and end in the posterior pituitary.

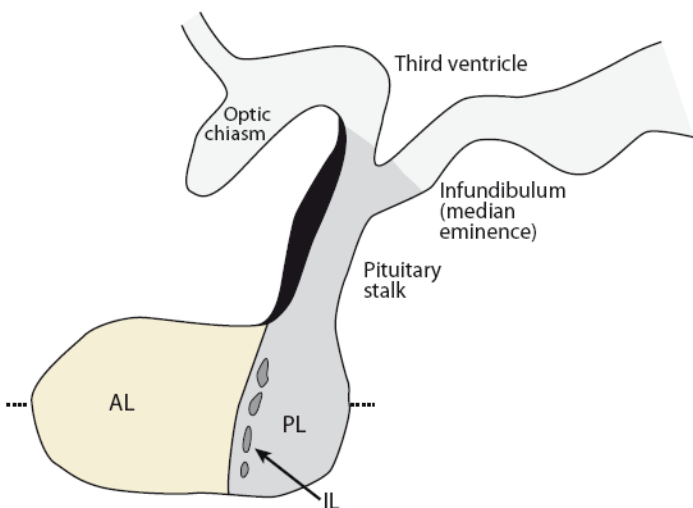


Fig.4 Pituitary anatomy.

The pituitary is composed of anterior lobe (adenohypophysis; AL), posterior (neurohypophysis; PL) and intermediate lobe. Neural tissue that derives from the hypothalamus and descends from the median eminence makes up the pituitary stalk and posterior lobe. Data source: (Asa and Ezzat, 2009).

The anterior pituitary is composed of six hormone-secreting cell types, including corticotrophs, somatotrophs, gonadotrophs, mammo-somatotrophs, thyrotrophs and lactotrophs (Table.2). These cells are supported in there acinar structure by folliculostellate cells expressing the glial markers S100 and glial fibrillary acidic protein (Hofler et al., 1984). Corticotroph cells in mainly the median wedge make the adrenocorticotrophic hormone (ACTH) which is derived from proopiomelanocortin (POMC), regulating the glucocorticoid synthesis and secretin in adrenal cortex. Somatotroph cells occupy the lateral wings, except a narrow posterolateral area and synthesize the growth hormone (GH) targeting the liver and adipose cells. The lactotroph cells synthesize prolactin and stimulate the milk production. The gonadotroph cells are scattered evenly throughout the intermediate lobes and produce follicle stimulating hormone (FSH) and leuteinzing hormone (LH), which regulate the germ cell development and sex steroid hormones. The following table summarizes the major hormones synthesized and secreted by the anterior pituitary lobe (Asa and Ezzat, 2002).

Table.2 Pituitary cells, hormones and target organs. Data source: (Asa and Ezzat, 2002).

Cell type	Hormone	Target organs	Major functions	Incidence
Somatotroph	GH	Liver and adipose tissue	Secretes IGF-I, protein synthesis, carbohydrate and lipid metabolism	10-15%
Lactotroph	Prolactin	Breast	Breast development and milk production (in male may facilitate reproductive function)	35%
Mammo-somatotroph	GH,Prolactin	As above	As above	5%
Thyrotroph	TSH	Thyroid	Secretes thyroxine, triiodothyronine	2%
Corticotroph	ACTH and other POMC derived peptide	Adrenal cortex	Secretes cortisol	10-15%
Gonadotroph	FSH,LH	Gonads	Germ cell development Secretes hormones (Female: Estrogen, progesteron, Male: Testosterone)	35%

1.3.2. Pituitary development

The pathway of pituitary development and cytodifferentiation are controlled by specific transcription factors that lead from a common pluripotent cell to differentiated cells of the different cell lineages (Asa and Ezzat, 2009; Scully and Rosenfeld, 2002) (Fig.5). In the early stages of pituitary organogenesis, *Rpx/HesX1*, a homeobox gene, regulates the formation of Rathke's pouch from the oral ectoderm (Hermesz et al., 1996; Sornson et al., 1996). Indeed *HesX1* null embryos display a severe reduction of forebrain structures (Dattani et al., 1998). The LIM homeobox genes (*Lhx3/4*) also implicate the formation of the pouch and the basic cellular structure of pituitary gland (Sheng et al., 1996). Pax6 (Paired box 6), Ptx1(Bicoid-related pituitary homeobox factor) and 2 (Structurally related pituitary homeobox factor2) are expressed throughout the oral ectoderm and in Rathke's pouch. Ptx1/2 are expressed in the adult pituitary, highly in the glycoprotein hormone alpha-subunit (α SU)-expressing thyrotropes, gonadotrophs and some POMC-producing cells (Crawford et al., 1997; Gage and Camper, 1997). Pit1 is a key protein required for the expression of the growth hormone gene allowing somatotroph differentiation. Together with Pit1, the estrogen receptor (ER) α induces the differentiation along the mammosomatotroph cell lineage (Day et al., 1990). SF1 (Steroidogenic factor 1) is the differentiation to the gonadotroph lineage (Asa et al., 1996). Thyrotroph differentiation requires the expression of TEF (Drolet et al., 1991), GATA2, GH repressor and Pit1 β (Dasen et al., 1999).

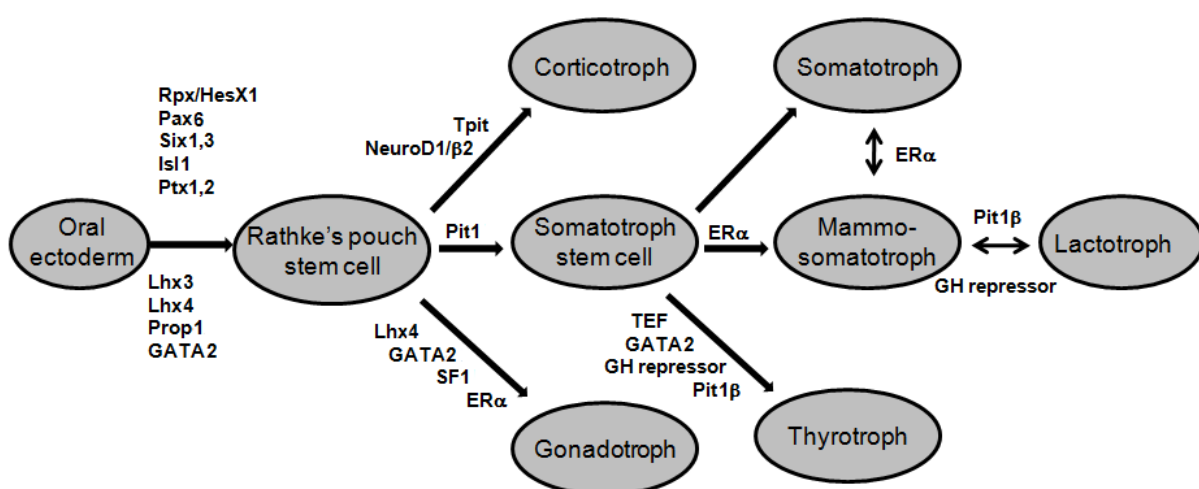


Fig.5 Adenohypophyseal cytogenesis. The adenohypophysis forms from the oral ectoderm through the activation of a series of transcription factors. Data source: (Asa and Ezzat, 2009).

1.3.3. Pituitary adenoma

Pituitary adenomas are common tumors of the anterior lobe of the pituitary gland and account for about 15% of intracranial neoplasm. They are typically benign and slow-growing neoplasms, although some pituitary adenomas often associated with significant morbidity, such as headache, local compressive effects to the normal parts to other parts of the body or invade the brain structure via the cerebrospinal fluid pathway or the extracranial tissues.

The several classifications of pituitary adenomas is based on several parameters, such as histological, immunocytochemical, and electron microscopic studies of the tumor cells, and keeps into account the hormone production of the tumor cells (Kovacs et al., 2001; Osamura et al., 2008).

Lactotroph adenomas secrete prolactin (PRL) and represent the most common hormone-producing pituitary tumors in humans, accounting for 25% to 41% of pituitary adenoma. Somatotroph adenomas produce growth hormone (GH), resulting in gigantism in younger patients and acromegaly in others (frequency ~ 13%). Corticotroph adenoma's main clinical manifestation is the secretion of the adrenocorticotrophic hormone (ACTH), which results in Cushing's syndrome (frequency 10%). Thyrotroph adenomas secrete thyroid-stimulating hormone (TSH), also known as thyrotropin, which results in hyperthyroidism without TSH suppression ($\leq 2\%$ of tumor samples). Gonadotroph adenomas may secrete follicle-stimulating hormone (FSH) and/or luteinizing hormone (LH), which, depending on gender, may result in ovarian overstimulation, increased testosterone levels, testicular enlargement, and pituitary insufficiency. Many gonadotroph tumors, however, are not associated with hormone excess and may be considered nonfunctioning tumors. They often show positive immunostaining for one or more pituitary hormones; although they are not associated with evidence of hormone excess. Nonfunctioning pituitary adenomas (NFA) cause symptoms when they compress the surrounding structures.

In the World Health Organization (WHO) classification, Ki-67 is a marker of proliferation and related to growth potential in many human tumors, also represents a major predictive indicator for pituitary adenomas (Lloyd, 2004). The high expression of Ki-67 associate with aggressive behaviour in human pituitary tumors (Thapar et al., 1996).

The majority of pituitary adenomas are sporadic, although some arise as a component of familial syndromes. So far, four genes have been identified that predispose to familial pituitary tumorigenesis. In addition to the multiple endocrine neoplasia type 1 (*MEN1*) gene causing the MEN1 syndrome, the protein kinase A regulatory subunit-1-alpha (*PRKARIA*)

gene has been associated with Carney complex (CNC), a familial multiple neoplasia syndrome presenting with growth hormone-producing pituitary adenoma (Veugelers et al., 2004; Yen et al., 1992). More recently, the *CDKN1B* and the aryl hydrocarbon receptor interacting protein (*AIP*) were identified as pituitary adenoma predisposing genes (Pellegata et al., 2006; Vierimaa et al., 2006). These last two genes are associated with a MEN1-like phenotype and with pituitary adenoma predisposition, respectively (Mulligan et al., 1993).

1.3.4. Current treatment of pituitary adenomas

Treatment of pituitary tumors usually involves surgery, radiotherapy and pharmacological therapy. The most common approach of surgery for pituitary tumors is the transsphenoidal surgery. This procedure is used to remove tumors of the pituitary gland through the nose and sphenoid (Buchfelder and Schlaffer, 2009). Radiation therapy can also be used in the treatment of pituitary adenomas, although it is not used as the first line of treatment in the majority of cases. The radiation comes in the form of high energy x-rays that results in damage to the DNA of cells, causing the tumor cells to die (Platta et al., 2010).

For some pituitary adenomas that secrete hormones, receptor-mediated treatment aimed at reducing hormone secretion can be effective rather than surgery or radiation, and is often the first treatment tried for these types of adenomas. Somatostatin (SRIF) and dopamine act as regulators of pituitary cell function, mainly controlling hormone secretion (Ben-Jonathan and Hnasko, 2001; Guillemin, 2005). SRIF and dopamine work through the binding to specific G-protein coupled receptors (GPCR): the somatostatin receptors type 1-5 (Sstr1-5) and subtype 2 of dopamine receptor (Drd2). mRNA of these receptors are expressed in both normal gland and pituitary tumors, but their expression is highly variable within and between tumor subtypes (Table.3).

Table 3 Gene expression of receptors in the different type of pituitary adenoma. Data source: (Saveanu and Jaquet, 2009).

Type of pituitary adenoma	Gene expression of somatostatin receptors (SSTRs) and dopamine receptor type 2 (Drd2)
Somatotroph	SSTR2/SSTR5/Drd2
Lactotroph	SSTR1/SSTR5/Drd2
Corticotroph	SSTR5/Drd2
Thyrotroph	SSTR2/SSTR5
NFA	SSTR1/SSTR2/SSTR3/Drd2

Most somatotroph express *Sstr2*, *Sstr5* and *Drd2* (Panetta and Patel, 1995; Stefaneanu et al., 2001). Lactotrophs express highly *Drd2*, and *Sstr1* and *Sstr5* are also present (Fusco et al., 2008). Nonfunctioning pituitary adenoma (NFA) expresses mostly *Sstr3*, whereas *Sstr2* is expressed at lower level. *Drd2* is found in most NFA, while *Sstr1* is present at extremely low levels (Taboada et al., 2007). Corticotrophs express mainly *Sstr5* and *Drd2*, whereas *Sstr2* is found at lower levels together with *Sstr1* and *Sstr3* (Pivonello et al., 2004).

Binding of SRIF to Sstr modulates a variety of signal transduction pathways, such as inhibition of adenylyl cyclase and guanylyl cyclase, activation of calcium channels, as well as stimulation of phosphotyrosine phosphatase or mitogen-activated protein kinase (MAPK) activity (Patel, 1999). Because of their function and widespread expression in pituitary adenoma, SRIF and Sstr have a potential target for therapy and diagnosis of pituitary adenoma. For this reason, SRIF-analogues (SSA) have been investigated for many years. The SRIF-analogues, such as octreotide and lanreotide, are available for clinical use due to a considerable longer half-life (about 2 hours) instead of the natural SRIF having a short half-life (less than 3 min). SSAs bind Sstrs similar to the natural SRIF, but show different binding affinities to the various receptors. Octreotide and lanreotide bind with high affinity to *Sstr2* and *Sstr5* (Lamberts et al., 1991). They treat successfully patients with somatotroph and thyrotroph tumors by normalizing growth hormone (GH) and insulin growth factor 1 (IGF-1) concentrations (Ezzat et al., 1992; Newman et al., 1995; Vance and Harris, 1991). Pasireotide (SOM230) is a novel SRIF-analogue that powerfully inhibits the growth of somatotroph and corticotroph adenomas both *in vivo* and *in vitro* (van der Hoek et al., 2004). SOM230 binds with high affinity *Sstr5* followed by *Sstr2* and *Sstr3*. Preclinical data showed that SOM230 induces downregulation of ERK phosphorylation and upregulation of p27 in pituitary adenomas, possibly impairing cell cycle progression and inhibiting cell growth more effectively than octreotide (Hubina et al., 2006).

The dopamine agonists, bromocriptine and cabergoline, bind to the dopamine receptors. They have shown the reduction of prolactin plasma level in most of prolactinoma patients (Bevan et al., 1992). Recently, a chimeric compound (BIM23A760) has been developed which binds to both dopamine receptors and Sstrs (specifically, *Sstr2* and *Sstr5*) and displays a potent inhibitory effect *in vitro* on GH and PRL release (Jaquet et al., 2005a; Jaquet et al., 2005b).

In contrast to the other types of pituitary adenoma, the issue of medical therapy for NFA is a matter of great debate. Transsphenoidal surgery is the treatment of choice for NFA but it is rarely curative. If residual tumor is discovered or if the tumor recurs after surgery, radiation therapy is performed for patients with NFA, but this approach is associated with long term

complications and is restricted to these patients at high risk for tumor growth (Ferrante et al., 2006). Currently available drugs for NFA, such as somatostatin analogue (octreotide and lanreotide) and dopamine (DA) agonist (bromocriptine), may be useful in some cases to prevent residual tumor growth. The novel compound, BIM23A760, also inhibits partially cell proliferation in 60% of NFA cell cultures (Florio et al., 2008) and SOM230 has inhibition effect on VEGF (vascular endothelial growth factor) secretion in 13 responders out of 25 NFA cell cultures (Zatelli et al., 2007a).

1.3.5. PI3K/AKT/mTOR pathway as a therapeutic target

Phosphatidylinositol 3-kinase (PI3K) and its downstream mTOR are often activated and play a critical role in development of many tumors, including breast, ovarian, prostate, pancreatic, thyroid and also pituitary adenoma. It has been known that over-activation aberrant pathway of PI3K/mTOR is frequently through various PI3K/AKT activating mutations (such as *PTEN* and *PIK3CA*) (Cully et al., 2006; Samuels et al., 2005). These findings suggest that such genetic alterations contribute to the uncontrolled PI3K activity.

Activated PI3K generates phosphatidylinositol-3,4,5-triphosphate, which recruits phosphatidylinositol-dependent kinase 1 (PDK1) and Akt serine/threonine kinase at the plasma membrane, resulting in activation of Akt through phosphorylation (Cantley, 2002; LeRoith and Roberts, 2003). To be fully active, Akt needs two phosphorylated residues: threonine 308 (T308-Akt) and serine 473 (S473-Akt). The phosphorylation is mediated by PDK1, while the identity of the kinase that mediates S473 phosphorylation is still debated (Alessi et al., 1997; Stokoe et al., 1997). Activated Akt phosphorylates downstream targets, most notably the mTOR kinase. mTOR is the catalytic subunit of two molecular complexes, mTOR complex-1 (mTORC1) and mTOR complex-2 (mTORC2) composed of different proteins (Sabatini, 2006; Wullschleger et al., 2006). mTORC1 molecule is complexed with raptor (regulatory associated protein of mTOR) and regulates protein synthesis through phosphorylation of S6K1 (p70 ribosomal protein S6 kinase), 4EBP1 and SGK (glucocorticoid-inducible kinase) (Hara et al., 1998; Kim et al., 2002). In an other complex, mTORC2, mTOR binds to the adaptor protein rictor and directly phosphorylates AKT on the S473 residue mediated by integrin-linked kinase (Heinonen et al., 2008; McDonald et al., 2008; Sarbassov et al., 2005) (Fig.6). Activation of AKT by PI3K pathway leads to the phosphorylation of p27 on threonine 157 (T157) and threonine 187 (T187). Phosphorylated

p27 translocates into cytoplasm where it is degraded thereby alleviating its inhibitory action on CyclinE/CDK2 complexes. Thus AKT activation promotes cell cycle progression (Liang et al., 2002).

The compounds that block PI3K/mTOR signaling cascade at various levels have been generated. The mTOR inhibitors, such as rapamycin analogues (rapalogs) and RAD001 (Everolimus) have been generated which are based on the structure of rapamycin, a natural antibiotics from *Streptomyces hygroscopicus* (Sehgal et al., 1975). These agents crosslink with FKPB12 and its complex (rapamycin-FKPB12) binds and inhibits mTOR, thereby blocking downstream pathways (Chung et al., 1992). mTOR inhibitors have been used as immunosuppressant drug used to prevent organ rejection, especially in kidney transplantation (Abraham and Wiederrecht, 1996). Recently mTOR inhibitors have shown antiproliferative effects on several tumor cell lines and tumors both *in vitro* and *in vivo*, including neuroendocrine tumors (Hudes et al., 2007; Panwalkar et al., 2004). Rapamycin, one of the mTOR inhibitor may have therapeutic potential for neurodegenerative disorders, such as Alzheimer's disease (AD), Huntington's and Parkinson's disease possibly through enhancement of autophagy (Hasty, 2010).

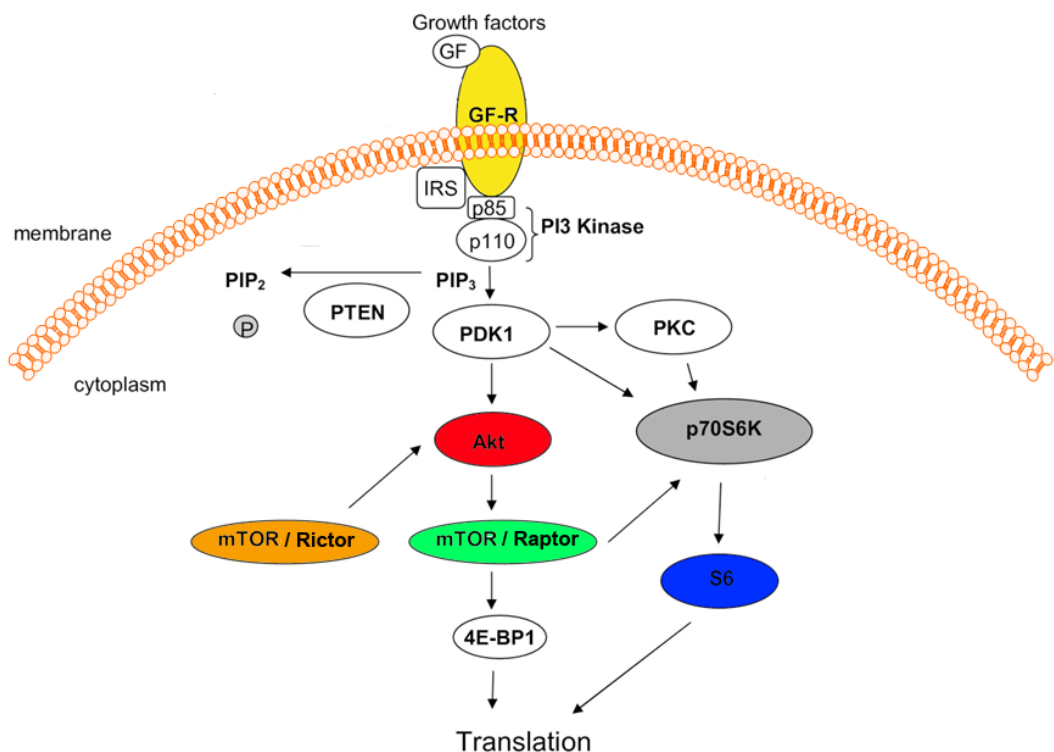


Fig.6 Graphic representation of PI3K/AKT/mTOR pathway

Insulin, hormones and growth factors activate the PI3K/AKT/mTOR signaling cascade. Akt is phosphorylated by PDK1 and an mTOR/riktor complex. The mTOR complex with raptor mediates the phosphorylation of 4E-BP1 and S6K1. Once activated, S6K1 phosphorylates ribosomal protein S6 and eIF4B. Data source: (Heinonen et al., 2008).

It has been recently observed that rapamycin and RAD001 significantly decrease cell viability of a rat GH-secreting pituitary tumor cell line (GH3 cell), of human GH-secreting pituitary tumors and human nonfunctioning adenoma (NFAs) (Gorshtein et al., 2009; Zatelli et al., 2010). These antiproliferative effects are caused by the induction of cell cycle arrest and apoptosis through the increase of p21 and p27 expression (Beuvink et al., 2005; Kawamata et al., 1998).

In addition, the inhibition of VEGF (vascular endothelial growth factor) secretion has been demonstrated to mediate the antiproliferative effect of mTOR inhibition. However, mTOR inhibitors also decrease p70S6K phosphorylation, thus impairing the inhibitory feedback loop to insulin receptor substrate 1 (IRS-1), results in the resistance to the effect of the inhibition because of an increase of AKT phosphorylation (O'Reilly et al., 2006; Um et al., 2004). Therefore, to overcome rapamycin-induced resistance, dual inhibitors target both PI3K (upstream to AKT) and mTOR have been recently developed, including the small molecules LU294003, PI-204, BGT225, XL765 and NVP-BEZ235 (Kong and Yamori, 2009). Recently, NVP-BEZ235 has shown successfully targeting the structurally related kinase domains of both PI3K and mTOR and inhibits several cancer cells proliferation more efficiently than single PI3K or mTOR inhibitors *in vitro* and *in vivo* (Baumann et al., 2009; Liu et al., 2009; Maira et al., 2008).

1.3.6. Animal models of pituitary adenoma

In the last years, several mouse models of cell cycle regulators have investigated (Table 3). These engineered mice develop pituitary tumors, alone or together with other tumor types. Mice with mutations that impair the function of the Rb pathway in cell cycle control (i.e. *Rb*^{+/−}, chimeric *Rb*^{−/−} mice) develop intermediate lobe (IL) pituitary tumors with high penetrance (Jacks et al., 1992; Williams et al., 1994). Tumor incidence due to the partial deletion of pRB is reverted by a mutation in pRB effectors such as E2F1 (Yamasaki et al., 1998) or E2F4 (Lee et al., 2002), indicating the relevance of the pRB/E2F pathway in pituitary tumorigenesis.

Inactivation of *Cdkn1b* (encoding p27^{Kip1}) alone (Fero et al., 1996) or *Cdkn1b* together with *Cdkn2c* (encoding p18^{INK4c}) (Franklin et al., 1998) induces 100% intermediate lobe pituitary adenoma formation. Mutant mouse strains (*Cdkn1b*^{ck−/ck−}) which are unable to bind and inhibit Cyclin/CDK complexes observed IL tumor with lower incidence (75%) (Besson et al., 2007). Mice with *Rb* or *Cdkn1b* mutation developed IL tumors, but they have different histological phenotype and the gene profile expression (Chien et al., 2007). Combination deletions of

Cdkn2c (encoding p18^{INK4c}) and *Cdkn1a* (encoding p21^{Cip1}) or *Rb* and *Cdkn1b* result in cooperation in pituitary tumor (Franklin et al., 2000; Park et al., 1999).

Deficiency in only *Cdkn2a* (encoding p16^{INK4a}) does not result in pituitary tumors. However, combination with *Cdkn2c* develop 50% IL tumors (Ramsey et al., 2007). Overall, mouse models generated by ablation of cell cycle develop pituitary adenoma, but due to their tumor location, these animal models do not really model human pituitary tumors that occur in the anterior lobe.

The other mouse models have been generated by deletions of the genes predisposing to hereditary pituitary tumors (*Men1* and *Prkr1a*), but often do not reflect the human diseases. Mice with *Prkar1a* deficiency do not show any consistent pituitary abnormalities (Griffin et al., 2004). *Hmga2* overexpression in mice results in pituitary tumorigenesis; transgenic mice overexpressing *Hmga2* develop pituitary adenomas secreting prolactin and GH (Fedele et al., 2002). Interestingly, the same phenotype is also seen in mice overexpressing *Hmga1* (Fedele et al., 2005), although neither rearrangement nor amplification of *HMGA1* locus have been detected in human pituitary adenomas. Taken together, the animal models available often show important phenotypic and biologic differences with respect to the human disease they were meant to model. Moreover, these mice models have been well studied at the phenotypic level but, with few exceptions, not at the molecular level to find additional genetic changes relevant to tumor development/progression not only in the mouse but also in humans.

Table.3 Mouse model of cell cycle-related proteins involved in pituitary tumors
Data source: (Quereda and Malumbres, 2009).

Model	Pituitary phenotype	Incidence (%)	Reference
<i>Rb</i> ^{+/-}	IL tumors	100	Jacks et al. (1992)
<i>Rb</i> ^{+/-} ; <i>E2f1</i> ^{-/-}	IL tumors	62	Yamasaki et al. (1998)
<i>Rb</i> ^{+/-} ; <i>E2f4</i> ^{-/-}	IL tumors	78	Lee et al. (2002)
<i>Cdkn1b</i> ^{-/-}	IL tumors	100	Fero et al. (1996)
<i>Cdkn1b</i> ^{ck/ck}	IL tumors	75	Besson et al. (2007)
<i>Rb</i> ^{+/-} ; <i>Cdkn1b</i> ^{-/-}	Cooperation in IL tumors	90	Park et al. (1999)
<i>Cdkn2c</i> ^{-/-}	Tumors in IL and AP	50	Franklin et al. (1998)
<i>Cdkn2a</i> ^{-/-} ; <i>Cdkn2c</i> ^{-/-}	IL tumors	50	Ramsey et al. (2007)
<i>Cdkn1a</i> ^{-/-} ; <i>Cdkn2c</i> ^{-/-}	Cooperation in IL tumors	90	Franklin et al. (2000)
<i>Cdkn1b</i> ^{-/-} ; <i>Cdkn2c</i> ^{-/-}	IL and AP undifferentiated tumors	100	Franklin et al. (1998)

IL: intermediate lobe AP: anterior pituitary

2. AIMS

Germline mutations in *Cdkn1b/CDKN1B* are associated with the predisposition to multiple endocrine tumors in both rats (MENX syndrome) and humans (MEN4 syndrome). The first aim of our study was to characterize at the molecular level the mutations in *Cdkn1b/CDKN1B*. We have identified which functions of p27 need to be altered/impaired for tumor predisposition to occur. This knowledge might then be exploited to provide a targeted therapeutic management of mutation-positive patients. MENX-affected rats develop, among other tumors, pituitary adenomas with complete penetrance. Since a comprehensive morphological and phenotypic characterization of the tumors is a prerequisite to exploit an animal model for preclinical therapy-response studies and for molecular studies aimed at elucidating the pathogenesis of such tumors, we set out to characterize the pituitary tumors that develop in MENX-affected rats. The aim of this study is to determine whether MENX-associated pituitary tumors could be a suitable model of human NFA, by testing primary rat pituitary tumor cultures with several therapeutic agents (SSA, chimeric drugs, rapalogs), comparing the results with human NFA studies. In addition, this study investigated more detail the downstream molecular events elicited by new rapalog NVP-BEZ235 in MENX-derived pituitary tumors, in relation to the genetic mutation in p27.

3. MATERIALS

3.1. Equipments

Applied Biosystems 7300 Real Time PCR system	Applera GmbH, Darmstadt (Germany)
Centrifuge Biofuge fresco	Heraeus Instruments, Osterode (Germany)
Centrifuge Biofuge pico	Heraeus Instruments, Osterode (Germany)
Centrifuge eppendorf 5415D	eppendorf, Hamburg (Germany)
Centrifuge Fisherbrand Mini	Fisher Scientific, Schwerte (Germany)
Centrifuge Rotanta 460R	Andreas Hettich, Tuttlingen (Germany)
Centrifuge Rotina 420R	Andreas Hettich, Tuttlingen (Germany)
Centrifuge Variofuge 3.0R	Heraeus Sepatech, Osterode (Germany)
Counting chamber Improved Double Neubauer Ruling	Brand, Wertheim (Germany)
Dispenser Multipette® plus	eppendorf, Hamburg (Germany)
Electrophoresis Cell GT MINI-SUB®	Bio-Rad Laboratories, Munich (Germany)
Electrophoresis Mini-Cell XCell <i>SureLock™</i> Novex	Invitrogen, Darmstadt (Germany)
Electrophoresis Transfer Cell Mini Trans-Blot®	Bio-Rad Laboratories, Munich (Germany)
Freezer -20°C Liebherr Comfort	Liebherr, Biberach an der Riss (Germany)
Freezer -80°C HFC86-360	Heraeus Instruments, Osterode (Germany)
Heating block Thermomixer® comfort 1.5 ml	eppendorf, Hamburg (Germany)
Microplate Reader Model 680	Bio-Rad Laboratories, Munich (Germany)
Microscope Apotome	Carl Zeiss, Jena (Germany)
Microscope Axiovert 135	Carl Zeiss, Jena (Germany)
Microscope EVOS xl	AMG, Bothell (WA, USA)
Microwave Privileg 1034HGD	Otto, Hamburg (Germany)
Multichannel pipette Finnpipette® 50-300 µl	Thermo LabSys., Waltham (MA, USA)
PCR cycler GeneAmp® PCR system 9700	Applied Biosystems, Carlsbad (CA, USA)
PCR cycler TPersonal Thermocycler	Biometra, Goettingen (Germany)
pH meter inoLab® Level 1	WTW, Weilheim (Germany)
Power supply Model 200/2.0	Bio-Rad Laboratories, Munich (Germany)
Spectrophotometer NanoDrop® ND-1000	Thermo Fisher Sci., Waltham (MA, USA)

Spectrophotometer UV/VIS Novaspec II	Pharmacia LKB, Uppsala (Sweden)
Tweezers No.5	A.Dumont&Fils, Montignez (Switzerland)
Vacuum Concentrator plus	eppendorf, Hamburg (Germany)
Vortexer Reax top	Heidolph Instr., Schwabach (Germany)
Water bath shaker #1083	G. f. Labortechnik, Burgwedel (Germany)
Water bath shaker SW21	Julabo Labortechnik, Seelbach (Germany)

3.2. Consumable materials

Adhesive seal films MicroAMP™	Applied Biosys., Foster City (CA, USA)
Blotting paper grade 3m/N 65 g/m ²	Munktell & Filtrak, Bärenstein (Germany)
Cell strainer Falcon™ 70 µm, nylon	BD Biosciences, Bedford (MA, USA)
Combitips® for Multipette® 12.5 ml	eppendorf, Hamburg (Germany)
Cover slips 12 mm round	Carl Roth, Karlsruhe (Germany)
Cryogenic vials sterile 2 ml freestanding Falcon®	BD Biosciences, Franklin Lakes (NJ, USA)
Cuvettes PLASTIBRAND® 1.5 ml semi-micro	Brand, Wertheim (Germany)
Gel cassettes 1.5 mm	Invitrogen, Grand Island (NY, USA)
Glass slides SuperFrost® 76 x 26 mm	Carl Roth, Karlsruhe (Germany)
Membrane for Western Amersham™ Hybond™-ECL	GE Healthcare, Munich (Germany)
Microplates, TC 96 well, clear bottomed, white walled	Lonza, Basel (Switzerland)
Needles Sterican® Ø 0.60 x 60 mm 23G x 2 3/8"	B. Braun, Melsungen (Germany)
Needles Sterican® Ø 0.80 x 50 mm 21G x 2"	B. Braun, Melsungen (Germany)
Parafilm®	Carl Roth, Karlsruhe (Germany)
PCR plate (0.2 ml) Thermo-Fast® 96-well, non-skirted	Abgene/Thermo Sci., Rockford (IL, USA)
PCR tube strips 0.2 ml	eppendorf, Hamburg (Germany)
Petri dishes 100 x 15 56.7 cm ² Nunclon™ Δ	nunc, Roskilde (Denmark)
Petri dishes glass bottom poly-D-lysine coated no. 1.5	MatTek, Ashland (MA, USA)
Photographic film Amersham Hyperfilm™ ECL	GE Healthcare, Little Chalfont (England)
Pipettes, Pasteur glass 3.2 ml	Carl Roth, Karlsruhe (Germany)
Pipettes, serological CELLSTAR® various volume	Greiner BioOne, Frickenhausen (Germany)
Pipette tips Graduated Filter Tips TipOne®	Starlab, Ahrensburg (Germany)
Reacion tubes 1.5 ml	eppendorf, Hamburg (Germany)
Reaction tubes Falcon™ Blue Max	BD Biosciences, Franklin Lakes (NJ, USA)
Reaction tubes, RNase-free 1.5 ml	Zymo Research, Orange (CA, USA)
Scalpel, sterile, disposable	Aesculap, Tuttlingen (Germany)
Syringe, single-use 50 ml (60 ml)	Henke-Sass-Wolf, Tuttlingen (Germany)
Tissue culture flasks, filter cap Nunclon™ Δ	nunc, Roskilde (Denmark)
Tissue culture plates MULTIWELL™ flat	BD, Franklin Lakes (NJ, USA)

3.3. Chemicals and reagents

β -mercaptoethanol	Sigma-Aldrich, Steinheim (Germany)
Agarose LE for gel electrophoresis	Biozym, Hessisch Oldendorf (Germany)
Albumin from bovine serum (BSA)	Sigma-Aldrich, Steinheim (Germany)
Ampicillin sodium salt	Sigma-Aldrich, Steinheim (Germany)
Ampuwa® water	Fresenius KABI, Bad Homburg (Germany)
Ammonium persulfate	Sigma-Aldrich, Steinheim (Germany)
Bis-acrylamide ProtoGel 30% (w/v)	national diagnostics, Atlanta (GA, USA)
BIM23A760	Ipsen Pharmaceuticals, Milford (MA, USA)
Bortezomib	LC-lab, Woburn (MA, USA)
Chemiluminescent substrate SuperSignal® West Pico	Pierce/Thermo Sci., Rockford (IL, USA)
Chloroform	Merck, Darmstadt (Germany)
Collagenase V	Worthington, Lakewood (NJ, USA)
Cycloheximide	Sigma-Aldrich, Steinheim (Germany)
Cresol red	AppliChem, Darmstadt (Germany)
DMEM + GlutaMAX™-I, 4.5 g/l D-glucose, pyruvate	Gibco/Invitrogen, Grand Island (NY, USA)
DMSO	Sigma-Aldrich, Steinheim (Germany)
DNA Molecular Weight Marker VIII	Roche Diagnostics, Mannheim (Germany)
Ethanol	Merck, Darmstadt (Germany)
Ethidium bromide	Sigma-Aldrich, Steinheim (Germany)
Fetal bovine serum (FBS)	Gibco/Invitrogen, Grand Island (NY, USA)
First strand buffer 5x	Invitrogen, Grand Island (NY, USA)
Fungizone™	Gibco/Invitrogen, Grand Island (NY, USA)
Gel loading dye, blue 6x	New England Biolabs, Ipswich (MA, USA)
Glycerol	Sigma-Aldrich, Steinheim (Germany)
HBSS 1x without CaCl ₂ /MgCl ₂	Gibco/Invitrogen, Grand Island (NY, USA)
HCl 5 M	neoLab, Heidelberg (Germany)
H8	Biaffin GmbH, Kassel (Germany)
H89	Biaffin GmbH, Kassel (Germany)
HA-1004	Biaffin GmbH, Kassel (Germany)
Hoechst 33258 bisBenzimide	Sigma-Aldrich, Steinheim (Germany)
Isopropanol	Merck, Darmstadt (Germany)
Kanamycin A monosulfate	Sigma-Aldrich, St. Louis (MO, USA)
Laemmli sample buffer 1x	Bio-Rad Lab., Hercules (CA, USA)
LB broth base	Invitrogen, Grand Island (NY, USA)
Methanol	Merck, Darmstadt (Germany)

MG132	Sigma-Aldrich, Steinheim (Germany)
NaCl EMSURE®	Merck, Darmstadt (Germany)
NP-40 Tergitol®	Sigma-Aldrich, St. Louis (MO, USA)
NVP-BEZ235	Novartis Pharma, Basel (Switzerland)
Octreotide	Sigma-Aldrich, St. Louis (MO, USA)
Paraformaldehyde	Merck, Darmstadt (Germany)
PageRuler™ prestained protein ladder	Fermentas, St. Leon-Rot (Germany)
PBS powder pH 7.4	Sigma-Aldrich, St. Louis (MO, USA)
Penicillin-Streptomycin, liquid	Gibco/Invitrogen, Grand Island (NY, USA)
Phenol Red	Sigma-Aldrich, Steinheim (Germany)
Photographic developer G153 A and B	Agfa Healthcare, Mortsel (Belgium)
Photographic fixer G354	Agfa Healthcare, Mortsel (Belgium)
Ponceau S practical grade	Sigma-Aldrich, Steinheim (Germany)
Protease inhibitor cocktail tablets complete mini	Roche Diagnostics, Mannheim (Germany)
Reverse transcriptase SuperScript® II	Sigma-Aldrich, St. Luis (MO, USA)
RNase inhibitor RNaseOUT™	Invitrogen, Grand Island (NY, USA)
RNaseZAP®	Sigma-Aldrich, St. Louis (MO, USA)
SDS 10% (w/v) solution	Bio-Rad Laboratories, Munich (Germany)
SDS-PAGE running buffer Rotiphorese®, 10x	Carl Roth, Karlsruhe (Germany)
Skimmed milk	Saliter, Oberguenzburg (Germany)
Sodium deoxycholate	Sigma-Aldrich, St. Louis (MO, USA)
Sodium hydroxide tablets EMSURE®	Merck, Darmstadt (Germany)
SOM230	Novartis Pharma, Basel (Switzerland)
Staurosporine	Biaffin GmbH, Kassel (Germany)
Taq DNA polymerase	Fermentas, St. Leon-Rot (Germany)
Stripping buffer for Western Blots Restore™ PLUS	Pierce/Thermo Sci., Rockford (IL, USA)
X-treamGENE siRNA transfection reagent	Roche, Manheim (Germany)

3.4. Buffers and solutions

1x PBS buffer (pH 7.4):

26.5 mM KCl
1.5 mM KH₂PO₄
137 mM NaCl
8 mM Na₂HPO₄

2x Laemmli buffer (pH 6.8):

100 mM Tris-Base
4% SDS
20% (w/v) Glycerol
10% (w/v) 2-Mercaptoethanol
0.01% (w/v) Bromophenolblue

RIPA buffer (pH 8.0):

50 mM Trizma® base
150 mM NaCl
0.1% (w/v) SDS
0.5% (w/v) sodium deoxycholate
1% (w/v) NP-40

10x Running buffer (pH 8.3):

500 mM Tris base
390 mM Glycin
0.039% (w/v) SDS

1x Transfer buffer:

10% (v/v) 10x Blotting buffer
20% (v/v) MeOH

5x TBE buffer (pH 8.3):

89 mM Tris base
89 mM Boric Acid
2 mM EDTA

LB media (pH 7.5):

10 g Bacto-Tryptone
5 g Yeast extract
10 g NaCl

LB Agar (pH 7.0):

10 g Tryptone
5 g Yeast extract
5 g NaCl
15 g bacterial Agar

Paraformaldehyde (2%, pH 7.4):

2% (w/v) paraformaldehyde in PBS
15 µl phenol red
add 10 M NaOH until dissolved (colour change from pink to colourless)
adjust pH to 7.4 with HCl using pH indicator strips

Separating gel (12%) for SDS-PAGE (10 ml):

4 ml 30% (w/v) acrylamide/bis
3.35 ml H₂O bidest
2.5 ml 1.5 M Tris (pH 8.8)
100 µl 10% (w/v) SDS
50 µl 10% (w/v) APS
5 µl TEMED

Stacking gel (4%) for SDS-PAGE (5 ml):

670 µl 30% (w/v) acrylamide/bis
3 ml H₂O bidest
1.26 ml 0.5 M Tris (pH 6.8)
50 µl 10% (w/v) SDS
25 µl 10% (w/v) APS
5 µl TEMED

3.5. Commercially available kits

BCA Protein Assay Pierce®	Thermo Sci., Rockford (IL, USA)
Cyclic AMP Assay Parameter™	R&D Sys., Minneapolis (MN, USA)
Miniprep Kit QIAprep® Spin (50)	Qiagen, Hilde (Germany)
Vialight® Plus Cell Proliferation and Cytotoxicity Kit	Lonza, Basel (Switzerland)
QuikChange™ Site-Directed Mutagenesis Kit	Stratagene, La Jolla (CA, USA)

3.6. Constructs

Rat wild-type *Cdkn1b* cDNA and cDNA carrying the MENX mutation, *Cdkn1bfs177*, were cloned into the pEGFP-C3 vector (BD Biosciences, Erembodegem, Belgium) in frame with GFP.

3.7. Software

7300 System SDS v1.4	Applied Biosystems, Carlsbad (CA, USA)
AimImageBrowser	Carl Zeiss, Jena (Germany)
AxioVision 4.6	Carl Zeiss, Jena (Germany)
Microplate Manager 5.2.1	Bio-Rad Laboratories, Munich (Germany)
MS Office 2003	Microsoft, Unterschleißheim (Germany)
Primer3	Whitehead Institute, Cambridge (MA, USA)
Simplicity 2.0	Berthold Det. Sys., Pforzheim (Germany)

4. METHODS

4.1. Mutagenesis

4.1.1. Primer design

For site-directed mutagenesis a mismatched oligonucleotide is extended, in order to incorporate a "mutation" into a strand of DNA that can be cloned. Therefore, mutagenic oligonucleotide primers are specially designed according to the respective mutation. These types of primers have to meet several requirements, the most important being that the primers should be 25-45 bases in length with the desired mutation in the middle and with 10 to 15 bases of correct sequence on both sides. The primers should furthermore have a melting temperature of below 78°C and feature a minimum GC content of 40% while terminating in one or more C or G bases. For the mutation of human wild-type p27, which had already been inserted into vectors pYFP-C1 (BD Biosciences Clontech) and pcDNA-HA (Invitrogen), the following primers were designed respecting after mentioned prerequisites (Table.4).

Table.4 Primers for mutations of *CDKN1B*

Name	Sequence
P69L fw	5'- CAGAACATCACAAACTCCTAGAGGGCAAG -3'
P69L rev	5'- CTTGCCCTCTAGGAGTTGTGATTCTG -3'
W76X fw	5'- GGCAAGTACGAGTAGCAAGAGGTGGAG -3'
W76X rev	5'- CTCCACCTCTTGCTACTCGTACTTGCC -3'
K96Q fw	5'- CCCCCGGGCCCCCAAGGTGCCTGCAAGG -3'
K96Q rev	5' CCTTGCAGGCACCTTGGGGGGCCGCGGGGC -3'
I119S fw	5'- CGGCGGCGCCTTAAGTGGGCTCCGGCTAA -3'
I119S rev	5'- TTAGCCGGAGCCCCACTTAAAGGCGCCGCCG -3'
I119D fw	5'- CGGCGGCGCCTTAGATGGGCTCCGGCTAA -3'
I119D rev	5'- TTAGCCGGAGCCCCATCTAAAGGCGCCGCCG -3'
I119E fw	5'- CGGCGGCGCCTTAGAAGGGCTCCGGCTAA -3'
I119E rev	5'- TTAGCCGGAGCCCCCTAAAGGCGCCGCCG -3'
I119A fw	5'- CGGCGGCGCCTTAGCTGGGCTCCGGCTAA -3'
I119A rev	5'- TTAGCCGGAGCCCCAGCTAAAGGCGCCGCCG -3'
I119T fw	5'- CGGCGGCGCCTTAAGTGGGCTCCGGCTAA -3'
I119T rev	5'- TTAGCCGGAGCCCCAGTTAAAGGCGCCGCCG -3'

4.1.2. PCR reaction

The polymerase chain reaction was completed in a normal plate with the following settings. Upon completion of the PCR, the samples were frozen at -20°C and kept in the dark until they could be processed. The duration of the extension step equates 1 min per kb of plasmid DNA. The number of cycles for single amino acid changes was set to 16 according to the protocol provided by Stratagene.

Reagent	
Forward primer	2.5 pmol/μl
Reverse primer	2.5 pmol/μl
dNTP Mix	10 mM
10X reaction buffer	1 μl (10%)
Template DNA	2-50 ng/μl
PfuUltra DNA polymerase	2.5 U/μl
final volume: 10 μl	

Step	Temperature	Time	Cycle(s)
Initial denaturation	95°C	30 sec	1
Denaturation	95°C	30 sec	
Annealing	55°C	1 min	
Extension	68°C	HA-vector: 5 min 30 sec YFP vector: 6 min 40 sec	2-18
Store	4°C	∞	

4.1.3. Digestion by *DpnI*

Since the transformation efficiency for the circular template plasmid is several orders of magnitude better than for the linear PCR product, *DpnI* digestion was performed to ensure transformation of the PCR product alone. As *DpnI* only cleaves at methylated sites, it digests the template plasmid but not the PCR product. Therefore, after the PCR reaction, the product was digested by *DpnI* incubation (0.5 U/μl) for 1 hour at 37°C.

4.1.4. Transformation & DNA extraction

For transformation of competent cells (XL-1 Blue) with DNA-constructs, 20 µl bacteria were taken from -80°C and thawed on ice. 1 µg of plasmid DNA was added and mixed gently. After incubation on ice for 30 min, cells were heat shocked for 30 seconds at 42°C in a water bath. Bacteria were then allowed to recover in 250 µl pre-warmed LB-medium for one hour at 37°C and 300 rpm. Bacteria were plated on agar and incubated at 37°C over night. Transformed bacteria were selected by adding respective antibiotics (ampicillin or kanamycin). The next day, positive clones were picked to inoculate 4-20 ml LB liquid cultures. After incubation over night at 37°C, bacteria were harvested for either plasmid isolation or for preparation of glycerol stocks. Plasmids were isolated from bacteria using a miniprep kit (Qiagen GmbH) and following the manufacturer's instructions.

For glycerol stocks, 20 ml selective LB over night cultures were inoculated. The next day, bacteria were harvested at 2500 x g and 4°C for 30 min. The cell pellet was resuspended in 3.4 ml LB plus 20% (v/v) glycerol. The suspension was divided into two cryo vials and stored at -80°C.

4.2. Dye-terminator sequencing

The method of dye-terminator sequencing (sometimes referred to as Sanger method) (Sanger and Coulson, 1975) is more efficient than the method of Maxam and Gilbert (Gilbert and Maxam, 1973). The key principle of the Sanger method is the use of dideoxynucleotides triphosphates (ddNTPs) as DNA chain terminators. In dye-terminator sequencing, the DNA sample is divided into four separate sequencing reactions, containing all four of the standard deoxynucleotides (dATP, dGTP, dCTP and dTTP) and DNA polymerase. To each reaction one of the four chain-terminating dideoxynucleotides (ddATP, ddGTP, ddCTP or ddTTP) is added. They lack the 3'-OH group that is required for the formation of a phosphodiester bond between two nucleotides and thus terminate DNA strand extension. This results in a number of DNA fragments of varying lengths. In our experiments, we used 'BigDye Terminator v3.1 Cycle Sequencing Kit' (Appelera GmbH). The BigDye terminators are labelled with dRhodamine acceptor dyes. The primers were designed to investigate the mutations of human patients (Table.5).

Table.5 Primers for sequencing to check mutagenesis

Name	Sequence
hCdkn1b 5 fw	5'- GTCGGGGTCTGTGTCTTTG -3'
hCdkn1b 622 rev	5'- CCATGTCTCTGCAGTGCTTC -3'
hCdkn1b 482fw	5'- TGTCTAACGGGAGCCCTAGC -3'
hCdkn1b 730 rev	5'- AGTAGAACTCGGGCAAGCTG-3'
hCdkn1b 882 rev	5'- GTCCGACGGATCAGTCTTG -3'
hCdkn1b 795 fw	5'- AGGAGAGGCCAGGATGTCAGC -3'
hCdkn1b intr 1 rev	5'- GCCAGGTAGCACTGAACACC -3'

The incorporation of the ddNTPs was conducted according to the protocol as follows:

Reagent	
Big Dye terminator mix (Applera)	2 µl
5x buffer (Applera)	0.94 µl
DMSO (Sigma)	0.3 µl
Template	250 ng
Primer	10 pmol
final volume: 10 µl	

Step	Temperature	Time	Cycle(s)
Initial denaturation	96°C	1 min	1
Denaturation	96°C	10 sec	
Annealing	50°C	5 sec	
Extension	60°C	4 min	35
Store	4°C	∞	

After the sequencing reaction and ethanol precipitation PCR extension products containing the mixture of strands, all of different length and all ending with a fluorescently-labelled ddNTP, underwent sequence analysis by the Genome Analysis Center core facility. Sequencing data (electropherograms of samples and sequence text files) were analyzed by using the Sequencher 3.0.

4.3. Animals

Animals were maintained according to animal husbandry regulations of helmholtzzentrum münchen (HMGU). Animals were subjected to complete necropsy either at the first indication of morbidity or at defined ages to analyze age-related tumour progression. Homozygous mutant rats were used for the analysis and are hereafter referred to as “mutant”. Age-matched unaffected littermates (controls) were also sacrificed at the ages indicated in the text.

4.4. Histology

For histological analysis, tissues were formalin-fixed, paraffin-embedded and cut in 1µm sections Hematoxylin and eosin (H&E) staining was used to confirm the diagnosis of hyperplasia or pituitary adenoma based on established criteria for neoplasia of the rat neuroendocrine system. Paraffin sections were rehydrated, stained and dehydrated according to the following protocol:

Step	Solution	Incubation
Rehydration	Xylene	2X 5 min
	100% ethanol	2X 5 min
	96% ethanol	5 min
	80% ethanol	5 min
	70% ethanol	5 min
	50% ethanol	5 min
	d H ₂ O	5 min
Staining	Hematoxylin	1-5 min
	d H ₂ O	10 sec
	Acid Alcohol	2 sec
	Tap Water	15 min
	Eosin	1 min
	d H ₂ O	10 sec
Dehydration	95% EtOH	1 min
	100% EtOH	1 min
	Xylene	2X 5 min
Mounting	Mounting solution (1 drop)	

Immunohistochemistry (IHC) is a method used to determine the expression of specific proteins in cells or tissues. The primary antibody binds to a specific antigen. This antibody-antigen complex is bound by a secondary, enzyme-conjugated antibody. In the presence of substrate and chromogen, the enzyme forms a colored deposit at the sites of antibody-antigen binding.

Paraffin sections were rehydrated according to the protocol described for H&E staining. After this step, samples were incubated with hydrogen peroxide (H_2O_2) solution (0.3% H_2O_2 in methanol) for 5 min to block endogenous peroxidase activity. This step results in the reduction of non-specific background staining. After washing with TBS buffer, antigen retrieval was performed to enhance antibody binding and consequently staining intensity: sections were microwaved for 30 min at 750 W in citric acid monohydrate buffer to break protein cross-links. After the microwaving, samples were left to cool down at room temperature for 5 min in TBS buffer and incubated with primary antibodies against specific proteins (Table.6) overnight at 4°C.

Table.6 List of primary antibody for IHC

Antibody	Company	Host	Dilution factor
anti-LH β	National Hormone and Peptide Program (CA, USA)	rabbit	1:500
anti- glycoprotein hormone alpha-subunit (α SU)	National Hormone and Peptide Program (CA, USA)	rabbit	1:1000
anti-GH	National Hormone and Peptide Program (CA, USA)	rabbit	1:500
anti-prolactin	National Hormone and Peptide Program (CA, USA)	rabbit	1:500
anti-SF1	Invitrogen (Karlsruhe, Germany)	mouse	1:100
anti-Ki67	BD Biosciences Pharmingen (NJ,USA)	mouse	1:200
anti-phospho-AKT (S473)	Cell signalling, (MA, USA)	rabbit	1:30
anti-AKT	Cell signalling, (MA, USA)	rabbit	1:30

In the avidin-biotin system we used, the secondary antibody is conjugated to biotin beads, which can bind to the avidin-enzyme complex. After incubation with primary antibody, samples were incubated with biotinylated secondary antibodies for 45 min and streptavidin-HRP conjugate (HSS-HRP) for 30 min. In between steps, samples were washed three times with TBS buffer for 5 min. For visualisation, the entire tissue section was covered with 1-5 drops of DAB/AEC Chromogen Solution and incubated for 3-20 min. After sufficient staining was affirmed under the microscope, dehydration was performed according to the protocol used for H&E staining.

Positive controls were always run in parallel to confirm the specificity of the staining. Images were recorded using a Hitachi camera HW/C20 installed in a Zeiss Axioplan microscope with Intellicam software (Zeiss MicroImaging). Image of tissue slides were acquired with an automatic high-resolution scanner (dotSlide System; Olympus). Area measurement was carried out using dotSlide software (Olympus).

4.5. Cell culture

All cells were only handled under a clean bench and incubated at 37°C in an atmosphere of 8% CO₂. When cells had reached a confluence of approximately 90% they were split 1:2 to 1:10 depending on their growth kinetics and intended use. Cells were cultured in special cell culture flasks that are available in different shapes and sizes. Primary mouse embryonic fibroblasts (MEFs) were obtained from *p27*^{-/-}, *p27*^{+/-} and *p27*^{+/+} mouse and primary rat fibroblasts (REFs) were obtained from rat embryo. They were cultured under sterile conditions as monolayers in Dulbecco's Minimal Essential Medium (DMEM), supplemented with 10% fetal bovine serum (FBS, Gibco-BRL), 100 units/ml of penicillin G sodium, 100 µg/ml streptomycin and 2.5 µg/ml Fungizone (Gibco-BRL).

MCF7 and HeLa cells from ATCC were maintained in RPMI1640 or DMEM medium, respectively, supplemented with 10% FBS, 20 mM L-glutamine, 100 units/ml of penicillin G sodium and 100 µg/ml streptomycin. GH3 cells were grown in F12 medium supplemented with 15% horse serum, 2.5% FBS, 20 mM L-glutamine, 100 units/ml of penicillin G sodium, and 100 µg/ml streptomycin.

To get the pituitary primary cells from MENX rats, fresh pituitaries were isolated from MENX-affected or wild-type control rats at autopsy. The tissues were transferred to 15 ml reaction tubes containing 10 ml sterile hank's buffered salt solution (HBSS) plus 100 units/ml of penicillin G sodium and 100 µg/ml streptomycin. The organ was then transferred to a Petri

dish with fresh HBSS. The organ was chopped with the help of two scalpels into equally sized pieces of about 2-3 mm². These pieces were transferred to a fresh Petri dish with fresh HBSS as means of washing. The organ was further chopped into pieces as small as possible. Tissue pieces were transferred to a fresh Petri dish containing serum-free medium and incubated for 90 min at 37°C with serum-free medium containing 1 ml collagenase V (5 mg/ml). During the incubation period, the Petri dish was carefully agitated every 30 min to ensure proper digestion of connective tissues. The digested organ was then pushed through a 21 gauge syringe ten times, subsequently through a 23 G syringe a minimum of ten times, until tissue pieces and larger cell aggregates were no longer visible. 1 ml of FBS was added and the single cell suspension centrifuged at 140 x g for five min at 4°C. After removing the supernatant, the cell pellet was resuspended in RPMI1640 supplemented with 10% fetal bovine serum, 100 units/ml of penicillin G sodium, 100 µg/ml streptomycin, Fungizone® antimycotic (Invitrogen) and D-valine to remove fibroblast contamination (Sordillo et al., 1988). The cell suspension was then passed through a 70 µm cell strainer to remove undigested tissues. The cells were seeded in 96 well plates (25000 cells per well) and left for 36 hours at 37°C in a humidified incubator with 5% CO₂ in air before beginning the treatments.

4.6. Cell viability

The effect of various anti-tumor drugs was tested on primary pituitary cell cultures plated in 96-well plates. Cells were treated with test substances or vehicle 36 hours after plating. Cell viability was assessed 48h after incubation with the test substances using the Vialight® Plus kit (Lonza). This cell viability assay is based upon the bioluminescent measurement of ATP that is present in all metabolically active cells. The bioluminescent method utilizes an enzyme, luciferase, which catalyses the formation of light from ATP and luciferin. The emitted light intensity is linearly related to the ATP concentration and is measured using a luminometer. 50 µl cell lysis buffers were added to each well in 96 well plates. After 15 min incubation at room temperature, 100 µl from each well were transferred to a white-walled 96 well luminometer plate. 100 µl of AMR (ATP Monitoring Reagent) Plus were added and incubated for two minutes to allow stabilisation of the signal. The plate was measured in a luminometer programmed to take a one second integrated reading of each well.

4.7. RNA interference

Cells were transfected with siRNAs targeting a variety of genes (Table.7). Cells were seeded in 6-well plates at a density of 5×10^5 cells in 2 ml complete medium per well or in 96-well plates to a density of 1.5×10^4 cells in 100 μ l medium. 24 hours after plating, the medium was removed and serum-free medium added. For transfection in 6-well plates, either 500 ng or 1 μ g siRNA were mixed with 15 μ l HiPerFect transfection reagent (Qiagen). siRNA was handled under RNase-free conditions. Untransfected cells, cells treated with transfection reagent and cells transfected with scrambled siRNA served as controls. Five to eight hours after transfection, the medium was changed to complete medium.

Table.7 List of siRNA.

Name	Description	Company
p27 siRNA (rat)	Pool of 4 different p27siRNA	Thermo Fisher Scientific (CO, USA)
SKP2 (rat)	Pool of 4 different SKP2 siRNA	Thermo Fisher Scientific (CO, USA)
KPC1 (rat) siRNA Silencer® Negative Control siRNA	Pool of 2 different KPC1siRNA	Ambion (CA, USA) Ambion (CA, USA)

4.8. Transient transfection

Asynchronously growing cells were transiently transfected with the different constructs when 70-80% confluent using the FuGene HD reagent (Roche). For one well, 500 ng-1 μ g of DNA was mixed with transfection reagent (3 μ l/ μ g of DNA) in 100 μ l serum-free medium. The components were mixed thoroughly and incubated for 15 min at room temperature, to ensure interaction between carrier molecules of the transfection reagent and DNA-molecules. After incubation, 100 μ l of transfection mix were added to each well and the plates carefully swirled to ensure even distribution. Five to eight hours after transfection, the medium was changed back to complete medium. Cells were collected and lysed 24-48h later in protein lysis buffer (10 mM Tris-HCl pH=7.4, 5 mM EDTA, 130 mM NaCl, 1% Triton) with added protease inhibitors.

4.9. Protein extraction and western blotting

For protein extraction, cells were collected after treatments, washed twice in PBS and lysed in RIPA-buffer (150 mM NaCl, 50 mM TrisHCl pH=8, NP-40 1%, Na-deoxycholate 0.5% and SDS 1%) with freshly added protease inhibitors. The volume of buffer varied from 25 µl to 200 µl, depending on the size of the cell pellet. After 15 min incubation on ice, the cell lysate was spun down at 13000 x g and 4°C for five minutes to remove cell debris. The protein-containing supernatant was transferred to a fresh tube and protein extracts stored at -80°C. Protein concentration was assessed by the bicinchoninic acid (BCA) protein assay (Smith et al., 1985). Total extracts were subjected to polyacrylamide gel electrophoresis using Bis-Tris 4-12% NuPAGE gels.

To target specific proteins from cell lysates, Western blot analysis was applied following SDS-PAGE. In order to make the proteins in the gel accessible to detection by antibodies, they were blotted from the gel onto a thin membrane with non-specific protein-binding properties. Transfer occurred overnight at 4°C. To prevent interactions between the membrane and antibodies used for detection, non-specific binding was blocked with 5% (w/v) skimmed milk in TBS-T. The membrane was incubated in milk for one hour under gentle agitation at room temperature. After three washes in TBS-T, a dilution of the primary antibody (Table.8) specific for the protein of interest was added and incubated over night at 4°C under gentle agitation.

Table.8 List of the primary antibodies for the western blotting studies

Antibody	Company	Host	Dilution factor
anti-p27	BD Biosciences (MA, USA)	mouse	1:300
anti-phospho-p27 (T187)	Santa Cruz (CA, USA)	rabbit	1:300
anti-phospho-AKT (S473)	Cell signalling, (MA, USA)	rabbit	1:1000
anti-AKT	Cell signalling, (MA, USA)	rabbit	1:1000
anti-phospho-S6 (S240/244)	Cell signalling, (MA, USA)	rabbit	1:1000
anti-S6	Cell signalling, (MA, USA)	rabbit	1:1000
anti-alpha-tubulin	Sigma-Aldrich (Steinheim, Germany)	mouse	1:1000
anti-Cdk2	Santa Cruz (CA, USA)	mouse	1:300
anti-Grb2	Santa Cruz (CA, USA)	rabbit	1:300

Unbound primary antibody was removed with three five-minute wash steps with TBS-T. Subsequently, a species-specific, horseradish peroxidise-coupled secondary antibody, diluted in 5% (w/v) skimmed milk in TBS-T, was added to the membrane. Incubation with the secondary antibody was carried out for 1h at room temperature. Following three more washes with TBS-T, a chemiluminescent agent was added and incubated for five minutes at room temperature in the dark. The membrane was exposed on a Kodak film for 30 seconds which was finally developed in an AGFA developing machine

4.10. RNA isolation

All RNA extractions were carried out under RNase-free conditions. For the isolation of total RNA from cells and tissues, the TRIzol method was applied. Cell pellets were mixed with 500 µl TRIzol® reagent and vortexed. During this step, reagent disrupts cells and dissolves cell components. 100 µl chloroform were added, samples were vigorously shaken and incubated at room temperature for 3 min. Samples were then centrifuged for 15 min at 4°C to separate the solution into an aqueous phase and an organic phase. RNA remains exclusively in the aqueous phase.

After transfer of the aqueous phase, the RNA was recovered by precipitation with 250 µl isopropyl alcohol. Samples were gently and centrifuged at 4°C for 30 min. The supernatant was discarded and 500 µl of 70% (v/v) ethanol were added. The ethanol was completely removed by from the RNA pellet. The RNA pellet was vacuum dried at room temperature and then dissolved in RNase free water. RNA extracts were stored at -80°C until further use. Concentration and quality of RNA samples were spectrophotometrically analysed using a NanoDrop device.

4.11. Reverse transcription

Reverse transcription (RT) was performed to gain complementary DNA (cDNA) from RNA templates. To this end, 0.1-1 µg of total RNA from cells was incubated for ten minutes at room temperature with 1 µg random primers in 11 µl reaction volume. After incubation, the following components were added per reaction batch:

Reagent	
DTT (0.1 M)	2 µl
dNTP Mix (10 mM each)	1 µl
RNaseOUT	1 µl
SuperScript™ II reverse transcriptase	1 µl
5x first strand buffer	4 µl
final volume: 11 µl	

Mixtures were incubated for one hour at 42°C. The reaction was stopped by heating to 95°C for five minutes. cDNA was stored at -20°C until further use.

4.12. Quantitative (q) RT-PCR

The qRT-PCR assay is based on Taq Polymerase 5'-3' nuclease activity. During the process of hybridization, the enzyme cleaves a dual-labeled probe to the complementary target sequence and fluorophore-based detection. The qRT-PCR probe, which is labeled with two fluorescent dyes, is created within the amplicon defined by a gene-specific PCR primer pair. The 5' end is labeled with a reporter dye (usually 6-carboxy-fluorescein, FAM), while the 3' end is labeled with a second fluorescent dye (6-carboxy-tetramethyl-rhodamine, TAMRA). As long as the probe is intact, the emission of the reporter dye is quenched by the second fluorescence dye. With the beginning of the extension phase of PCR, the polymerase enzyme starts to cleave the TaqMan probe, which results in a release of reporter dye. An automated sequence detector, equipped with specific software, is used to monitor the increasing amount of reporter fluorescent dye. For our experiments, specific genes were amplified by TaqMan PCR using gene expression assays from Applied Biosystems (Table.9). The following mix was prepared for each sample:

Reagent	
2x TaqMan master mix	10 µl
Assay-on-Demand	1 µl
final volume: 16 µl	

Table.9 List of Assay for qRT-PCR

Gene Symbol	Assay ID	Sequence
<i>Sstr1</i>	Rn02532012_s1	acctgcaatggtcgaatgcactgtt
<i>Sstr2</i>	Rn00571116_m1	ctcgtaaaaagcaagatgtcacgat
<i>Sstr3</i>	Rn00591732_m1	agcaacccctaaggttggctag
<i>Sstr5</i>	Rn00563577_m1	cctgcacagagacacgcgtggctg
<i>Drd2</i>	Rn00561126_m1	ggtgtgggt gagtgaaattcagcaggat
<i>B2m</i>	Rn00560865_m1	gcttgcattcagaaaactccccaa

16 µl of mixture were aliquoted into 96-well PCR-plates and 4 µl of RT product were added. For each assay negative control samples (H_2O) and calibrator (rat brain), which was used to create standard curves for the genes of interest, were added. For normalization, we used an endogenous control, β_2 microglobulin. The 7300 Real Time PCR System was run for 40 cycles (steps 3 to 4) with the following program:

- 1) 50°C 2 min
- 2) 95°C 10 min
- 3) 94°C 15 sec
- 4) 60°C 1 min
- 5) 4°C pause

The system quantifies PCR reaction products during each cycle by calculating the cycle threshold (Ct) value for each sample. Relative quantification was performed using the pre-recorded standard curve and analysis data of the 7300 Sequence Detection System. Linear regression analysis was used to calculate the relative amount of mRNA in samples. The relative mRNA expression level was normalized for RNA input with rat β_2 -microglobulin (*B2m*) gene expression in the sample. The relative mRNA expression level (CR) in each sample was calculated using the comparative cycle time (Ct) method as CR= 2 - (Ct rat normal tissue - Ct *B2m*) - (Ct target tissue - Ct *B2m*) (Pellegata et al., 2006).

4.13. Immunofluorescence

To visualize the location of the Yellow Fluorescent Protein (YFP)-p27 fusion proteins within the cell, cells were plated on poly-lysine coated cover slips (12 mm). Cells were incubated for 24 hours and then transfected with the appropriate vector constructs. After 24 hours of incubation, cells fixed with 2% (w/v) para-formaldehyde (Merck). Afterwards, the cells were washed 3 times with cold PBS. If necessary, fixed cells were stored in PBS at 4°C for up to 1 week. Pictures were taken using a Laser Scanning Microscope (LSM) provided by Zeiss. Image processing of the stained cells was carried out with Zeiss computer software.

4.14. Glutathione-S-transferase (GST) pull down assay

GST pull-down experiments are used to identify interactions between a probe protein and unknown targets and to confirm suspected interactions between a probe protein and a known protein. The probe protein is fused to GST and cloned into an isopropyl- β -D-thiogalactoside (IPTG)-inducible expression vector. In our experiments, we used GST-Grb2 (Upstate) and GST-CDK2 (Abnova) recombinant proteins. HeLa cells were transfected with YFP-p27wt, YFP-p27P69L or YFP-p27K96Q. The cells were collected 24 h after transfection and lysed in 5 mM EDTA, 1% Triton-X (IP buffer) for 20 min on ice and centrifuged at 13000 rpm for 5 min at 4°C. 500 μ g of total protein were incubated with 5 μ g of Grb2-GST recombinant protein already bound to Glutathione-agarose beads for the Grb2 binding assay or incubated with 2 μ g of recombinant Cdk2-GST (Abnova) and 20 μ l of Glutathione Agarose (Santa Cruz) overnight at 4°C . Samples were washed 5 times in IP buffer and resuspended in 25 μ l of Laemli buffer. 50 μ g of the cellular lysate (INPUT) and the whole pull-down was loaded on 12% bis-acrylamide SDS gels. Electrophoresis and blotting were performed as described above.

4.15. Apoptosis assay

Many different methods have been devised to detect apoptosis. In our experiments, we used DAPI staining for cell lines or caspase-3/7 measurement for primary cells. Diamidino-2-phenylindole (DAPI) is a DNA-specific dye that can pass through the intact membranes of viable cells and displays blue fluorescence. Apoptotic increases cell membrane permeability and uptake of DAPI, leading to a stronger blue stain. The morphology of the cells' nuclei was

used as additional feature to distinguish live cells from apoptotic cells. The nuclei of normal cells appear round, clear-edged and uniformly stained. In contrast, apoptotic cells show irregular edges around the nucleus, chromosome concentration in the nucleus, heavier coloring, and, with nuclear pyknosis, an increased number of nuclear body fragments.

For DAPI staining, HeLa cells were grown on cover slips and transfected with various plasmids during their exponential growth phase. At 24h or 48h post-transfection cells were fixed as described above. Fixed cells were completely covered with DAPI solution (300 nM) and incubated for 1-5 min in the dark. Afterwards, the cells were washed 3 times with cold PBS. Pictures were taken using a Laser Scanning Microscope (LSM) provided by Zeiss. Image processing of the stained cells was carried out with Zeiss computer software.

The members of the caspase family play key effector roles in apoptosis of mammalian cells. Therefore, apoptosis rates of primary cells after treatment were assessed by measuring the activity of cysteine aspartic acid-specific proteases (caspase)-3/7 using the Caspase-Glo® 3/7 Assay kit (Promega). This assay provides a luminogenic caspase-3/7 substrate, which contains the tetrapeptide sequence DEVD, in a reagent optimized for caspase activity, luciferase activity and cell lysis. Primary cells were plated in 96-well plates and treated with NVP-BEZ235 (10 nM, 100 nM) or vehicle 36 hours later. 24 h after treatment, reagent was added directly to the wells. This resulted in cell lysis, followed by the cleavage of the substrate by caspases and generation of a luminescent signal. Luminescence was measured using a luminometer (Berthold).

4.16. Clonogenic assay and growth curve

Clonogenic assay is an *in vitro* cell survival assay based on the ability of a single cell to grow into a colony. In our experiments, this assay was used to test for the effects of p27 mutant genes on the growth and proliferative characteristics of cells. To examine clonogenic activity, GH3 cells were plated (500,000 per well) in 6-well plates and transfected with p27wt, p27W76X or p27P69L as described above. The day after the transfection, the cells were diluted 1:6 and, starting from the day after, selected for 6 weeks by adding 0.4 mg/ml G418 (geneticin) to the culture medium. Cells were stained with 0.3% crystal violet in 30% ethanol. Colonies of ≥ 50 cells were scored. p27W76X GH3 stable clones, and untransfected GH3 cells were plated in duplicate (100,000 per well) in 12-well plates, in full medium plus 400 µg/ml G418. The number of cells was counted every two days over a 9 day-period using a cell counter.

4.17. Statistical analysis

Results of the cell viability assays are shown as the mean of values obtained in independent experiments \pm SEM (standard error of the mean). A paired two-tailed Student's *t*-test was used to detect significance between two series of data and p-value (*p*) <0.05 was considered statistically significant.

5. RESULTS

5.1. Germline *Cdkn1b* (p27^{Kip1}) mutation in the MENX rat syndrome

5.1.1. The MENX mutation in *Cdkn1b* affects p27 stability

Our group recently identified a variant of the MEN syndromes that spontaneously developed in a Sprague-Dawley rat colony (Pellegata et al., 2006). Affected rats are homozygous for a tandem duplication of 8 nucleotides starting at codon 177 (c. 520-528dupTTTCAGAC) in exon 2 of the *Cdkn1b* gene encoding the p27 protein. This mutation is never found in normal control DNA from commercially available rat strains. The mutated *Cdkn1b* mRNA encodes for a predicted 22 amino acid longer than p27 wild-type and protein 218 amino acid long containing a p27-unrelated C-terminal domain. We refer to this mutant protein as p27fs177 (Fig.7). Rats homozygous for the *Cdkn1b* mutation have very little, if any, immunoreactivity for the p27fs177 protein in their tissues, suggesting that this mutation behaves as a loss-of-function mutation.

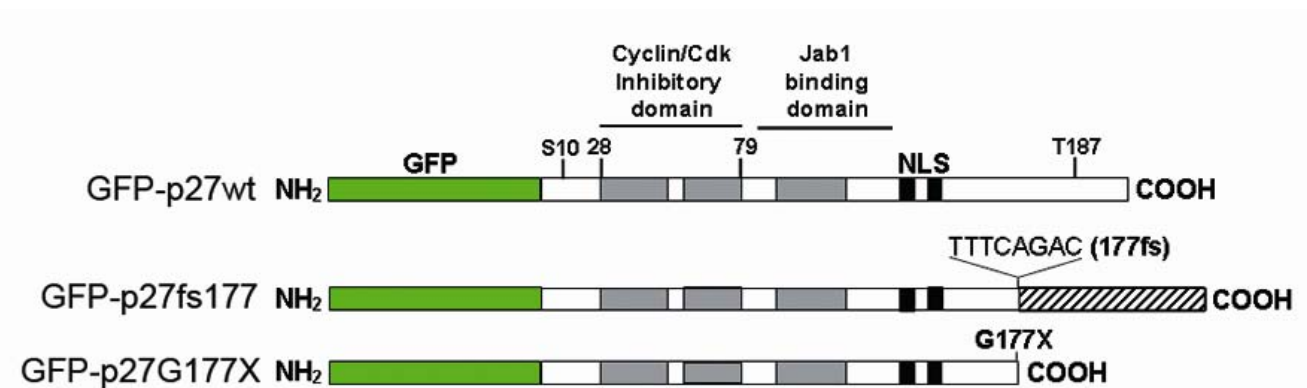


Fig.7 Schematic representation of GFP-p27wt (wild-type p27), GFP-p27fs177 and GFP-p27G177X expression vectors.

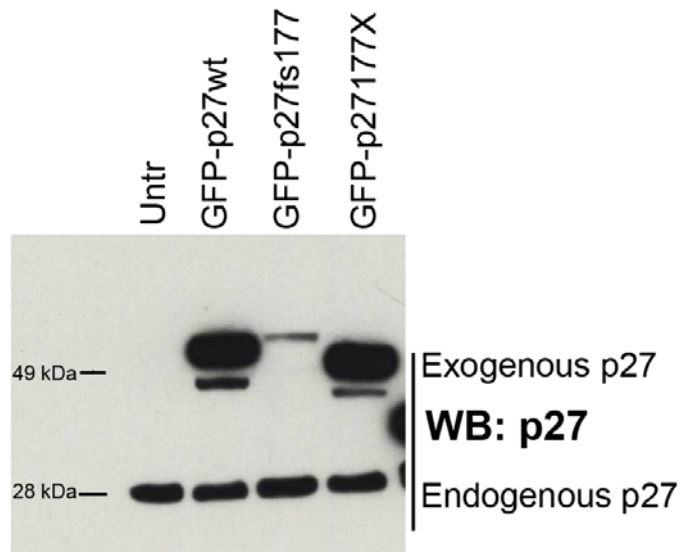


Fig.8 Expression of the p27 proteins. GFP-p27wt (wild-type p27), GFP-p27fs177 or GFP-p27G177X were transfected in MCF-7 cells. After 24h, cells were collected and total protein was extract, in parallel with untransfected MCF-7 cells (Untr). The levels of exogenous and endogenous p27 proteins were analyzed by western blotting with anti-p27 antibody.

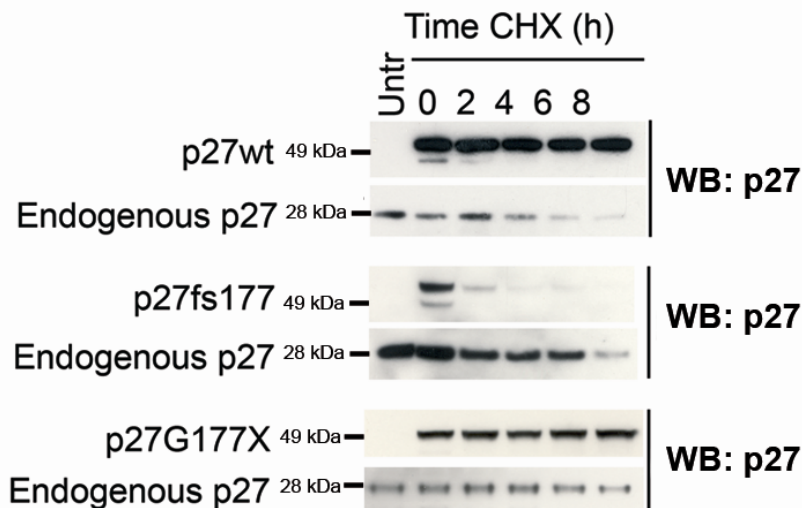
To better understand the functional properties of p27fs177, vectors that express p27fs177, p27wt (wild-type p27), or p27G177X (encoding a p27 protein with a premature stop codon at amino acid 177) tagged with the green fluorescence protein (GFP) were generated for *in vitro* experiments. All plasmids were transfected in MCF-7 cells and analyzed 24h later. All fusion proteins were expressed and their size was consistent with the predicted protein length (Fig.8). Exogenous p27fs177 was expressed at much lower level than p27wt and showed a band with higher molecular weight than the normal protein. In contrast, p27G177X was expressed at the same level of p27wt, and migrated more rapidly. The lower expression of the p27fs177 protein *in vitro* is consistent with the little immunoreactivity of MENX mutant rat tissues for p27. Since we observed clear bands of p27 by western blotting, we showed only part of western blotting in the following experiments.

The low expression level of p27fs177 could be due to enhanced instability of this mutant protein. To assess the stability of p27fs177, we treated GFP-p27fs177- or GFP-p27G177X-transfected MCF-7 cells with cycloheximide (CHX) to block new protein synthesis. p27wt and p27G177X were very stable after incubation with CHX for 8h. However, the p27fs177 protein was rapidly degraded already 2h after CHX treatment (Fig.9A).

Live cell imaging of MCF7 cells transfected with p27fs177 also showed a very fast degradation of the mutant p27 protein, degraded already 45min after addition of CHX (Fig.9B). Interestingly, within the time frame of the live cell imaging experiment (from 15

min up to 2 hr post-CHX treatment) the fluorescent signal associated with GFP-p27fs177 expression was detected only in the nucleus. This suggests that the mutant p27 protein is degraded in this cell compartment.

A



B

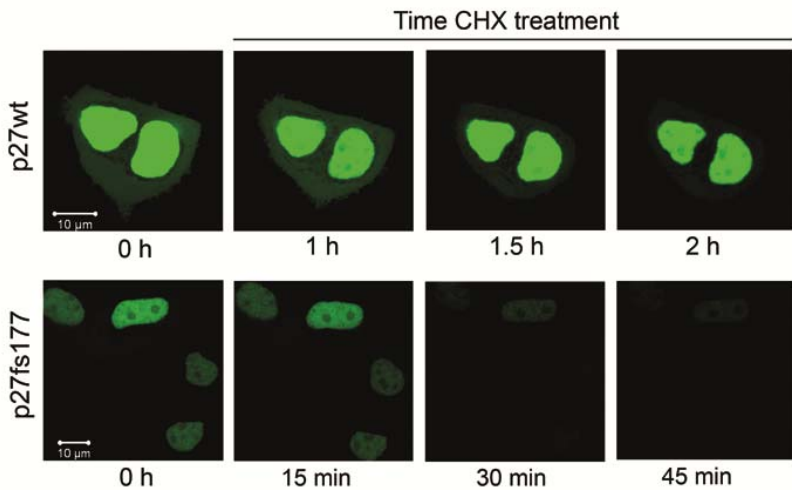


Fig.9 Stability of p27 proteins. (A) MCF7 cells transfected with GFP-p27wt, GFP-p27fs177 or GFP-p27G177X were treated for the indicated times (from 0 to 8h) with cycloheximide (CHX) (25 µg/mL) or without CHX (Untr). Expression level of p27 was analyzed by western blotting (WB) with anti-p27 antibody. (B) Live cell imaging of MCF7 cells transfected with p27wt or p27fs177 and treated for the indicated times with CHX. To recreate a more physiological condition (37°C and 5% CO₂), dishes were put under a microincubation chamber (Zeiss, Jena, Germany) mounted on a confocal laser scanning microscope (Zeiss). Images were taken every 15 min using always the same settings. Here only some relevant time points are shown.

5.1.2. Proteasome-mediated degradation of p27fs177 *in vitro*

p27fs177 is rapidly degraded compared to p27wt or p27G177X. In physiological conditions, p27wt is degraded through ubiquitin-dependent proteasomal degradation (Kamura et al., 2004). To verify whether the proteasome also mediates the aberrant degradation of the mutant p27fs177 protein, we generated stably-transfected cells expressing this mutant. MCF7 cells were transfected with p27wt, p27fs177 or p27G177X constructs and selected for resistant to the geneticin (G418) for 3 weeks. Each stably transfected clone constitutively expressed the appropriate protein, as demonstrated by western blotting (Fig.10). For further studies, clones 3, 8 and 9 were expanded and studied as representatives of each transfection condition.

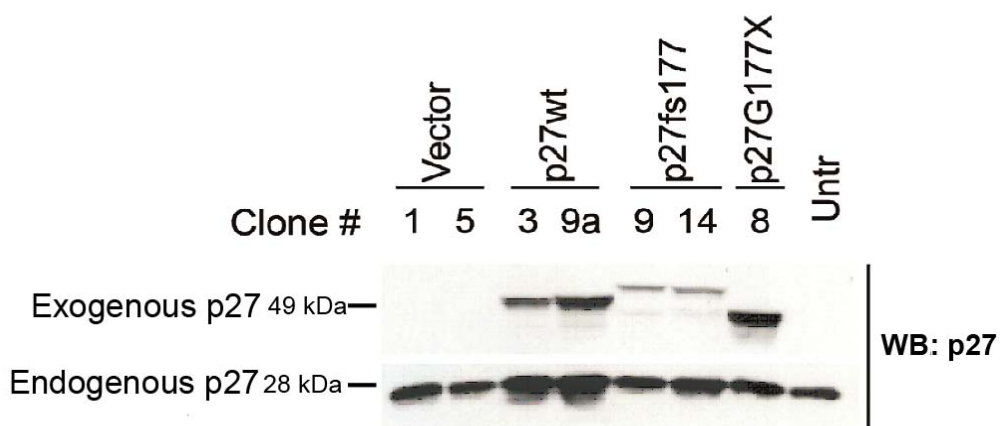


Fig.10 Clones stably expressing mutant p27 proteins. Western blotting (WB) was performed to identify the p27 expression level in different clones after transfection and selection, in parallel with untransfected cells (Untr). Clones stably express the indicated p27 mutants.

To confirm the results obtained incubating transiently transfected MCF-7 cells with CHX, the selected clones (clone 3, 8, 9) stably expressing the three p27 proteins were incubated with CHX for 2, 4, 6, 8 hours. Similar to our previous results, clone 3 (p27wt) and clone 8 (p27G177X) did not show rapid degradation after CHX treatment (Fig.11A and 11B). In contrast, clone 9, which expresses p27fs177, showed rapid degradation of the protein already 20 min after CHX treatment similarly to what we previously observed upon transient transfection (Fig.11C).

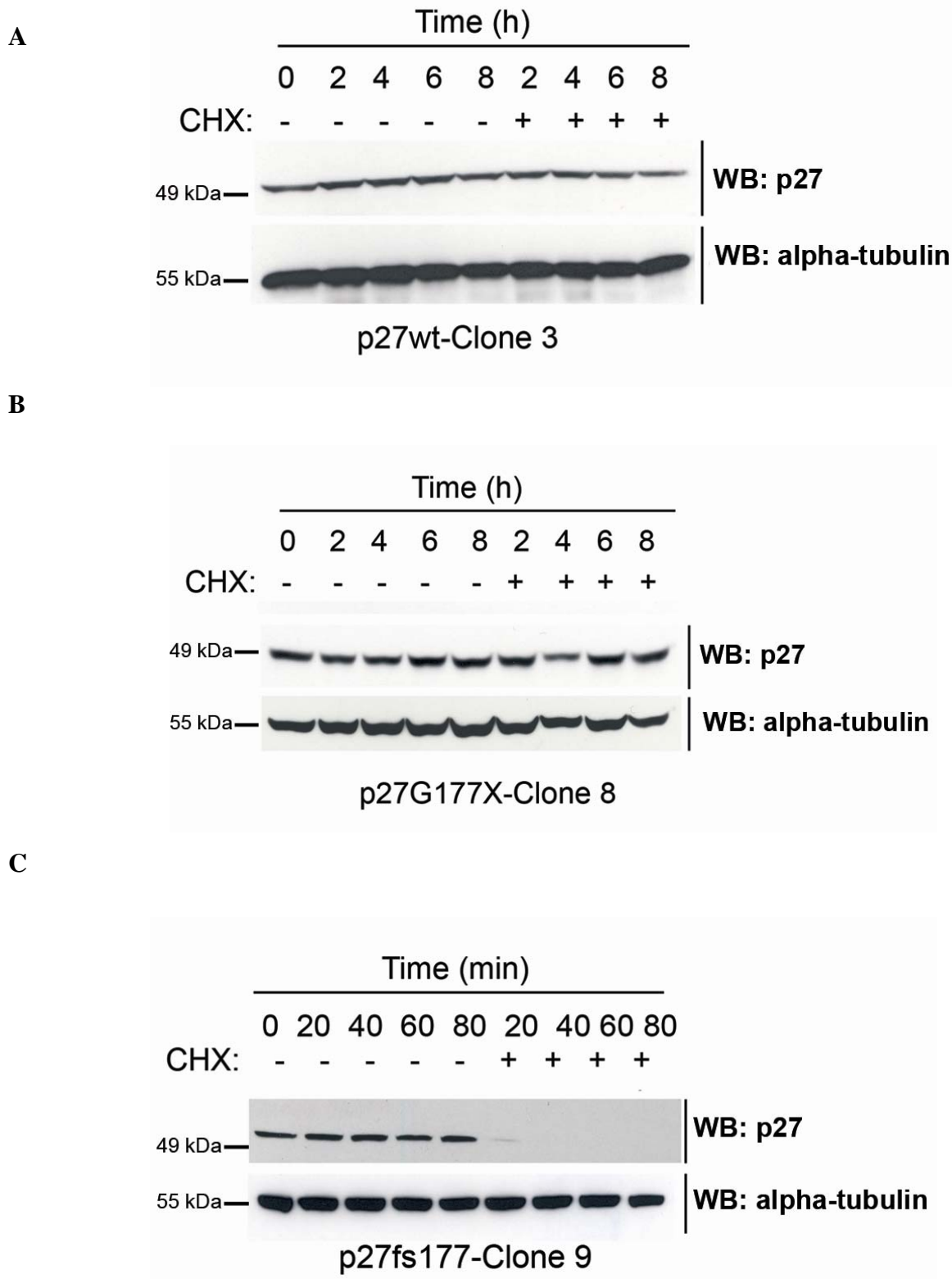


Fig.11 Stability of p27 proteins. Stably transfected (A) p27wt (clone3), (B) p27G177X (clone8) and (C) p27fs177X (clone9) were incubated with CHX (25 µg/mL) for the indicated times in complete medium. Western blotting (WB) only shows the exogenous p27 proteins. The membranes were also probed for alpha-tubulin to check equal loading.

The above experiments illustrated that p27fs177 is degraded very rapidly. Since p27wt is mainly degraded through the proteasome, we decided to check whether this is also the case for the degradation of p27fs177. Therefore, stably transfected p27fs177-clone 9 cells were incubated with CHX for 8h in the presence or absence of the proteasome inhibitor drug epoxomycin (EPOX) (Meng et al., 1999) to determine whether the proteasome mediates p27fs177 degradation. As shown in Fig.12, epoxomycin partially inhibits the degradation of p27fs177, although the protein level is not completely restored back to that of untreated cells. The efficacy of the epoxomycin treatment was confirmed by the increase of endogenous p27 expression levels. The experiments performed by the proteasome-inhibitor drug suggest that p27fs177 is degraded, at least in part, through proteasome-mediated proteolysis, just as wild-type p27.

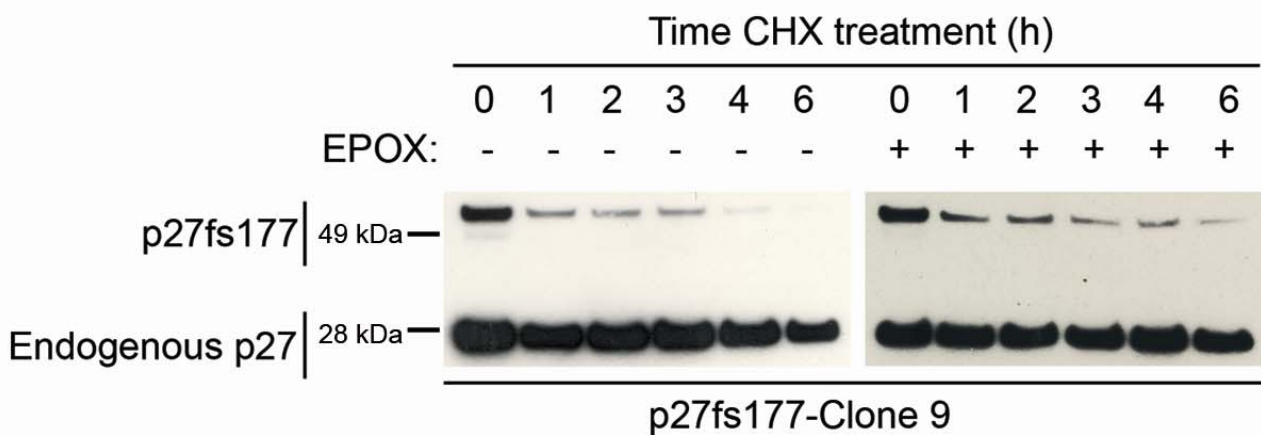
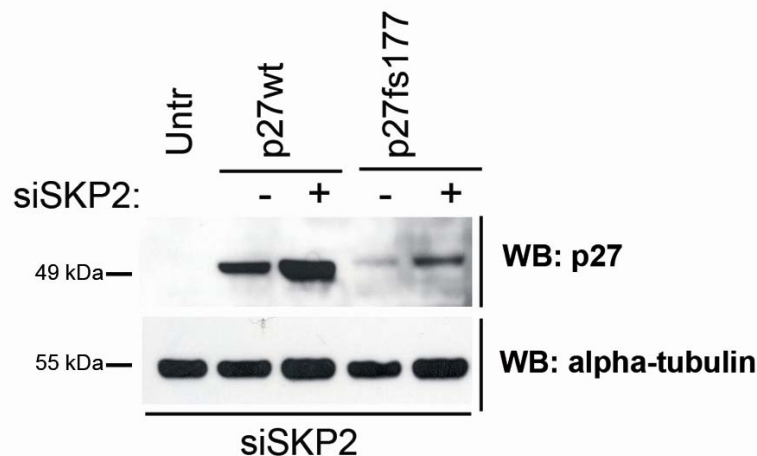


Fig.12 p27fs177 is degraded by the proteasome. Proliferating p27fs177-Clone 9 cells were treated with CHX (25 µg/mL) and epoxomycin (EPOX, +) or DMSO (-) for the indicated times. Expression levels of exogenous and endogenous p27 were shown by western blotting using anti-p27 antibody.

We previously showed (see Fig.9B) that p27fs177 is mainly a nuclear protein. As we mentioned, p27 is degraded in the nucleus by the Skp2-dependent SCF (Skp-cullin-f-box) E3 ligase. p27 phosphorylation at the threonine (Thr) 187 residue by cyclin E/Cdk2 is recognized by the SKP2 ubiquitin ligase, inducing p27 poly-ubiquitylation and subsequent degradation by the proteasome (Carrano et al., 1999). The p27fs177 protein does not possess the Thr187 residue (see Fig.7). Thus, it could be an interesting observation to determine whether Skp2 is also involved in degradation of the mutant p27fs177 protein through a pathway independent from the Thr 187 residue. To test this hypothesis, MCF7 cells were transfected with the p27wt

or p27fs177 and we reduced Skp2 expression by siRNA-mediated knock-down. As shown Fig.13A, reduction of Skp2 induced increasing level of both p27wt and p27fs177. Moreover, efficient knockdown of Skp2 was tested using different DNA concentrations of p27wt and p27fs177 plasmid (Fig.13B).

A



B

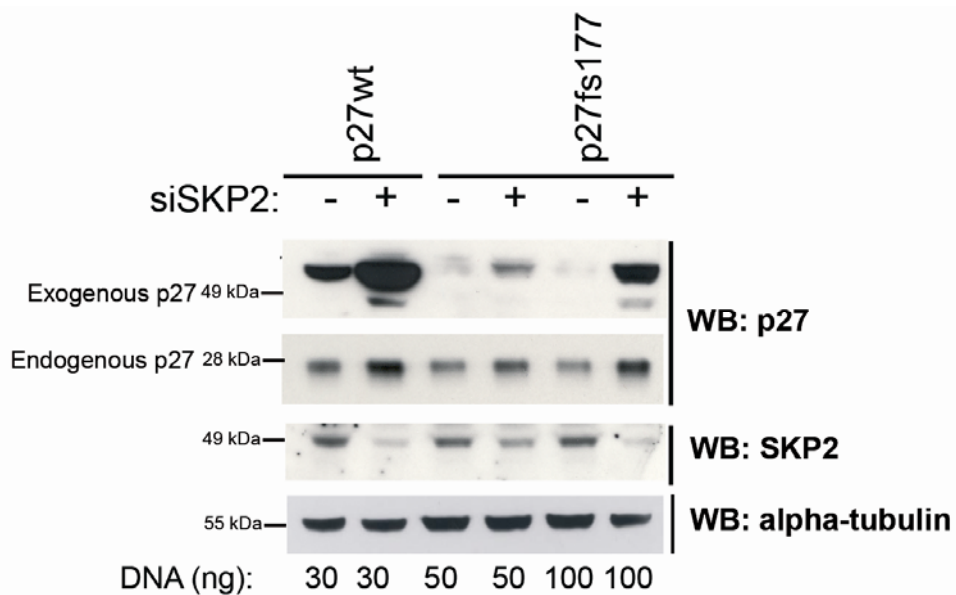


Fig.13 SKP2 regulates p27fs177 degradation. (A) SKP2 specific siRNA oligos were transfected in parallel with p27wt or p27fs177 in MCF-7 cell. Expression of p27 was assessed by western blotting (WB). The membranes were also probed for alpha-tubulin to check equal loading. (B) To test the efficiency of siRNA-mediated SKP2 knock-down, 50 ng or 100 ng p27fs177 plasmid were transfected with SKP2 siRNA same as A.

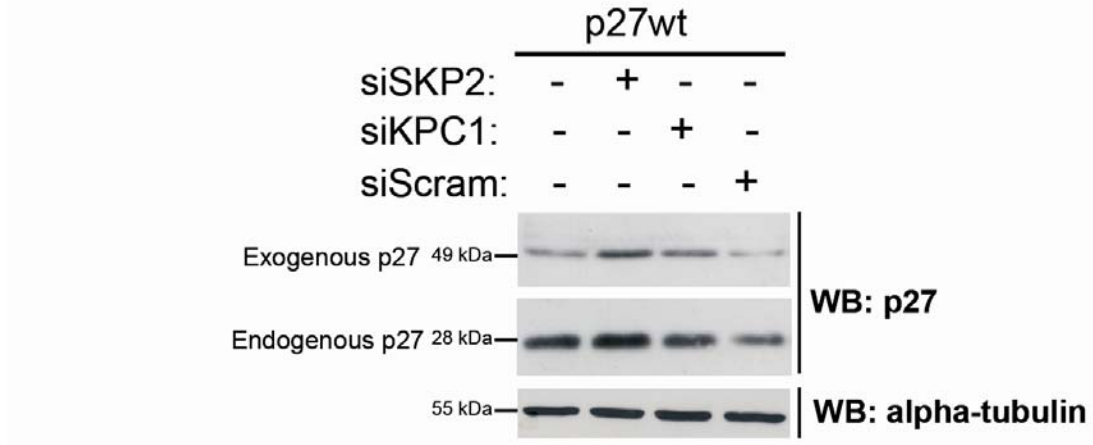


Fig.14 Scrambled siRNA has no effect on p27wt levels. siRNA oligos against SKP2, KPC1 or same amount of scrambled siRNA oligos were transfected in parallel with the p27wt plasmid in MCF-7 cells. Probing of the membrane by western blotting (WB) was done with anti-p27. The membranes were also probed for alpha-tubulin to check equal loading.

To attest the specificity of the effect of Skp2 siRNA, unspecific scrambled siRNA was used as a negative control and showed no effect on p27wt levels (Fig.14). In parallel, siRNA mediated knock-down of KPC1 was also included as positive control, since this ligase also induces degradation of p27wt. Thus, p27fs177 is still a substrate of the Skp2-SCF complex for ubiquitination despite the absence of the Thr187 residue.

The above findings demonstrate that p27fs177 is an unstable p27 mutant, at least in part, degraded by the proteasome, and also by SKP2-mediated mechanisms. Poly-ubiquitination is often a pre-requisite for proteasomal turnover and it is required for the degradation of p27wt. To test whether poly-ubiquitination is also required for p27fs177 degradation, we used a ubiquitin mutant that lacks its seven internal lysines (pUbr7) and thereby inhibits ubiquitin chain elongation allowing only monoubiquitination. pUbr7 was transfected together with p27wt or p27fs177 in MCF-7 cells. As shown in Fig.15, cotransfection of this mutant ubiquitin increased the steady-state abundance of p27wt (control) but not that of p27fs177. Therefore, polyubiquitination is required for p27wt but not for p27fs177 degradation. We speculated that p27fs177 may be directly degraded by the proteasome due to its altered conformation.

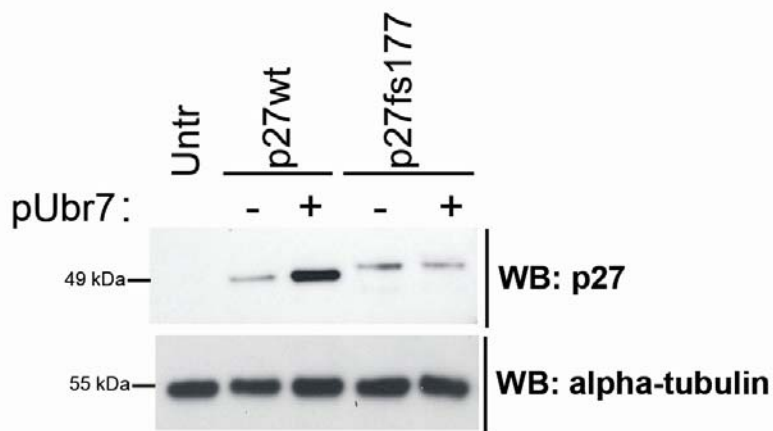


Fig.15 Poly-ubiquitination of p27fs177 is not required for its proteolysis. A ubiquitin mutant (pUbr7) was co-transfected without (Untr) or with the p27wt and p27fs177 in MCF7 cells. The expression of p27 was analyzed by western blotting (WB) of p27, in parallel with untransfected cells (Untr). The membranes were also probed for alpha-tubulin to check equal loading.

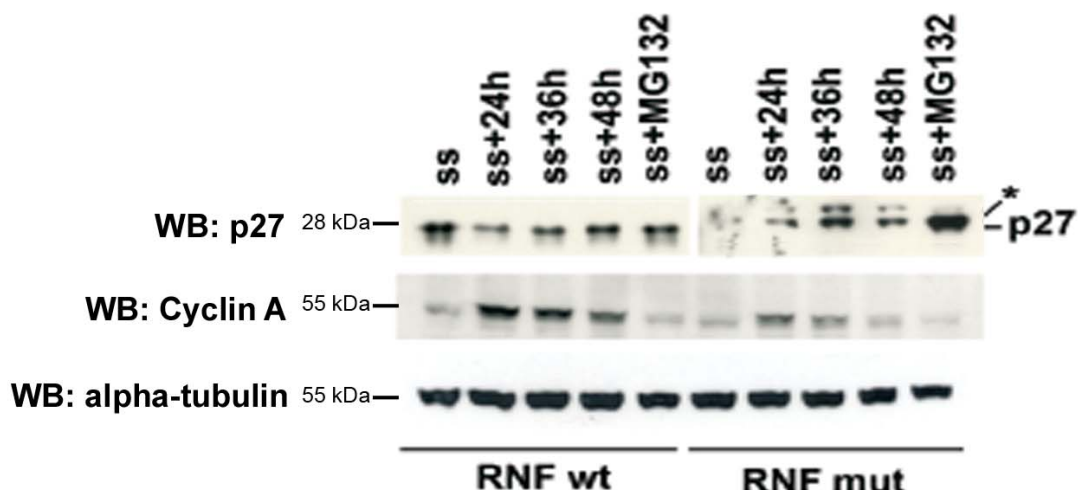
5.1.3. Instability of p27fs177 in primary rat cells

Ectopically expressed p27fs177 is more unstable than p27wt *in vitro*. To study the degradation of p27fs177 in a more physiological system, primary skin fibroblast cell lines from newborn wild-type (RNFwt) and mutant (RNFmut) MENX rat littermates were generated. To check whether the expression of p27 is normally regulated in these cells, serum-starvation and release experiments were performed. As shown in Fig.16A, the level of p27fs177 oscillated in RNFmut cells, but the protein could not be detected in serum-starved cells. The level of p27fs177 in quiescent RNFmut cells increased by adding the proteasome inhibitor MG132, indicating that proteasomal degradation is active also during this phase. Analysis of cyclin A (an S-phase cyclin) expression confirmed the progression of RNFs (both wt and mut) through the cell cycle.

To better understand the stability of p27fs177 in RNFmut cell, RNFs were treated with CHX and epoxomycin (+) or DMSO (-) for the indicated times (Fig.16B). In proliferating RNFmut cells, p27fs177 is degraded within minutes following treatment with CHX, and if we add epoxomycin (EPOX) it is stabilized. This indicated that endogenous p27fs177 is in part degraded by the proteasome. Therefore, the low level of endogenous p27fs177 protein in RNFs is caused by its rapid degradation mediated, at least in part, by the proteasome, as seen *in vitro*. The mutant p27 protein is even less stable in this more physiological system than

following transfection. In REFmut cells a nonspecific band migrating slower than p27fs177 can be observed at long exposure times, which is not affected by any treatment. In summary, these studies demonstrated that the p27fs177 mutant protein associated with the MENX syndrome is highly unstable *in vitro* and it is degraded in part through the proteasome.

A



B

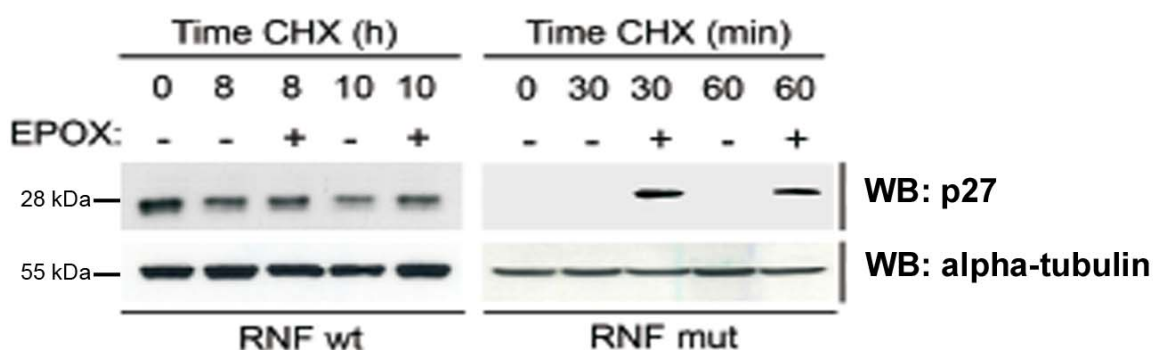


Fig.16 p27fs177 is highly unstable in primary rat fibroblasts. (A) RNFwt and RNFmut cells were incubated in medium with 0.1% FCS for 72hr (serum starvation=ss). Serum (10%) was then added and cells were collected 24h, 36h or 48h post-release from starvation. The 'ss+MG132' have represents cells treated with the proteasome inhibitors during the serum starvation. Western blotting (WB) were performed for p27 and cyclin A. The membranes were also probed for alpha-tubulin to check equal loading. The asterisk (*) indicates a non-specific band. (B) CHX were added on exponentially growing RNFwt or RNFmut in the presence or absence of EPOX.

5.2. Characterization of MENX-associated pituitary tumors

5.2.1. Macroscopic and histological analysis

To exploit the MENX model for preclinical studies *in vitro* and *in vivo*, it is necessary to fully characterize the neoplasms that the affected rats develop from the histological and immunohistological point of view. In this thesis, we focused on the multifocal pituitary tumors associated with MENX. In order to identify the histopathological features of the pituitary tumors that develop in rats affected by the MENX syndrome, macroscopic and histological analysis were performed on pituitary glands from wild-type and MENX-affected rats at different ages.

As shown in Fig.17A, rats homozygous for the MENX-associated *Cdkn1b* germline mutation develop multifocal pituitary neoplasms. The lesions begin from around 4 months of age as multiple nodules. Wild-type rats may spontaneously develop pituitary adenomas with age, but spontaneous tumors are typically small, single lesions, and they arise at much older age (>20 months). None of the wild-type animals showed pituitary tumors at age 10±2 months, as all mutant rats do. At the age of about 6 months, hyperplastic lesions merge in larger lesions and acquire the characteristics of a pituitary adenoma. By 8 months of age, all affected animals have macroscopically visible tumors (Fig.17B). Taken together, these results indicate that affected rat develop adenomatous tumors in the anterior lobe of the pituitary gland.

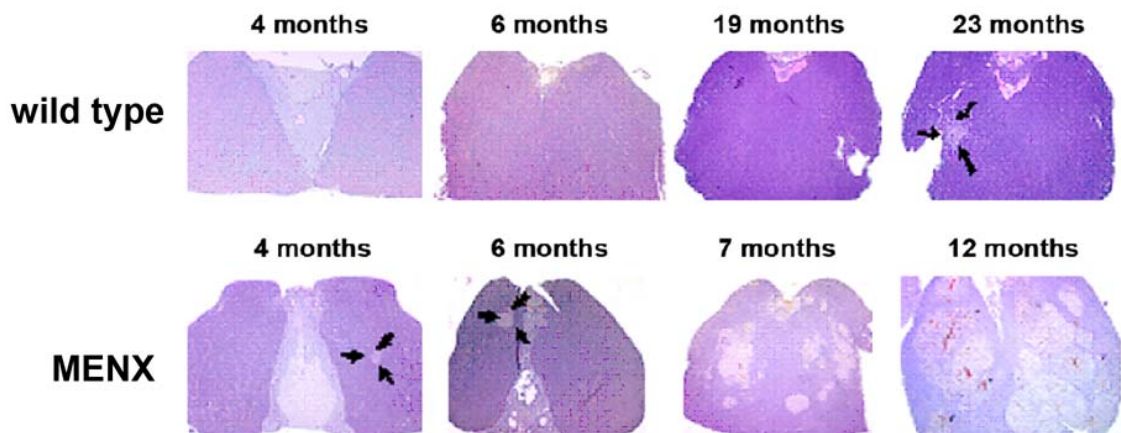
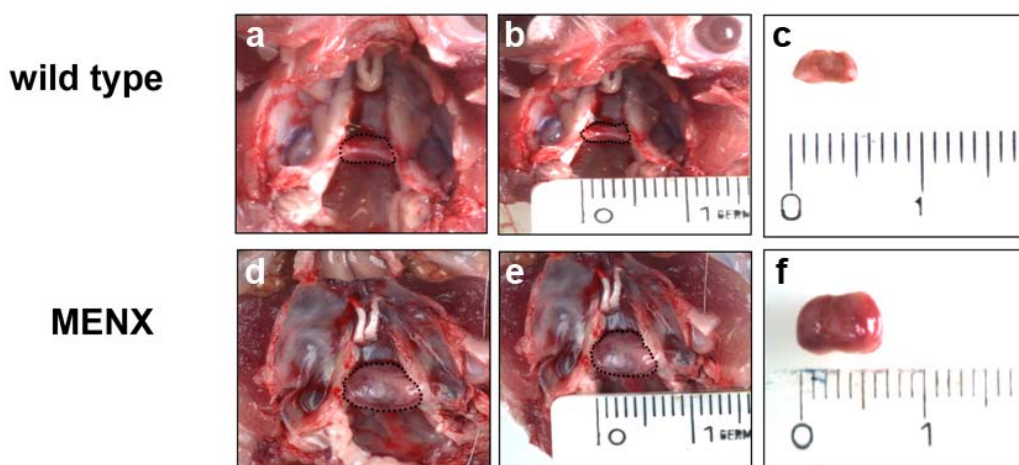
A**B**

Fig.17 Histology and dorsal photographs of pituitary gland. (A) Histology of pituitary glands of wild-type and mutant rats at different ages. Hyperplastic lesions in the anterior pituitary are visible in mutant rats staining at 4 months of age. Then, the lesions progress and by 6-8 months affected rats have multifocal, highly vascularized tumors. Normal animals may eventually develop spontaneous, single pituitary adenomas much later in life (Top panel). H&E staining original magnification: X25. (B) Dorsal photographs of representative in sellae (a,b,d,e) pituitaries or glands removed from the sella (c,f). Eight-month-old wild-type and homozygous mutant (p27^{mut/mut}) rats were sacrificed. Original magnification: $\times 2$.

5.2.2. Immunophenotype of the pituitary tumors

Human pituitary tumors are classified based on the hormone they secrete, if any. To better characterize the pituitary tumors of MENX rats, it is important to determine which hormone is secreted by the tumor cells. Therefore, we performed immunohistochemistry (IHC) for the expression of the pituitary hormones GH, PRL, ACTH, TSH β , FSH β LH β and α -subunit of glycoprotein hormone (α SU) on 55 individual pituitary lesions from 10 homozygous mutant rats. Most of tumor lesions could not express the PRL, GH and ACTH. However, α SU is expressed at high level in over 90% of cells in the lesions regardless of their size. Smaller lesions might occasionally show positivity for FSH β (29%), LH β (43%), and much less frequently PRL (17%). ACTH (5.8%) and GH (7.8%) are very rarely expressed in the neither big nor small lesions. The results of the immunohistochemistry are summarized in Fig.18.

In humans, gonadotroph nonfunctioning adenoma synthesize FSH β , LH β and also α SU (Snyder et al., 1985). To verify whether MENX-associated tumors are indeed gonadotroph tumors, we performed IHC for steroidogenic factor 1 (SF1), a marker of gonadotroph cell lineage.

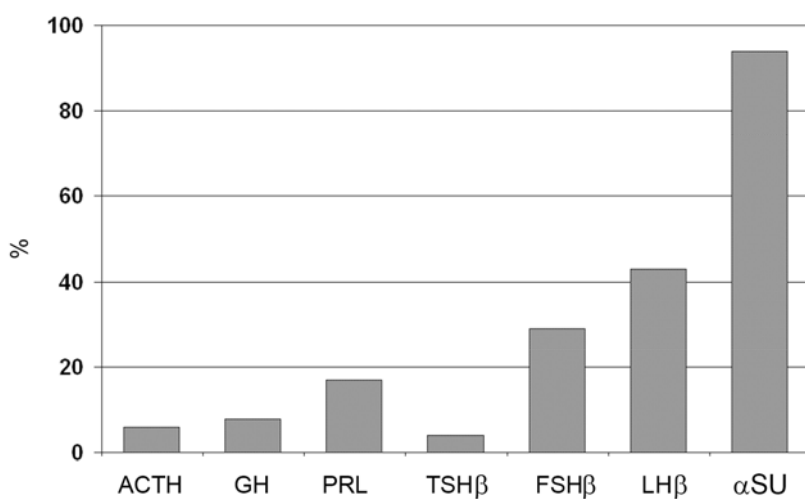


Fig.18 Expression of the pituitary hormones in mutant rats lesions. Immunohistochemical staining for the indicated hormones was performed on a total of 55 individual pituitary lesions from 10 mutant rats.

We observed strong nuclear staining with SF1 (Fig.19). SF1 is transcription factor that regulates the expression of the genes encoding α SU, LH β and FSH β . Thus, we performed IHC of α SU, LH β and FSH β in hyperplasia and adenoma having different SF1 expression level. We observed α SU, LH β and FSH β expressed in SF1 positive lesions of hyperplasia. However, as we mentioned previously, the big lesions (adenoma) expressed only α SU. Taken together, based on the hormone profiling and SF1 expression, the pituitary adenomas in MENX most closely resemble gonadotroph non-functioning pituitary adenomas.

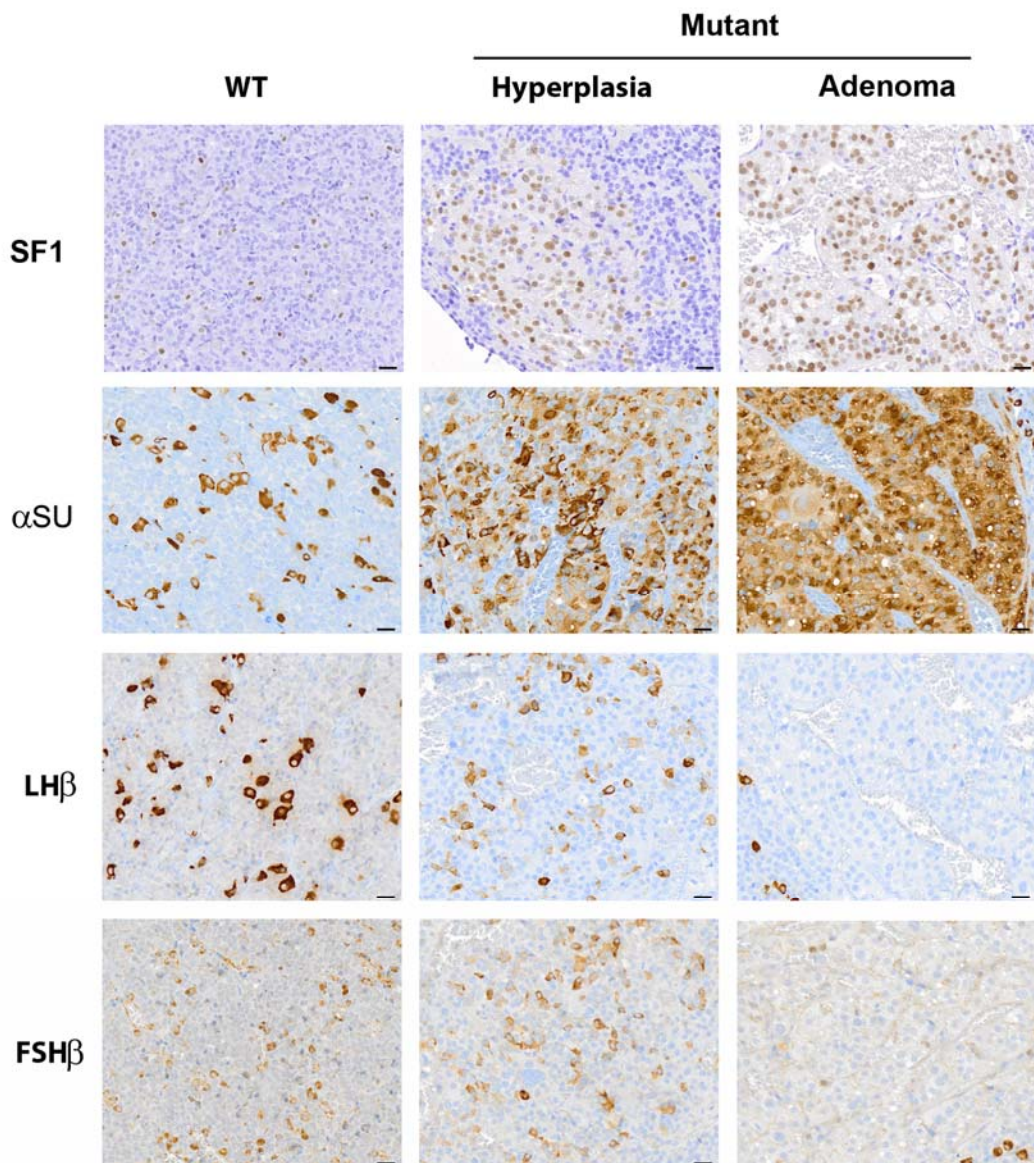


Fig.19 Expression of gonadotrope cell markers in normal pituitary tissue and rat pituitary lesions. Immunohistochemical staining was performed on tissues from 8 months old wild-type (WT) or mutant rats. Hyperplasia are composed of cells immunoreactive for α SU and, to a lesser extent, for LH β and FSH β . Bigger tumors express α SU but no other hormones. SF1 is expressed in every lesion. scale bar: 125 μ m.

5.2.3. Proliferative index of rat pituitary tumors

To precisely determine the proliferation rate of the rat pituitary tumors, immunohistochemical staining for the Ki-67 antigen, which is found in growing and dividing cells but that is absent in the resting phase of cell growth, was performed. As shown in Fig.20, hyperplasia and tumor showed higher Ki-67 immunoreactivity than pituitary tissues of wild-type rats. High levels of Ki-67 indicate a highly proliferative tumor and usually predict a poor prognosis, thus making of Ki-67 an important tumor marker. Automated quantification of the number of Ki-67 positive cells was obtained using a slide scanner and commercially available software. The proliferation rate of the individual lesions varies within and among pituitary glands, and has a range from 1% to 21%. Together with the hormone immunophenotyping, these data suggest that MENX-associated pituitary adenomas are similar to aggressive non-functioning pituitary adenoma of gonadotroph origin.

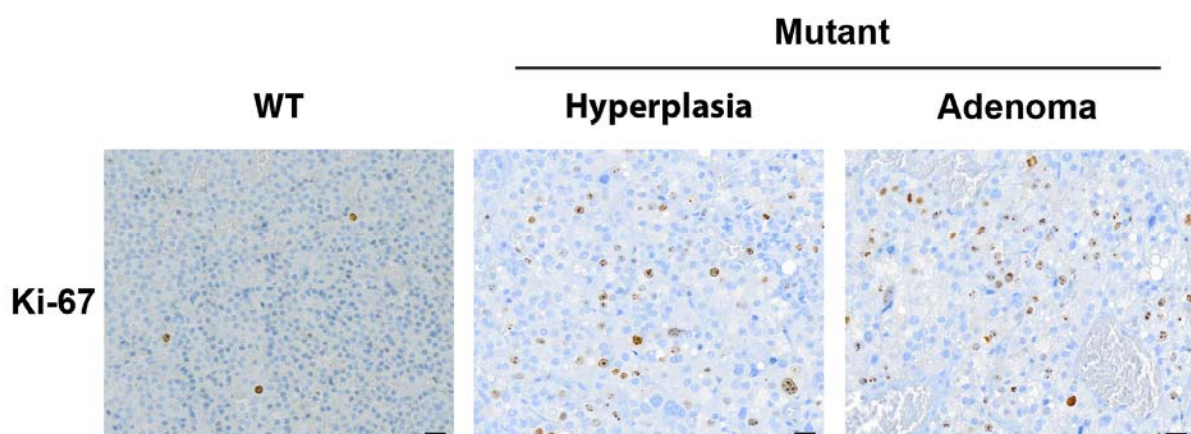


Fig.20 Expression of the Ki-67 antigen in normal pituitary tissue and rat pituitary lesions. Immunohistochemical staining was performed on tissues from 8 months old wild-type (WT) or mutant rats. The proliferation rate increases with tumor progression. scale bar: 125 μ m.

5.3. MENX as a preclinical model to evaluate compounds with therapeutic activity against neuroendocrine tumors

5.3.1. Establishing a protocol to obtain single pituitary primary cells from MENX

In order to perform therapy-response studies *in vitro*, a mechanic and enzymatic disaggregation protocol was optimized to obtain single primary cells from pituitary tumors of MENX rats (see detail in Methods) (Fig.21A). Continuous monitoring of the cells for the following 5 days demonstrated that using this protocol most cells attached to the plates and were viable (Fig.21B). To determine whether the cells survive and grow *in vitro*, pituitary primary cells from MENX cultured in complete medium (10% FCS) were employed for growth curves over a period of 4 days. In contrast to established cell lines, primary cells were not proliferating and their number remained constant over time. Primary cells could survive at the most one week in culture.

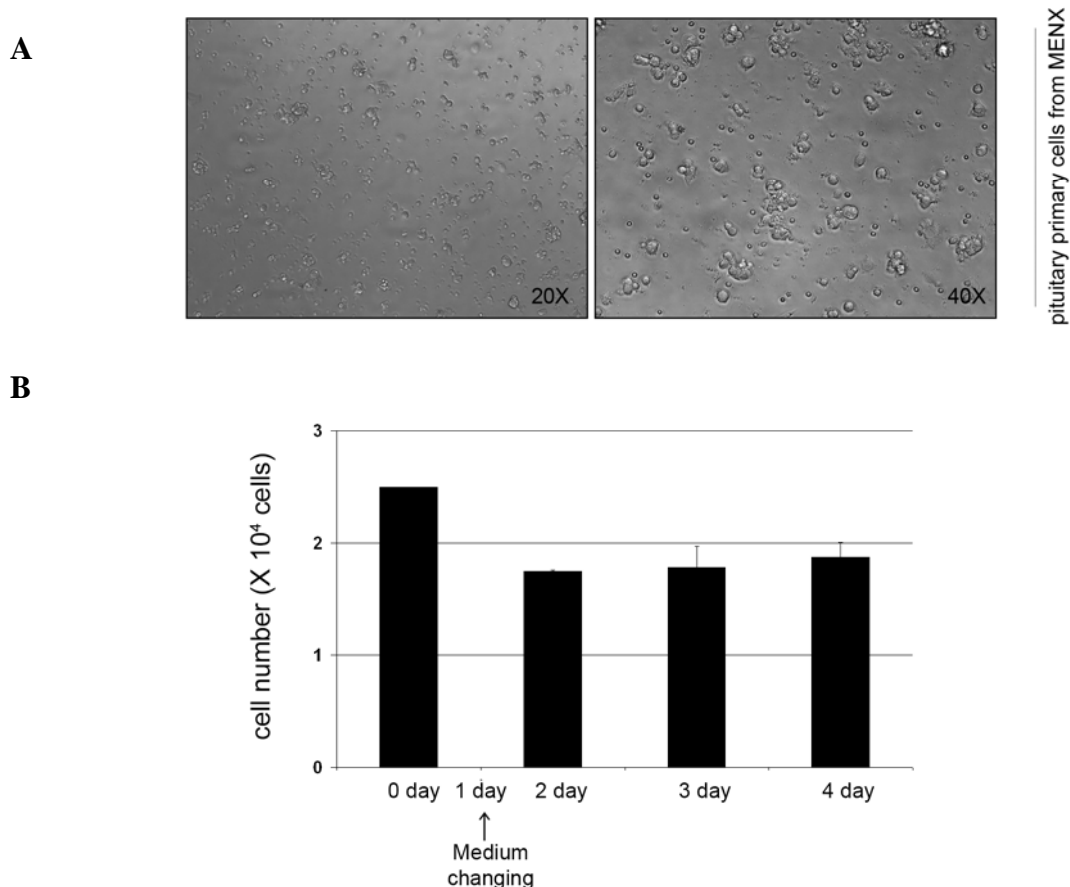


Fig.21 Pituitary primary cell cultures. (A) Picture of primary pituitary cells. Cells from pituitary of an affected MENX rat after 48 hours in culture with complete medium. (B) Growth curves of primary cells. For 4 days, cells were counted after trypan blue staining to exclude dead cells. Values are the mean of 3 independent experiments \pm SD.

5.3.2. Receptor profiling of pituitary primary cells from MENX

Since somatostatin/dopamine receptors are expressed at highly variable levels within and between pituitary tumor subtypes, the somatostatin receptor (*Sstr* subtypes 1,2,3,5) and dopamine receptor (*Drd2*) gene expression profile was determined in pituitary tumor cells in primary cultures and compared with the profile of pituitary cultures obtained from wild-type rats. These genes were amplified using specific real-time quantitative RT-PCR (qRT-PCR) primers and probes. *Sstr4* was not included in the analysis as it has been shown that this receptor subtype is not expressed in most pituitary tumors. All the above genes are expressed at detectable levels in both culture types (tumor and normal). When we compared the results obtained analyzing the mutant rats with the wild-type ones, higher expression of *Sstr2* and *Sstr3* in tumor cells was observed compared to normal pituitary cells, while expression of *Sstr5* was lower in cultures of mutant cells and *Drd2* was expressed at similar level in both culture types (Fig.22A).

To verify whether there is a correlation between the level of *Sstrs* mRNA and that of the encoded proteins, IHC was performed on the pituitaries of 4 mutant rats. In parallel, normal pituitary tissue from wild type rat was stained as a control. Only anti-*Sstr2* antibody gave specific staining, while the antibodies against *Sstr1,3* and *5* showed no signal or high background in both normal and tumor rat tissues. As shown in Fig.22B, we found positive *Sstr2* staining in some lesions having high mRNA expression of *Sstr2* by qRT-PCR (> 5 folds vs. wild type). Interestingly, there was more frequent and stronger expression of *Sstr2* in small lesions in MENX mutant rats, while most of the big lesions lost the expression of the SSTR2 receptor.

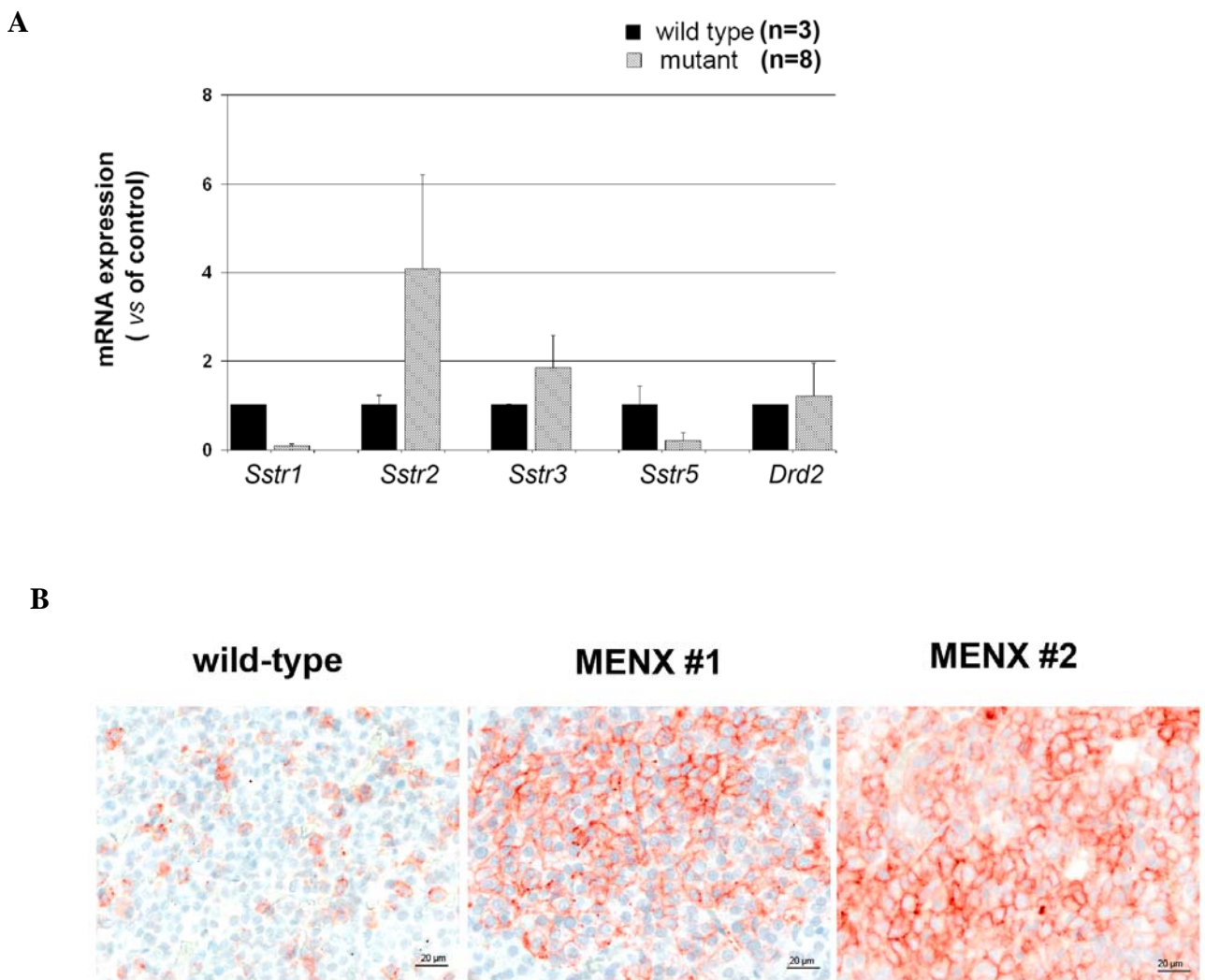


Fig.22 Expression of the somatostatin receptors and dopamine receptor in pituitary cells from wild type and mutant rats. (A) Primary cells from wild-type (control, n=3) and mutant rats (n=8) were incubated with normal medium (10% FCS) for 24 hours and then RNA was extracted RNA. We performed qRT-PCR using primer and probe sets specific to rat *Sstr2*, *Sstr3*, *Sstr5* and *Drd2*. (B) Immunohistochemical staining of *Sstr2* was performed on pituitary tissue from wild-type and mutant rats (MENX). scale bar: 20 μ m.

5.3.3. Effect of somatostatin-related drugs on the viability of rat primary pituitary cells

The observation that neuroendocrine cells usually express somatostatin receptors (Sstr subtype 1 through 5) and dopamine receptors has lead to the clinical use of somatostatin analogues (SSA) and somatostatin-dopamine chimeric molecules (dopastatin) for the treatment of neuroendocrine tumors. Since the mRNA expression of somatostatin and dopamine receptors was detectable in the pituitary tumor cells from MENX rats, primary pituitary cultures were treated with SSAs (octreotide, SOM230) and dopastatin (BIM23A760). The functional characteristics of the drugs are the following: octreotide is a SSA that binds preferentially Sstr2 and it is used to treat acromagalic patients (GH-producing pituitary adenoma); SOM230 is a multiligand SSA that binds to Sstr1,2,3 and 5; BIM23A760 is a chimeric compound having both SSA and dopamine agonist properties. Previous studies showed that pituitary primary cells from MENX mutant rats do not grow, thus effect of treatments were measured by assessing cell viability. When a reduction in cell viability of at least 20% compared to control was observed, the culture was considered a “responder” to the drug, otherwise it was considered “nonresponder”. A cut-off of 15%-20% is commonly used in this type of studies (Zatelli et al., 2007b). Treatments were performed for all compounds using a range of concentrations based on studies on primary cells from human patients or on pituitary tumor cell lines (i.e. GH3 cell): octreotide, from 1 pM to 100 pM; SOM230, from 10 pM to 1 nM; BIM23A670, from 10 pM to 1 nM.

The GH3 pituitary adenoma cell line shows a reduction of cell proliferation after octreotide treatment at low concentration (Hubina et al., 2006). As shown in Fig.23A, treatment with octreotide reduced cell viability in 6 out of 11 cultures at 1 pM (-30% cell viability vs. control, $P<0.05$) and also 10 pM (-21%, $P<0.05$). In agreement with GH3 cell, octreotide showed significant reduction of cell viability at lower and not higher concentration.

SOM230 is capable to bind to multiple somatostatin receptor subtypes (Sstr1, 2, 3 and 5), closely mimicking the action of natural somatostatin. However, in primary cell cultures from MENX pituitary tumors, SOM230 induced 30% reduction of cell viability in 3 out of 11 primary cultures ($P<0.05$) (Fig.23B). The treatment with SSA/DA chimeric compound BIM23A760 reduced the cell viability in 3 out of 11 rat tumor cultures (dose 100 pM: -23% cell viability, $P<0.05$), like SOM 230 (Fig.23C).

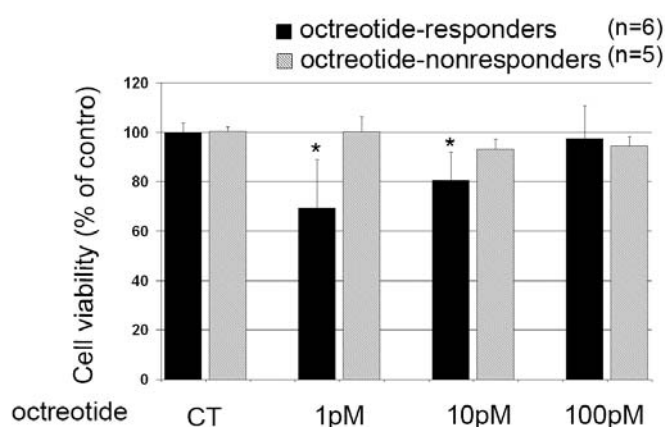
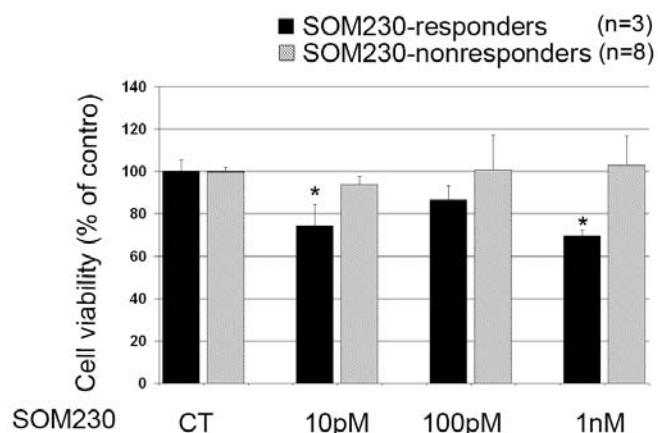
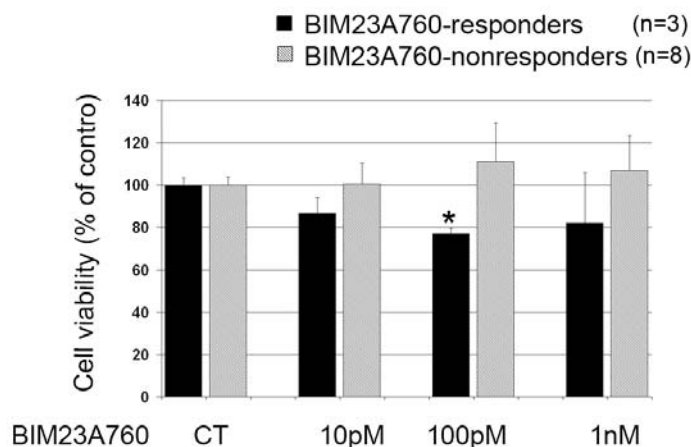
A**B****C**

Fig.23 Cell viability of primary pituitary tumor cells after treatments. Primary rat pituitary cells from MENX mutant rats were incubated in 96 well plates for 48h in culture medium supplemented with increasing concentrations of octreotide (A) from 1 pM to 100 pM, SOM230 (B) from 10 pM to 1 nM, and BIM23A760 (C) from 10 pM to 1 nM. Control cells were incubated with vehicle solution (CT). Data from primary cultures are evaluated independently with six replicates each and are expressed as the means \pm SD. *, P<0.05 versus CT.

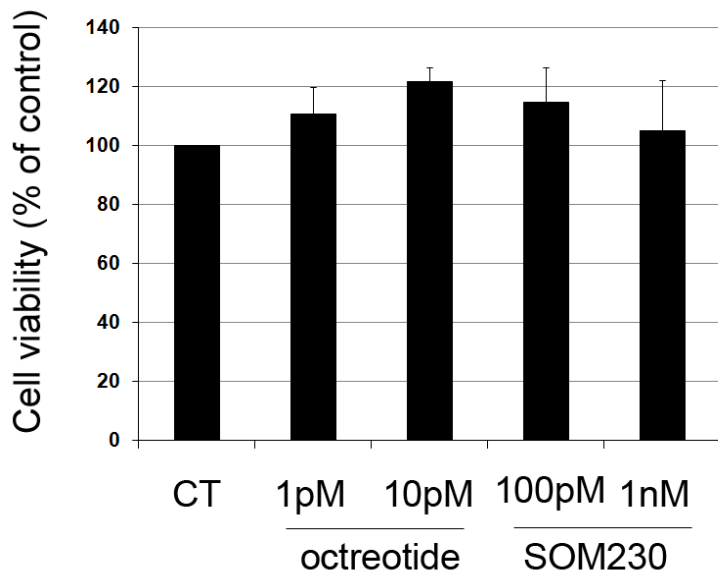


Fig.24 Cell viability of primary normal pituitary cells after treatments. Primary rat pituitary cells form wild-type rats ($n=3$) were incubated in 96 well plates for 48h in culture medium supplemented with increasing concentrations of octreotide (1 pM and 10 pM), SOM230 (100 pM and 1 nM) or vehicle solution (CT). Data from primary cultures are evaluated independently with six replicates each and are expressed as the means \pm SD.

In contrast to the human pituitary tumor samples which are mostly devoid of normal cells, the rat pituitary glands invariably contain a proportion of non-tumoral cells. To exclude the potential influence of non-tumoral cells included in rat tissue samples on the response of the tumor cells to the various compounds, pituitary primary cultures from three wild-type rats were treated with octreotide and SOM230 and showed no response (Fig.24).

Moreover, the pituitary glands of 7 mutant rats with tumors were cut in half: one part was used for establishing primary cultures and the other part was fixed in formalin and embedded in paraffin for histological examination. In addition to the H&E staining, we performed IHC for the α -subunit hormone, which is expressed in all pituitary lesions in MENX mutant rats. The percentage of tumor and non-tumoral regions in each gland was automatically determined (Fig.25). The results showed that the tumor regions vary among individual rats ranging from 15 to 65% (Table.10). However, in our hand, there was no significant relationship between drug response and percentage of tumor region. Therefore, taken together, these results indicated that the amount of non-tumoral endocrine cells is not likely to affect the response of the tumor cells to the drug treatment. Normal pituitary cells behave as an inert population concerning drug treatment.

Table.10 Tumor areas in pituitary tissues of 7 individual rats

# of MENX rats	Sex	Tumor area
688	Female	32%
728	Female	15%
818	Female	19%
835	Female	65%
743	Male	29%
760	Male	60%
819	Male	45%

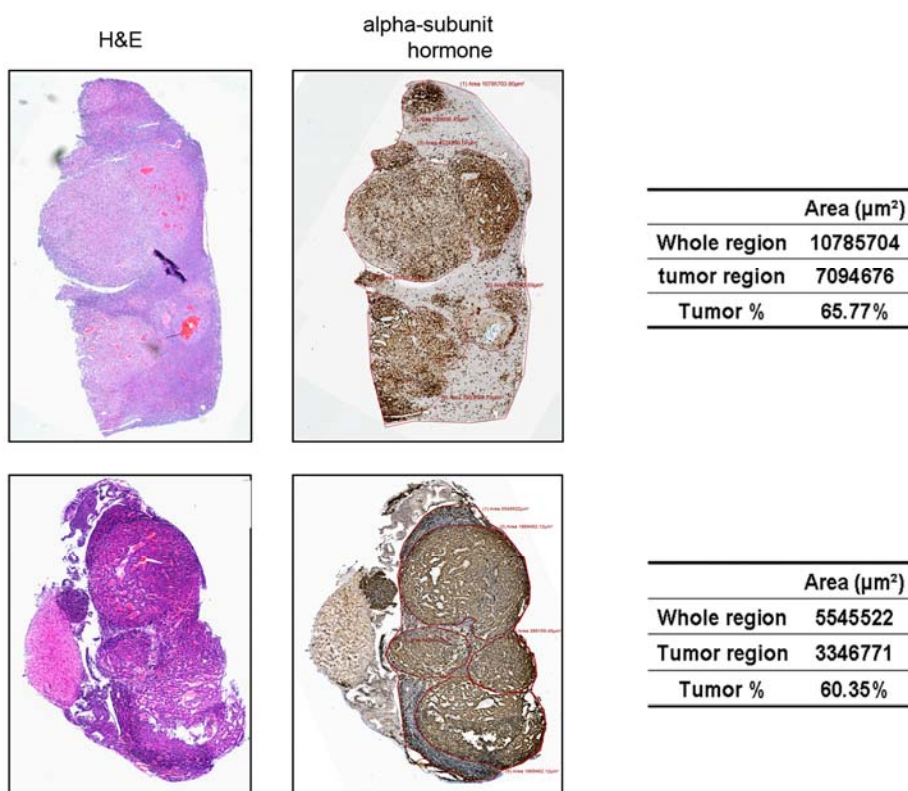


Fig.25 Tumor and normal areas in pituitary tissues from MENX mutant rats. (A) We performed hematoxylin and eosin staining and immunohistochemistry on paraffin-embedded pituitary tissues from mutant rats using an antibody against the α -subunit of glycoprotein hormones (1:1000) and hematoxylin as counter stain. Images of tissue slides were acquired with an automatic high-resolution scanner (dotSlide System; Olympus). Area measurement was carried out using dotSlide software (Olympus).

5.3.4. Correlation of response to SSA with somatostatin receptor expression

Ligand/agonist binding was reported to upregulate G protein-coupled receptors (GPCRs) (Filtz et al., 1994; Zhang et al., 1994), including somatostatin receptors (Bruno et al., 1994; Hukovic et al., 1999). However, no significant changes were observed in *Sstr2,3* and *Drd2* mRNA levels following treatment with all three SSA or chimeric compounds, while there was a slight increase in *Sstr5* mRNA expression following octreotide and SOM230 treatment (Fig.26).

In human pituitary adenoma, response to SSA is related to the expression of the somatostatin receptors (Zatelli et al., 2007a). To determine whether the response of the rat primary cultures to octreotide or SOM230 might also be associated with the level of receptors, mRNA expression of somatostatin or dopamine receptors between responder and non-responder primary cultures were compared by qRT-PCR. We observed no significant correlation between *Sstr2,3* and *Drd2* mRNA expression and reduction in cell viability following octreotide treatment. Interestingly, a significant negative correlation was found between *Sstr5* mRNA level and reduction of cell viability after octreotide (Fig.27A). No significant difference in *Sstrs* and *D2dr* mRNA levels was observed between SOM230 and BIM23A760 responder and nonresponder cultures (Fig.27B and C). In summary, *Sstr5* mRNA expression level might be a candidate marker of the response to SSA in our animal model.

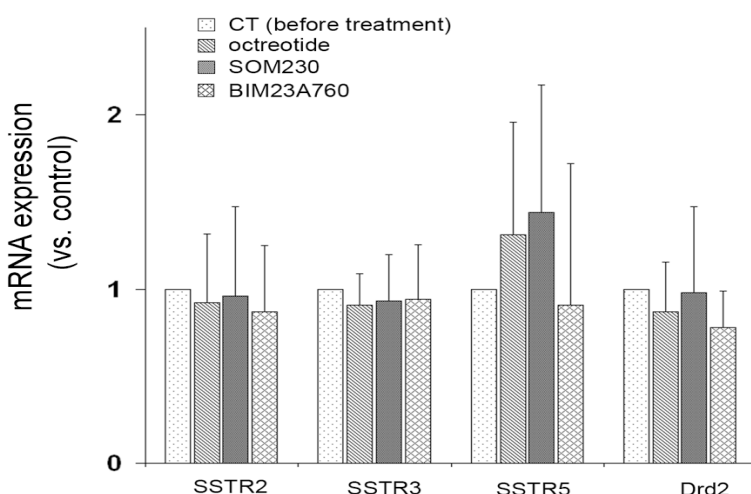


Fig.26 mRNA expression level of *Sstrs* and *Drd2* genes before and after treatments. qRT-PCR were performed using primary cells from MENX mutant rats (n=8) incubated with vehicle solution (CT) with the indicated compounds (octreotide, SOM230 or BIM23A760) for 24h. Values reported are normalized against the untreated control (CT). Data from primary cultures are expressed as the means \pm SD.

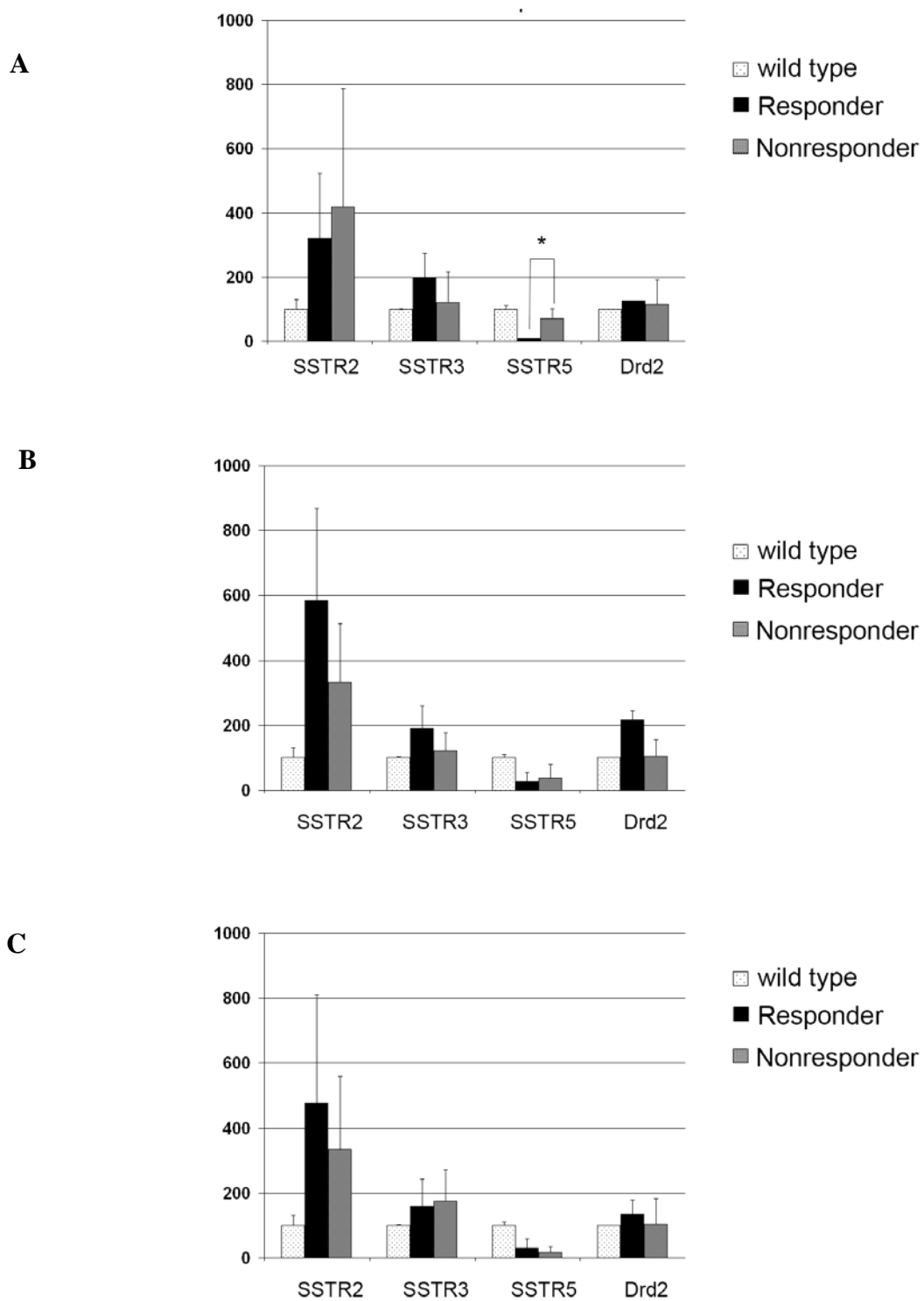


Fig.27 Comparison of the expression level of *Sstrs* and *Drd2* genes between responder and non-responder primary pituitary tumor cultures. Primary cells from wild-type (control) and mutant rats were incubated with different compounds; octreotide (A), SOM230 (B) or BIM23A760 (C) for 24 hours. Total mRNA was extracted and the qRT-PCR was performed using primer and probe sets specific to rat *Sstr2*, *Sstr3*, *Sstr5* and *Drd2*. The values are normalized against the wild-type. Data are expressed as the means \pm SD. *, P<0.05 versus nonresponder.

5.3.5. Overactivation of the PI3K/mTOR/AKT pathway in rat pituitary tumor cells

To assess whether high AKT phosphorylation levels, indicative of PI3K pathway overactivation was happening in rat pituitary tumors, western blotting for total AKT and phosphorylated AKT (p-AKTS473) expression was performed using protein extracts from primary cells established from mutant and wild-type rats (Fig.28A). The amount of phosphorylated AKT was higher in mutant compared to wild-type pituitary primary cells. To confirm this finding, we also determined the average intensities measured by band densitometry, using western blotting with lysates from 2 wild-type and 4 mutant pituitary primary cultures for phosphorylated AKT and total AKT. The average of phosphorylated AKT levels in mutant rats ($n=4$) is 1.5 folds that in wild-type rats ($n=2$) (Fig.28B).

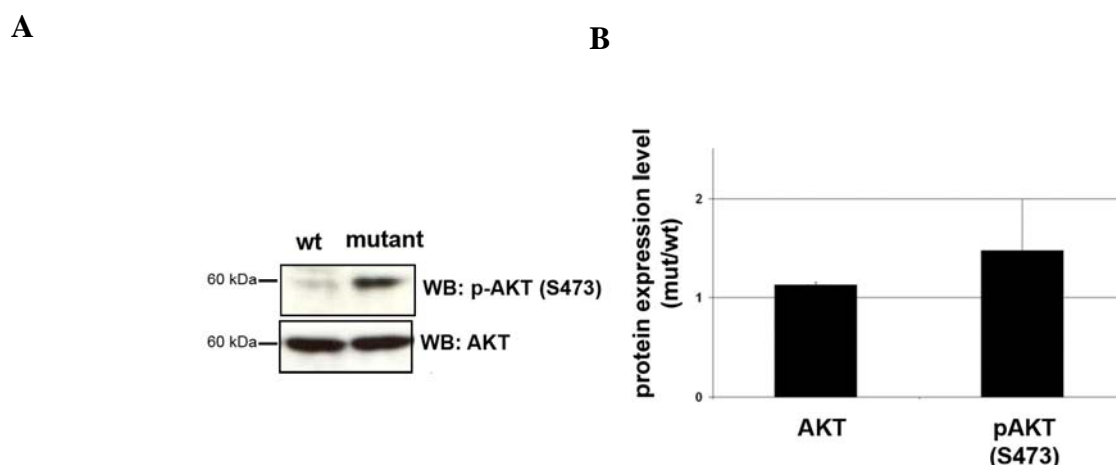


Fig.28 Expression of p-AKT and total AKT in primary cells from wild-type and MENX rats. (A) Protein lysates from primary rat pituitary cells from wild-type (wt) and mutant rats were used for western blotting with anti-pAKT (S473), anti-AKT. (B) Diagrams were obtained by band densitometry. Data are expressed as the means \pm SD.

To confirm these finding, IHC was performed with antibodies against both forms of AKT (total and phosphorylated) on pituitary tissues from adult mutant rats (bearing tumors) and age-matched wild-type controls. In agreement with the western blotting results, normal and tumor areas in mutant rats showed similar expression of total AKT, while cytoplasmic immunostaining for phosphorylated AKT (p-AKTS473) was stronger in pituitary tumor lesions than in normal adjacent tissue (Fig.29A). As shown in Fig.29B, IHC was also performed on pituitary glands from unaffected rats (control), which expressed total AKT but no phosphorylated AKT. This suggests that AKT signaling is activated in MENX-associated pituitary adenomas similarly to what happens in human NFA patients.

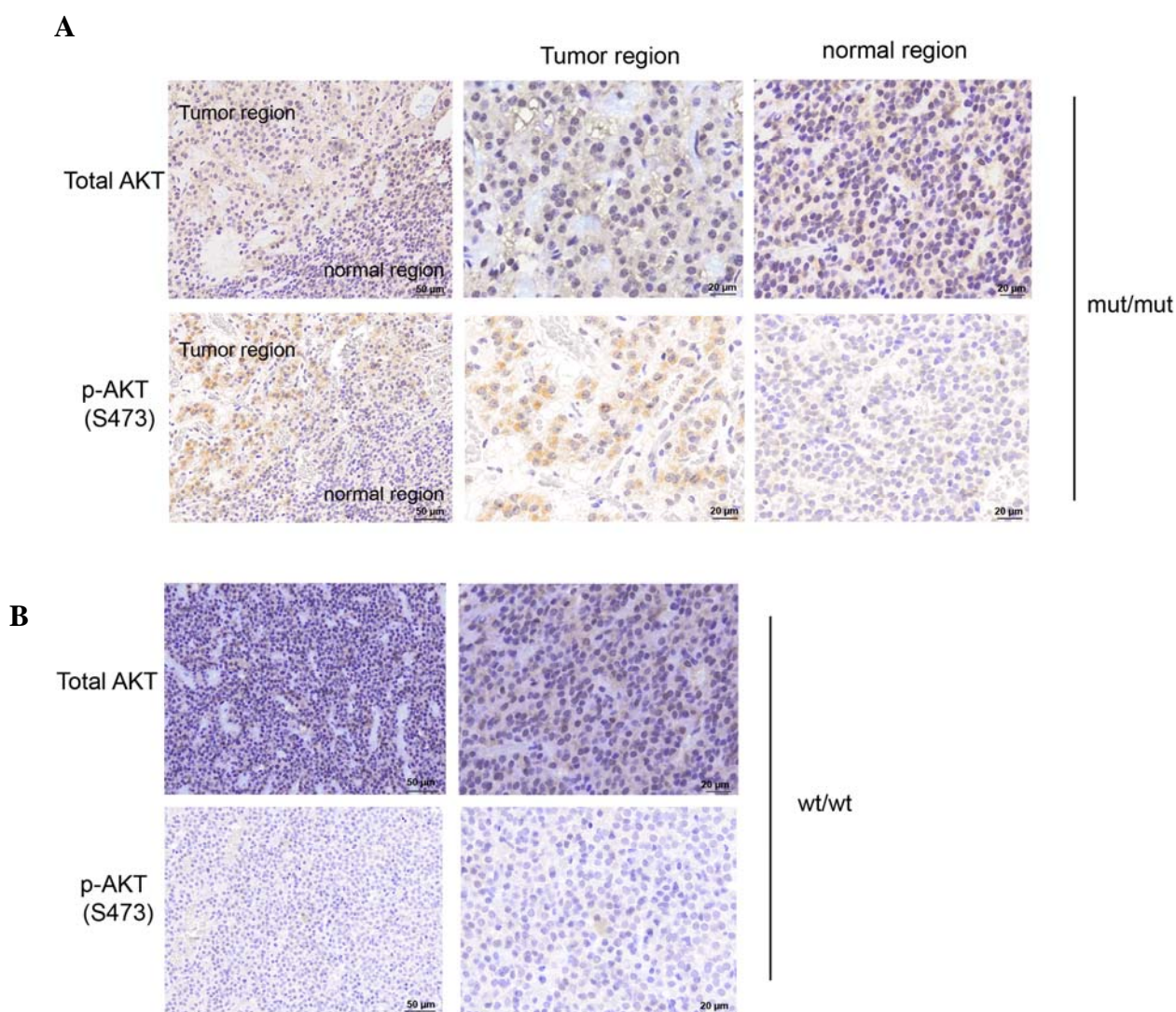


Fig.29 Expression of p-AKT and AKT in pituitary tissues from wild type and MENX rats. Immunohistochemistry was performed a paraffin-embedded pituitary tissues from mutant rat (A) and wild-type rats (B) using p-AKT(S473) (1:30) antibody, AKT (1:30) antibody, and counterstained with hematoxylin. scale bar: indicated in each figure.

5.3.6. Effect of RAD001 and NVP-BEZ235 in rat pituitary tumor cells

Since we identified a overactivation of the AKT pathway in the pituitary tumors of mutant rats, primary cultures from these lesions were treated with RAD001. As shown in Fig.30A, RAD001 caused a dose-dependent reduction in cell viability which reached statistical significance at the 100 nM concentration (-36% ; $P < 0.01$ vs. control) in 5 out of 11 primary cultures. To verify whether treatment of MENX-derived pituitary tumor cells with RAD001 indeed affects the mTOR/AKT pathway, the expression of the phosphorylated form of AKT and of S6, a kinase downstream of mTOR was determined in primary cells from one mutant rat. We observed a dose-dependent inhibition of S6 phosphorylation (Fig.30B). Interestingly, we found an increase in the expression level of phosphorylated AKT in primary pituitary tumor cells after RAD001 treatment.

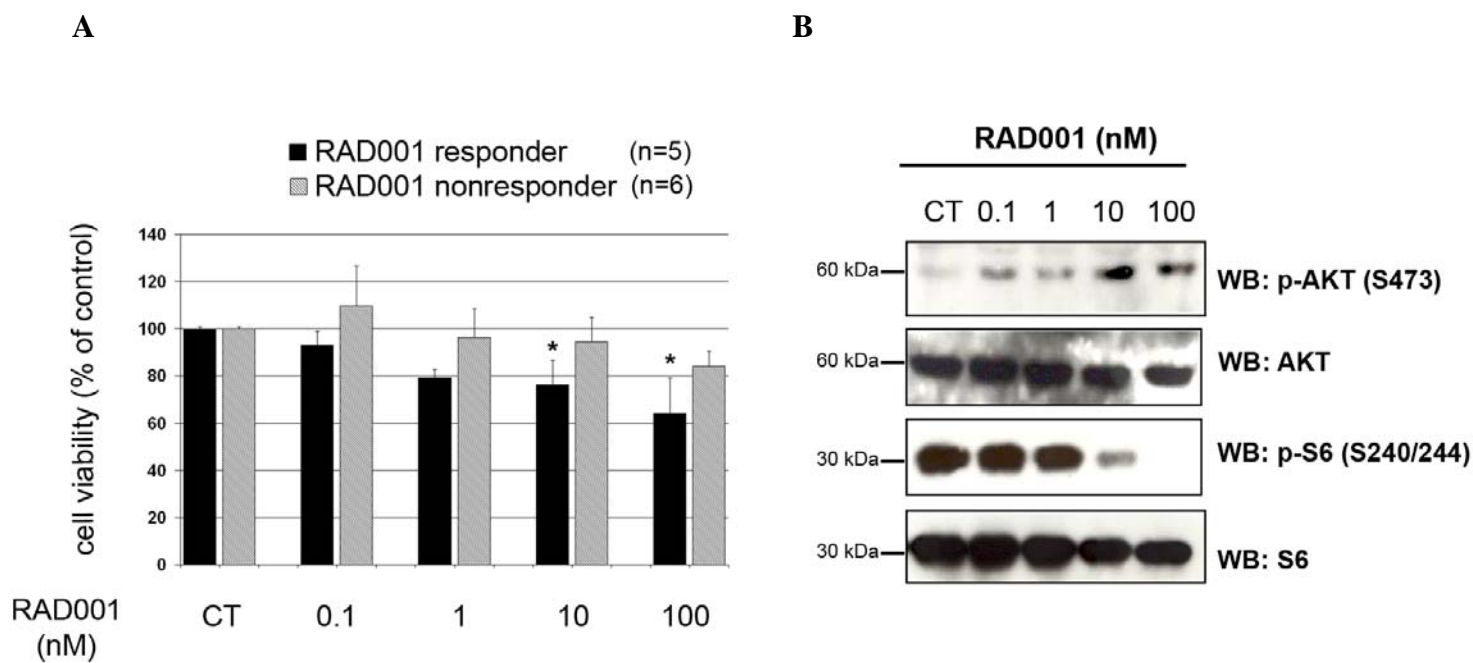


Fig.30 Effect of the single mTOR inhibitor RAD001 on the primary cells from MENX mutant rats. (A) Primary rat pituitary cells were incubated for 48 hr in culture medium supplemented with RAD001 (dose from 0.1 nM to 100 nM) or vehicle solution (CT). Data from primary cultures are evaluated independently with six replicates each and are expressed as the mean \pm SD. *, $P < 0.05$ versus CT. (B) Protein lysates from primary cells after RAD001 treatment for 24h were used for western blotting with anti-pAKT (S473), AKT, pS6 (S240/244) and S6.

To prevent AKT activation following single mTOR inhibitor, pharmaceutical research has recently developed a new class of compounds, including NVP-BEZ235 (Maira et al., 2008), that inhibits both mTOR and the upstream PI3K kinase, thus preventing the feedback loop. In contrast to RAD001, incubation with the dual PI3K/mTOR inhibitor NVP-BEZ235 reduced cell viability up to 25% at the 10 nM concentration ($P < 0.001$ vs. control) and up to 37% at 100 nM ($P < 0.001$ vs. control) in all (10/10) the primary tumor cultures tested (Fig.31A), making this compound the most effective in our experimental model. To identify whether NVP-BEZ235 treatment reduces cell viability inducing apoptotic cell death, we measured caspase-3/7 activity, as marker of apoptosis. Incubation with NVP-BEZ235 for 24h induced the caspase-3/7 activity (+24% vs. control), suggesting that this drug reduced the cell viability of MENX rats primary cultures, at least in part, by promoting apoptosis (Fig.31B)

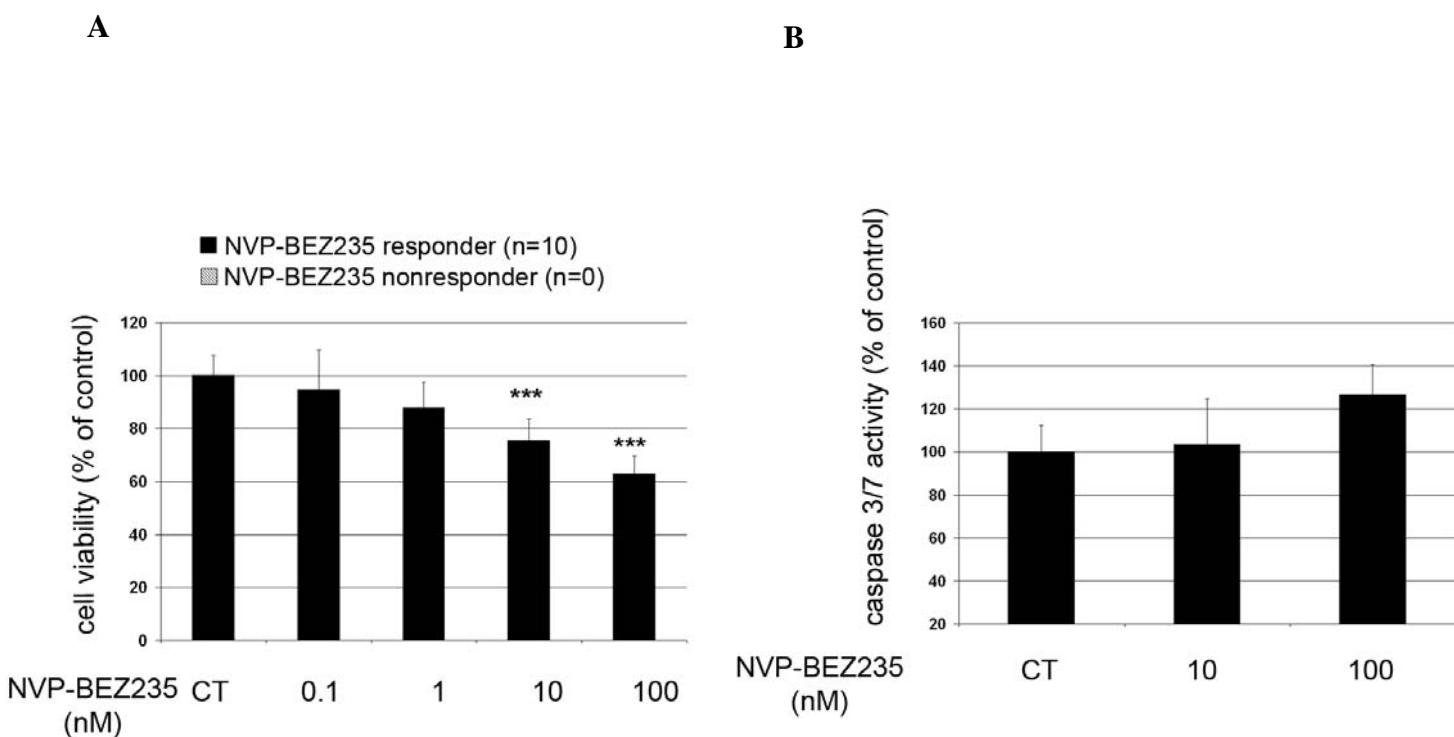


Fig.31 Effect of dual PI3K/mTOR inhibitor, NVP-BEZ235 on primary cells from MENX. (A) Primary rat pituitary cells (n=10) were incubated for 48 hr in culture medium supplemented with increasing concentration of NVP-BEZ235 or vehicle solution (CT). (B) Caspase-3/7 activity was measured to monitor apoptosis of primary cells (n=3) after 24h NVP-BEZ235 treatment. Data from primary cultures are evaluated independently with six replicates each and are expressed as the mean \pm SD. ***, $P < 0.001$ versus CT.

To determine whether treatment of MENX tumor cells with NVP-BEZ235 indeed regulates the PI3K/mTOR/AKT pathway, the expression level of phosphorylated AKT and S6 proteins was analyzed in primary cultures from three different mutant rats following treatment with this compound by western blotting. As shown in Fig.32, NVP-BEZ235 induced significant inhibition of both AKT (A) and S6 (B) phosphorylation in a dose-dependent manner.

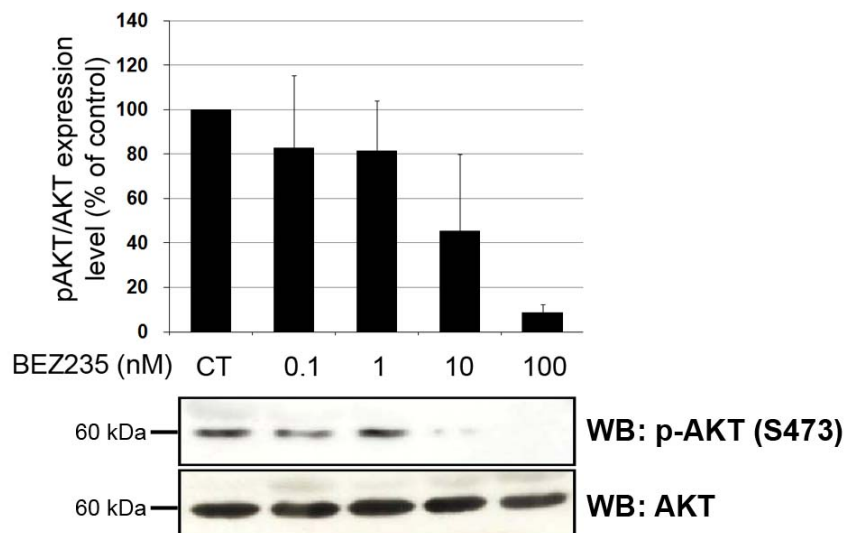
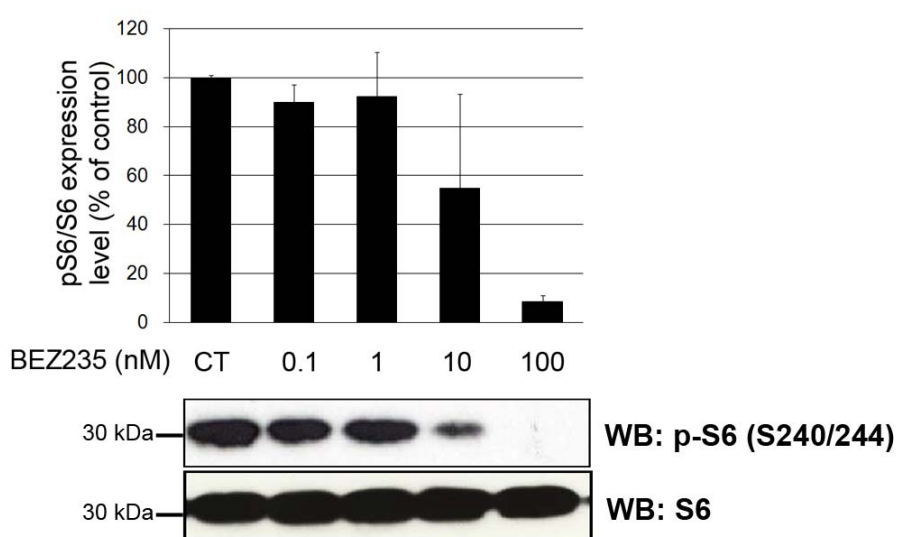
A**B**

Fig.32 Effect of phosphorylated protein after NVP-BEZ235 treatment. Protein lysates from 3 different primary cultures after 24h incubation with NVP-BEZ235 or vehicle (CT) were used for western blotting. We analyzed the expression of anti-pAKT (S473), anti-AKT, anti-pS6(S240/244) and S6 by band densitometry. Diagrams showed the average of expression of indicated proteins. The lower panels show representative western blotting experiments.

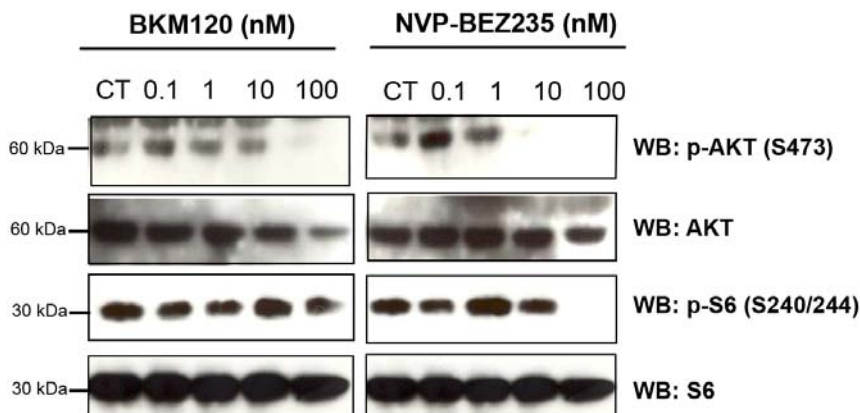


Fig.33 Effect of the single PI3K inhibitor BKM120 and dual PI3K/mTOR inhibitor NVP-BEZ235 on the primary cells from MENX mutant rats. Protein lysates from primary cells after BKM-120 or NVP-BEZ235 treatment for 24h were used for western blotting with anti-pAKT (S473), AKT, pS6 (S240/244) and S6.

To investigate the extent to which the downstream signaling pathway is suppressed by the dual NVP-BEZ235 inhibitor, primary pituitary tumor cultures were also incubated with the single PI3K inhibitor, BKM120, and compared with those incubated with the dual PI3K/mTOR inhibitor NVP-BEZ235. BKM120 downregulated AKT-Ser473 but did not affect S6-S240/244 phosphorylation (Fig.33). We already showed that treatment with the single mTOR inhibitor RAD001 downregulates only phosphorylated S6-Ser240/244 in (see Fig.30B). Exposure to NVP-BEZ235 caused downregulation of both phosphorylated AKT-Ser473 and phosphorylated S6-Ser240/244.

5.3.7. p27 expression sensitizes to NVP-BEZ235 treatment

MENX mutant rats bear a germline frameshift *Cdkn1b* mutation which encodes a p27 mutant protein (named p27fs177). This mutant p27 protein is highly unstable, although it maintains several characteristics of the wild-type protein (localization and protein binding). As a consequence of this mutation, there is very little or no p27 protein in the cells/tissues of affected rats. To determine how the mutant p27fs177 protein, expressed at low level in MENX rat cells, might affect the response to NVP-BEZ235, primary embryonic fibroblasts from wild-type (REF7) and mutant (REF10) rats were treated with the drug and their viability was assessed. As shown in Fig.34A, REF10 cells express a lower level of the p27fs177 protein compared to the level of p27wt in REF7 cells.

We observed that REF7 cells respond to NVP-BEZ235 (cell viability -37% vs. control), while REF10 cells do not (cell viability -8%) (Fig.34B). This suggests that functional p27 expression enhances the response of primary fibroblasts to NVP-BEZ235. Following incubation with NVP-BEZ235, p27 expression slightly increased in REF7 cells while no change in the amount of mutant p27fs177 was observed in REF10 cells.

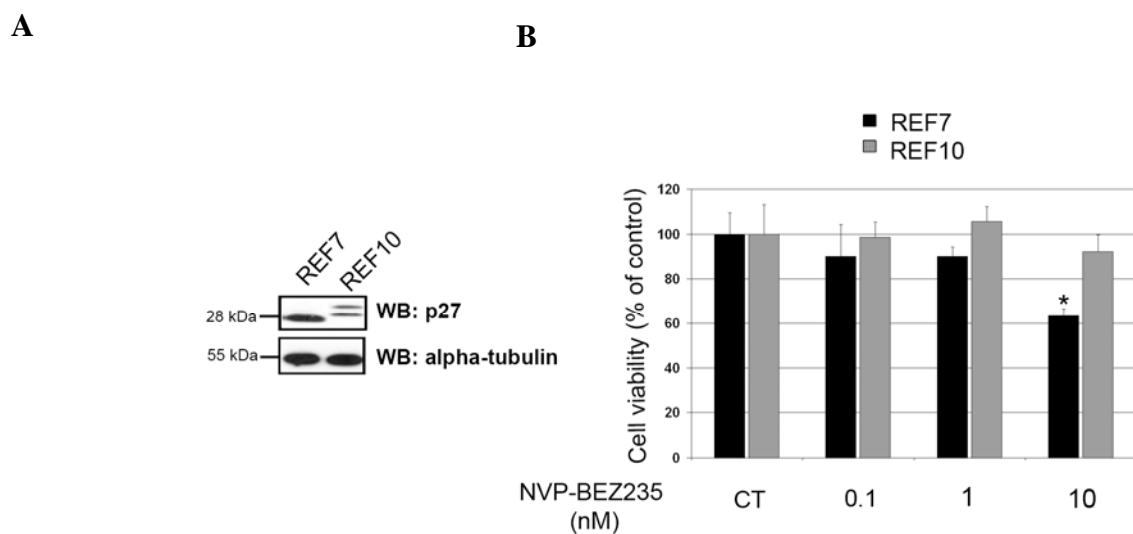


Fig.34 Wild-type p27 expression enhances the response to the NVP-BEZ235 in REF cell lines. (A) To determine the p27 expression level, western blotting was performed on REF7 and REF10 cell lysates with anti-p27 and anti-alpha-tubulin (to check for equal loading) antibodies. (B) REF7 or REF10 cells were incubated with BEZ235 for 24h. Cell viability assays were done by measuring the ATP levels. Data were performed independently with six replicates each and are expressed as the mean \pm SD. *, P<0.05 versus CT.

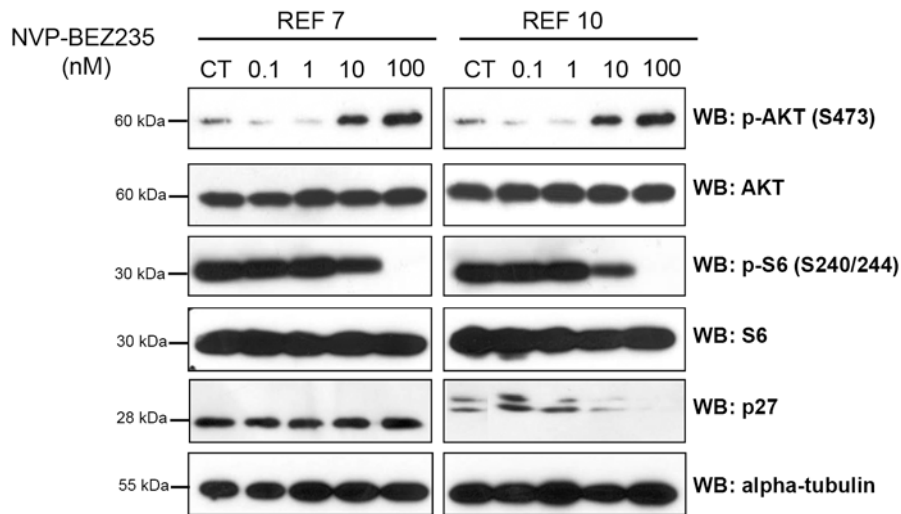


Fig.35 Downstream regulation of NVP-BEZ235 in REF cells. Parallel cultures to Fig.34B were used to extract total proteins and perform western blot analysis to assess the expression level of total AKT, p-AKT (S473), total S6, p-S6(S240/244), p27. Alpha-tubulin was used to check for equal loading.

Upon drug treatment phosphorylated S6 levels decreased in both REF7 and REF10 cells confirming that both cell types respond to NVP-BEZ235 administration at the molecular level. Surprisingly, incubation of both REF7 and REF10 cells with NVP-BEZ235 increased phosphorylated AKT levels similar to what is observed in some human cells after treatment with single mTOR inhibitors (Fig.35).

To confirm the role of p27 in sensitizing cells to NVP-BEZ235, we used mouse embryonic fibroblasts (MEFs) from *p27^{+/+}*, *p27^{+/−}* and *p27^{−/−}* mice. We established MEF clone 12 cells expressing p27 wild-type and MEF clone 19 cells devoid of p27. MEF clone 21 cells were derived from a *p27^{+/−}* mouse and have an intermediate level of p27 expression compared to MEFs derived from *p27^{+/+}* and *p27^{−/−}* mouse (Fig.36A). In agreement with REFs, following incubation with 10nM NVP-BEZ235 *p27^{+/+}* MEFs showed a more pronounced reduction in cell viability than cells from *p27^{−/−}* mice, while heterozygous *p27^{+/−}* MEFs showed an intermediate inhibition (Fig.36B). GH3 rat pituitary adenoma cells do not express p27 because of hypermethylation of the *Cdkn1b* promoter (Qian et al., 1998). GH3 cells transfected with p27wt responded better to NVP-BEZ235 treatment compared to cells transfected with the mutant p27fs177, supporting our hypothesis that p27 sensitizes to NVP-BEZ235 (Fig.36D).

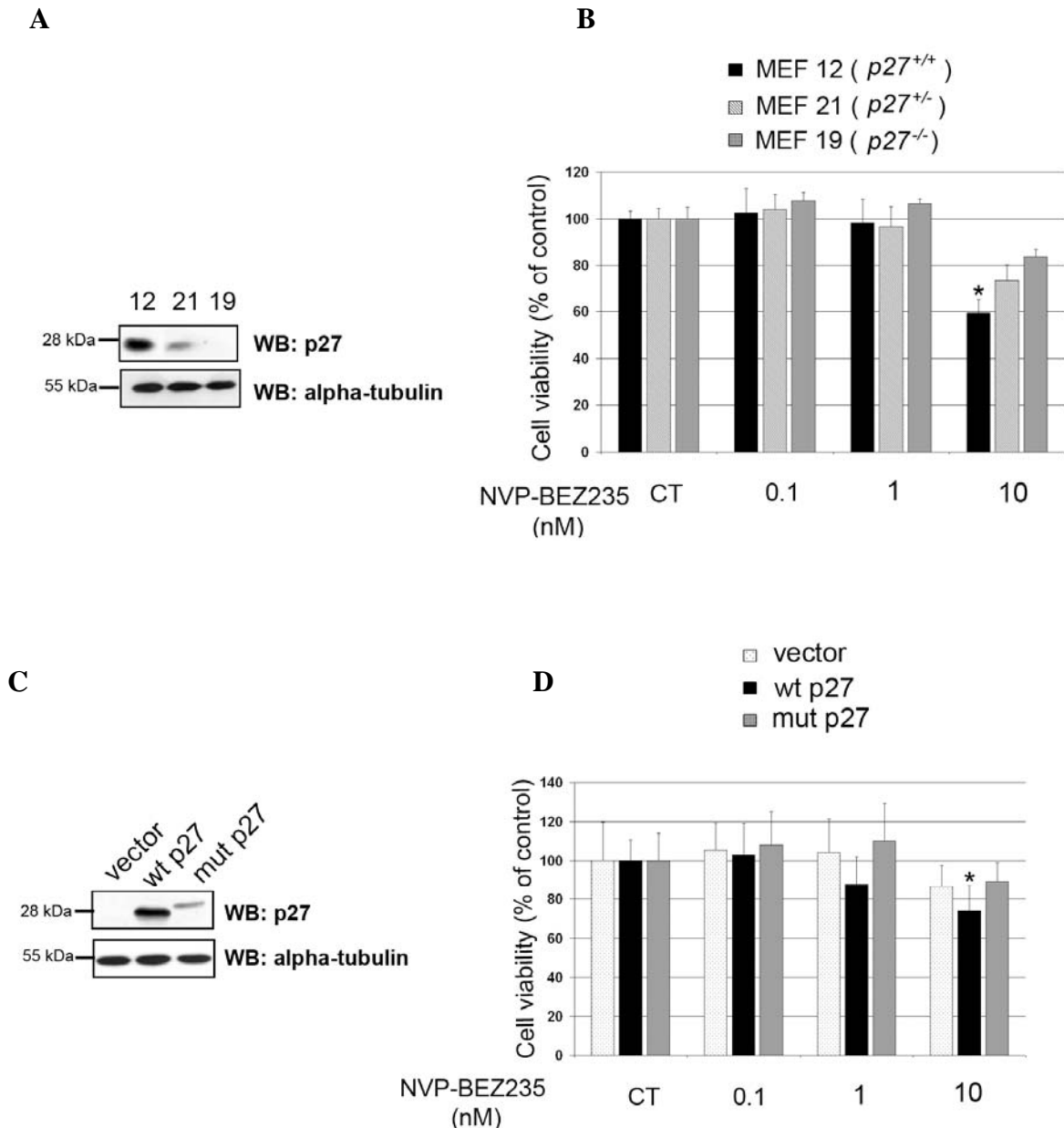


Fig.36 Wild-type p27 expression enhances the response to the NVP-BEZ235 in MEF and GH3 cells. (A) To determine the p27 expression level, western blotting was performed with MEF12 (p27^{+/+}), MEF21 (p27^{+/-}) and MEF19 (p27^{-/-}) cell lysates. Alpha-tubulin was used to check for equal loading. (B) We treated the MEF cell lines with NVP-BEZ235 for 24h and then measured cell viability. (C) GH3 cells were transfected with GFP-vector, GFP-wt p27 and GFP-mut p27 (p27fs177) constructs. Expression level of exogenous p27 proteins was determined by western blotting 24 hours later. Alpha-tubulin was used to check for equal loading. (D) In parallel to (C), transfected GH3 cells were incubated with different concentrations of NVP-BEZ235 for additional 24 hours. We then measured cell viability. Data were performed independently with six replicates each and are expressed as the mean \pm SD. *, P<0.05 versus CT.

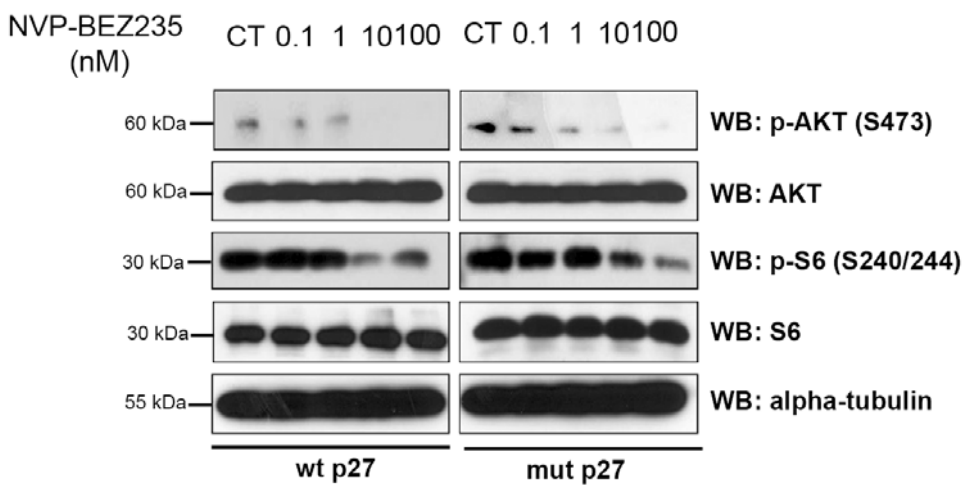


Fig.37 Downstream regulation of NVP-BEZ235 in GH3 cells. Parallel samples to Fig.36D were employed to extract total proteins and perform western blot analysis to monitor the expression level of total AKT, p-AKT (S473), total S6, p-S6(S240/244), p27. Alpha-tubulin was used to check for equal loading.

Incubation with NVP-BEZ235 reduced phosphorylation of both AKT and S6 in both types of GH3-transfected cells, excluding unspecific disabling action of the mutant p27 on the upstream signalling pathways mediating the response to the drug (Fig.37). Taken together, these results support the hypothesis that the presence of functional p27 expression enhances the cytotoxic effect of NVP- BEZ235 in various rodent cells (fibroblasts, pituitary adenoma).

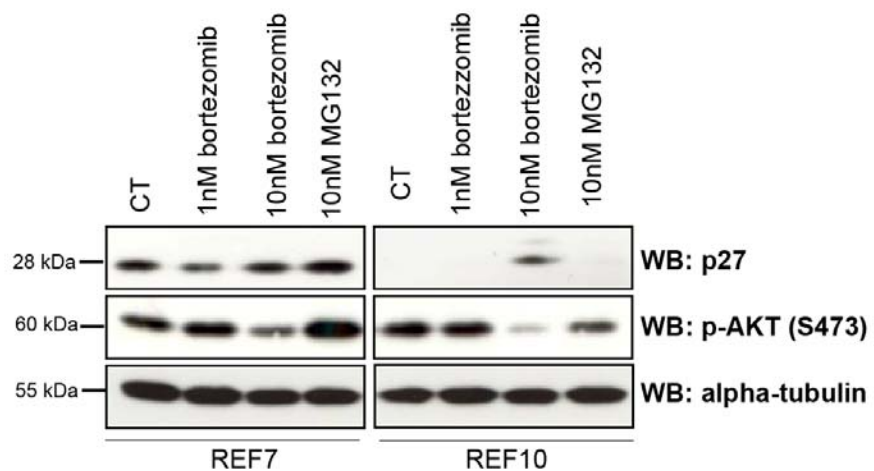
5.3.8. The proteasome inhibitor improves the response to NVP-BEZ235.

A previous study demonstrated that the reduced level of p27fs177 in REF10 is only in part explained by proteasome-mediated degradation. Thus, to further clarify whether the changes in sensitivity to NVP-BEZ235 displayed by the various cell systems were indeed due to p27 expression, two different proteasome inhibitors, bortezomib (Velcade®) and MG132, were employed to stabilize the p27 expression in REF cells. MG132 is commonly used in experimental studies, while bortezomib is also used for the treatment of patients with various types of cancers. Incubation of REF7 cells (p27wt) and REF10 cells (p27fs177) with bortezomib or MG132 for 24hr increased the level of p27 (Fig.38A). However, in REF10

cells, bortezomib treatment was more effective than MG132 at reinstating p27fs177 expression in a dose-dependent manner (Fig.38B). Interestingly, we also observed that bortezomib, at the dose associated to higher p27 expression, inhibited phosphorylation of AKT in both cell types.

The restoration of p27fs177 expression lasted until 48 hr post-treatment and was evident already at 3 hr, in keeping with the usual short half-life of this protein (Fig.39A). Based on these results, bortezomib was used for further experiments. Combined treatment of primary fibroblasts (REF10) from mutant rats with NVP-BEZ235 and bortezomib resulted in decreased cell viability compared with the application of each individual drug (10 nM bortezomib, -27%; 10 nM NVP-BEZ235, -7%; together, -40%) (Fig.39B) and concurrently led to a significant inhibition of S6 phosphorylation (Fig.39C). Inhibition of AKT phosphorylation was also observed following the combined treatment, while addition of NVP-BEZ235 alone increased AKT phosphorylation due to the feedback loop (See Fig.35).

A



B

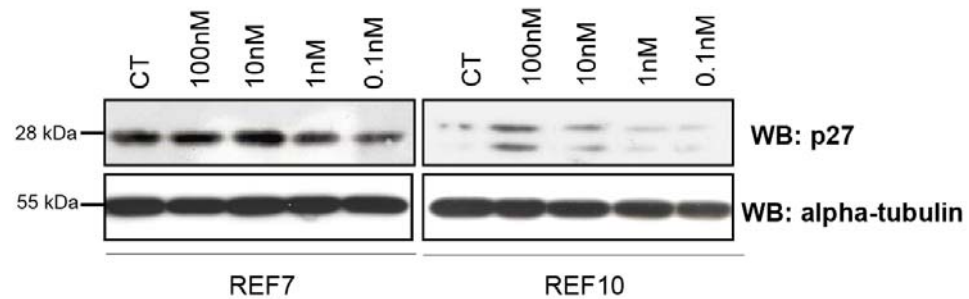


Fig.38 p27fs177 can be stabilized by bortezomib in primary rat fibroblasts. (A) Exponentially growing REF7 and REF10 cells were treated with the proteasome inhibitors, bortezomib (1 nM/10 nM), MG132 (10 nM) or vehicle (CT) for 24 h. Western blotting was performed for p27, pAKT (S473). Alpha-tubulin was used to check for equal loading. (B) REF7 and REF10 were incubated with bortezomib (dose from 0.1 nM to 100 nM) or vehicle (CT) for 24h. Then western blotting was performed for p27. Alpha-tubulin was used to check for equal loading.

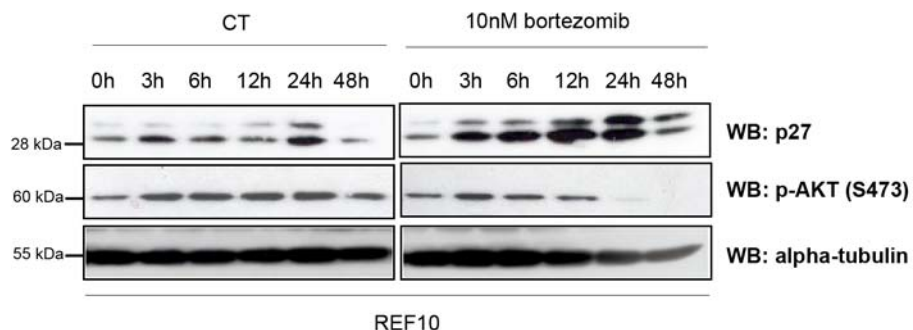
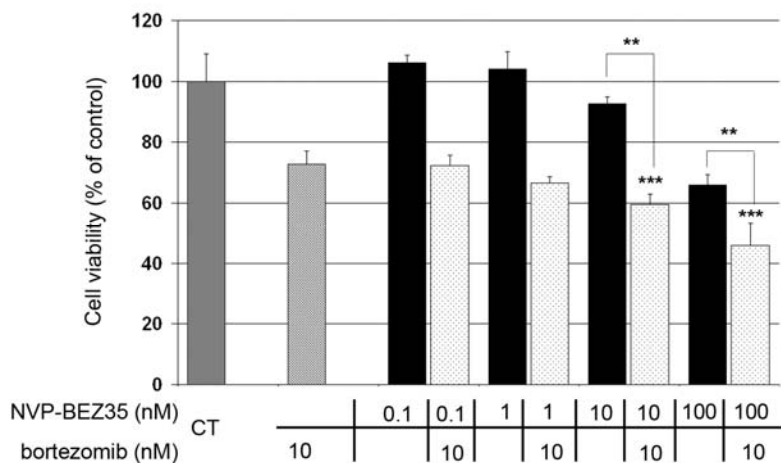
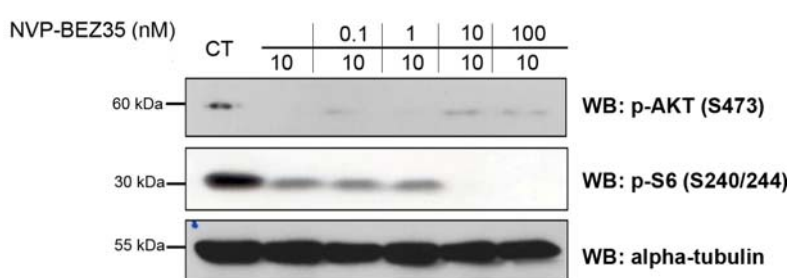
A**B****C**

Fig.39 Bortezomib enhances the effect of NVP-BEZ235 (A) REF10 cells were incubated with 10 nM bortezomib or vehicle (CT) for the indicated time. Western blotting was performed for p27, pAKT(S473). Alpha-tubulin was used to check for equal loading. (B) REF10 cells were incubated with NVP-BEZ235 in the presence or absence of bortezomib (10 nM) for 24 hr, and then we measured cell viability. Data were performed independently with six replicates each. (C) Using pituitary primary cells in parallel to B, we monitored the p-AKT (S473), AKT, p-S6 (S240/244) and S6 expression level by western blotting. alpha-tubulin was used to check for equal loading. Data were performed independently with six replicates each and are expressed as the mean \pm SD. **, P<0.01 comparing single *versus* combined treatment; ***, P<0.001 *versus* untreated control (CT).

Bortezomib can recover the expression of p27fs177 in REF10 cells and enhance their response to NVP-BEZ235. We then tested whether this drug would also work on primary pituitary tumor cells from MENX rats: incubation with 10 nM bortezomib increases the amount of the mutant p27fs177 protein (Fig.40). To identify the effect of increased p27 expression on the response to NVP-BEZ235 in our model, primary pituitary tumor cells from 3 mutant MENX rats were incubated with both NVP-BEZ235 and bortezomib.

As shown in Fig.41A, a synergistic effect of both drugs in inhibiting the viability of rat primary pituitary tumor cells in culture was observed: 10nM bortezomib, -27%; 10 nM NVP-BEZ235, -34%; together, -54%. Thus, the combination of NVP-BEZ235 and bortezomib caused a more potent inhibition of cell viability than the incubation with the individual drugs. Moreover, both phosphorylated AKT and S6 levels were dramatically reduced 24 hours after the combined treatment with 10 nM NVP-BEZ235 and 10nM bortezomib similar to results obtained following co-treatment of REF10 cells (Fig.41B). Taken together these data attest to a role of p27 in mediating the antiproliferative action of NVP-BEZ235.

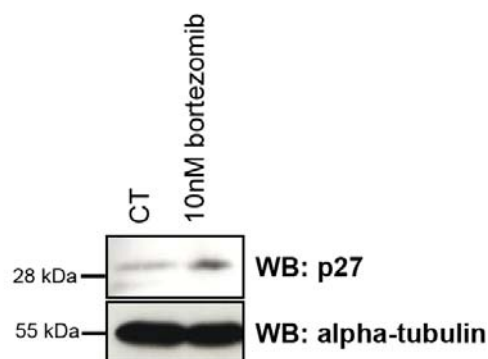


Fig.40 p27 expression level after bortezomib treatment in primary pituitary tumor cells. Pituitary primary cells from a mutant rat were incubated with 10 nM bortezomib for 24h. p27 expression level was analyzed by western blotting. Alpha-tubulin was used to check for equal loading.

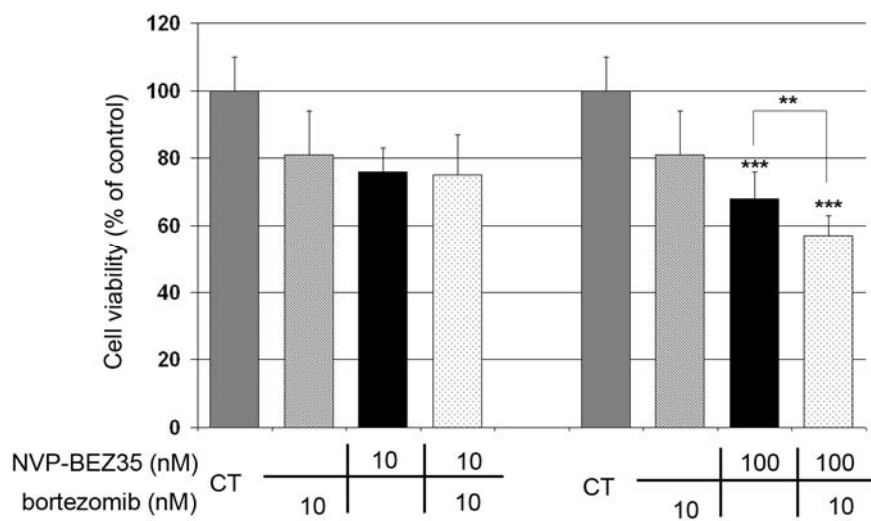
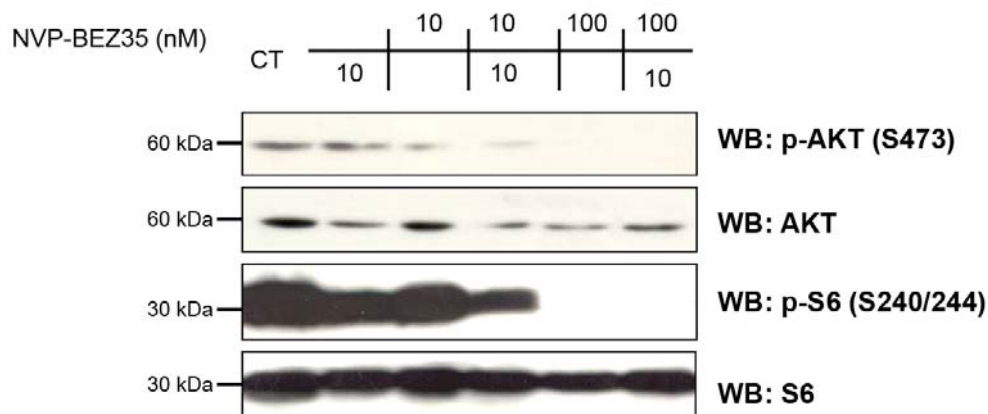
A**B**

Fig.41 Effect of the combined bortezomib and NVP-BEZ235 treatment on NFA primary cultures (A) We incubated pituitary primary cells from 3 MENX mutant rats with vehicle (CT) or with bortezomib (10 nM) and/or NVP-BEZ235 (dose from 10 nM to 100 nM) for 24 hr, and then we measured cell viability. Data were performed independently with six replicates each and are expressed as the mean \pm SD. **, P<0.01 comparing single *versus* combined treatment; ***, P<0.001 *versus* untreated control (CT). (B) Using the samples in (A), we monitored the p-AKT (S473), AKT, p-S6 (S240/244) and S6 expression level by western blotting.

5.4. Germline *CDKN1B* mutations in human neuroendocrine tumor patients

5.4.1. Germline genetic changes and clinical presentation

Studies of MENX rats have demonstrated that *Cdkn1b* is a novel susceptibility gene for multiple endocrine tumors. Not all patients with classical MEN syndromes show mutations in *RET* or *MEN1*, indicating that other genes may be responsible for multiple endocrine syndromes. The genomic DNA of *MEN1* mutation-negative patients was screened for *CDKN1B* germline changes. The first *CDKN1B* mutation was a germline heterozygous nonsense mutation at codon 76 (c.692G>A, p.W76X) found in a 48-year-old Caucasian female affected by a GH-secreting pituitary tumor (acromegaly) and hyperparathyroidism. This was the first germline mutation ever identified in this gene. By screening a series of Italian patients with MEN1-related tumors, we identified a second mutation. This *CDKN1B* germline mutation was a variant at codon 69 (c.678C>T, p.P69L) in a 79-year-old Caucasian female patient diagnosed with bilateral multiple lung metastases of a bronchial carcinoid and type 2 diabetes mellitus. A sellar magnetic resonance imaging (MRI) revealed a pituitary microadenoma in this patient.

We could also analyze 30 patients affected by familial isolated pituitary adenoma (FIPA) and identified two missense mutations. The first was a missense change at condon 96 (c.286A>C, p.K96Q) found in one female patient with a past history of prolactinemia and with recently discovered breast cancer (age 41). The second, a missense change at codon 119 (c.356C>T, p. I119T) was identified in one acromegalic patient (GH-secreting pituitary adenoma). These variations were not observed in over 300 healthy control individuals.

5.4.2. Functional characterization of the p27 variants

To investigate which functional properties of p27^{wt} are affected by the P69L, W76X, K96Q and I119Q changes, plasmid vectors that express various p27 mutants as fusion proteins with the YFP tag located at the N-terminus were generated. Expression and size of the fusion proteins were verified by western blotting following transfection into MCF-7 (Fig.42A) or HeLa cells (Fig.42B). Interestingly, p27P69L was consistently expressed at reduced level compared to p27^{wt} in all cell lines, and p27I119T migrated higher than p27^{wt} in SDS-PAGE. The other mutants were expressed at the same level as p27^{wt}. We then checked the localization of the mutant p27 proteins. Following transfections of mutations were done in growing *p27*^{-/-} mouse embryonal fibroblasts (MEFs) to avoid any possible interference from endogenous p27. As shown in Fig.43, p27P69L localized mainly to the nucleus, like p27^{wt}. Transfected p27K96Q and p27I119T also localize to the nucleus. However, W76X shows a higher proportion of cytoplasmic localization compared to p27^{wt}.

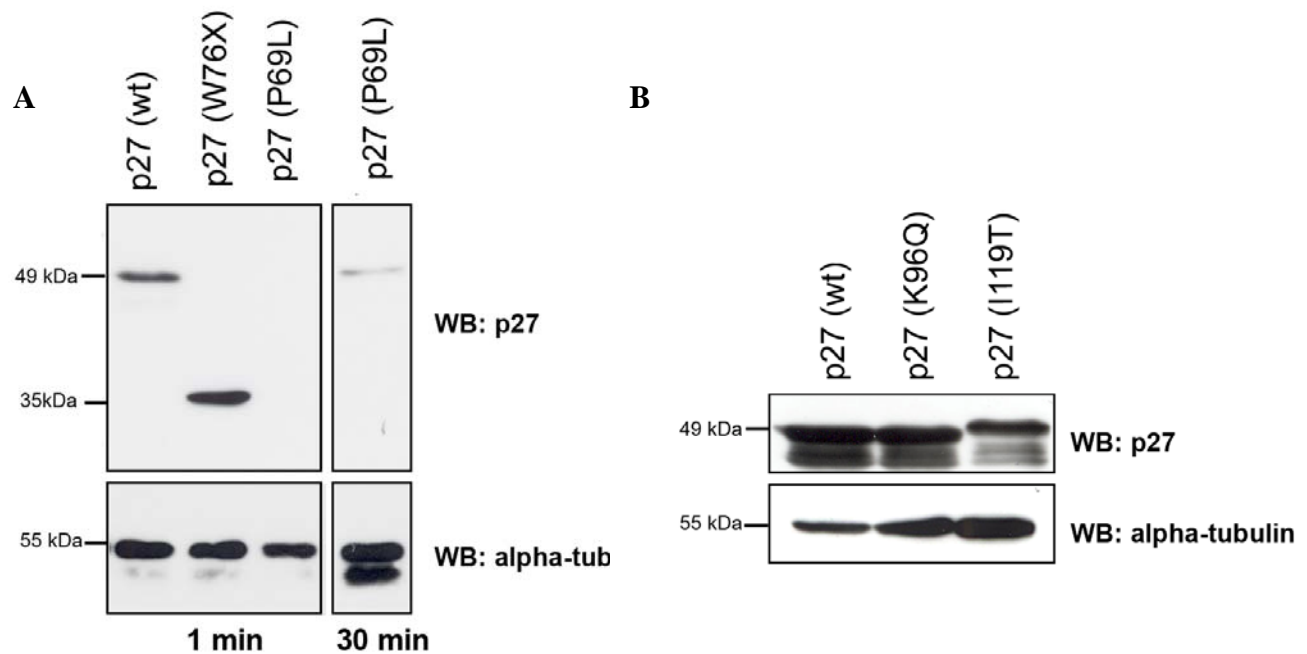


Fig.42 Expression of p27 mutant proteins. (A) Expression of the p27W76X and p27P69L mutant proteins 24h after transfection of MCF7 cells. Western blotting was performed with a monoclonal anti-p27 antibody. The membrane was exposed 1min and 30 min on X-ray film to better evaluate the expression of p27P69L. The membranes were also probed for alpha-tubulin to check equal loading. (B) Expression of the p27K96Q and p27I119T mutant protein 24h after transfection in Hela cells. Western blotting was performed as (A).

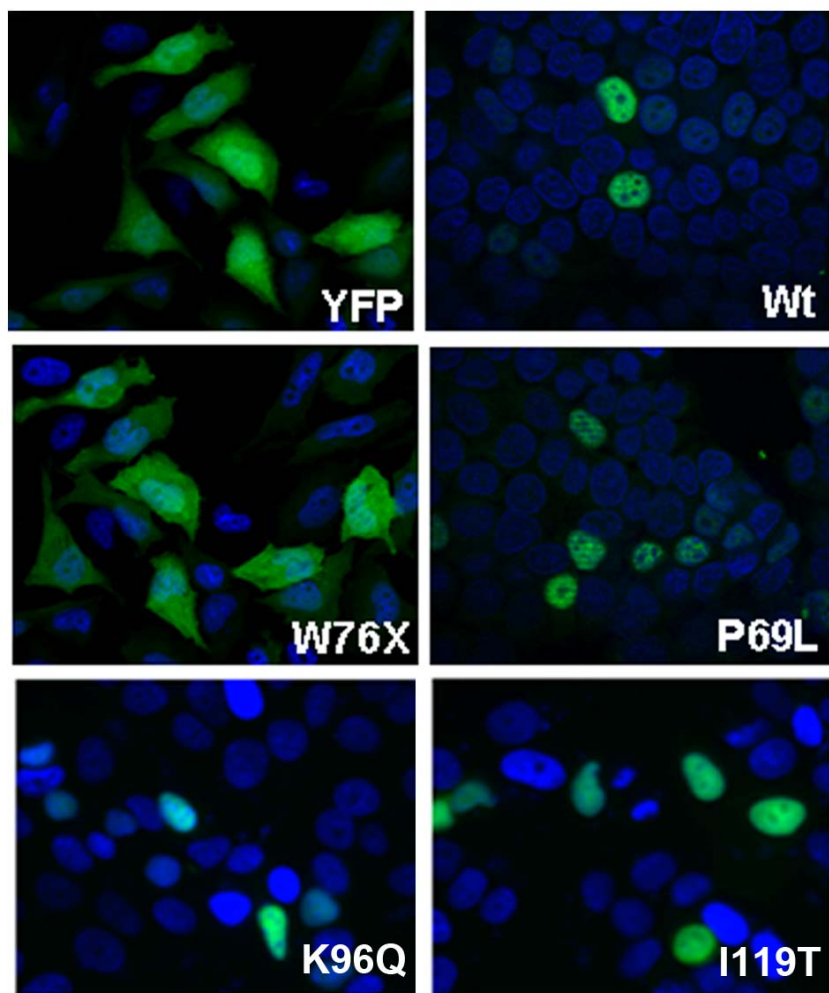


Fig.43 Localization of the p27 proteins. Asynchronously growing p27-negative mouse MEFs were plated on coated cover slip. MEFs were transiently transfected with the YFP backbone vector, YFP-p27wt, YFP- p27W76X, YFP- p27P69L, YFP-p27K96Q or YFP-p27I119T. Cells were fixed 24h later with 2% paraformaldehyde and nuclei were counterstained with DAPI. Cells were examined for direct YFP fluorescence under a fluorescent microscope.

5.4.3. Stability and protein binding ability of p27P69L and p27W76X

p27P69L is consistently expressed at lower steady-state level compared to p27wt. This could be due to enhanced protein degradation by the proteasome, the mechanism responsible for p27 down-regulation in many human tumors (Loda et al., 1997; Pagano et al., 1995). To check the stability of the p27P69L and p27W76X, exponentially growing MCF7 cells were transfected with p27wt, p27P69L or p27W76X and then incubated with Cycloheximide (CHX) to block new protein synthesis. The expression level of exogenous p27 proteins was analyzed at different time points thereafter. As shown in Fig.44A, up to 8h post-treatment with CHX, we observed no change in p27wt and p27W76X amount, while p27P69L showed reduced expression after 6h. This indicates that p27P69L is degraded slightly faster than p27wt. In parallel, the time-dependent reduction of endogenous p27 expression levels confirmed the efficiency of CHX treatment.

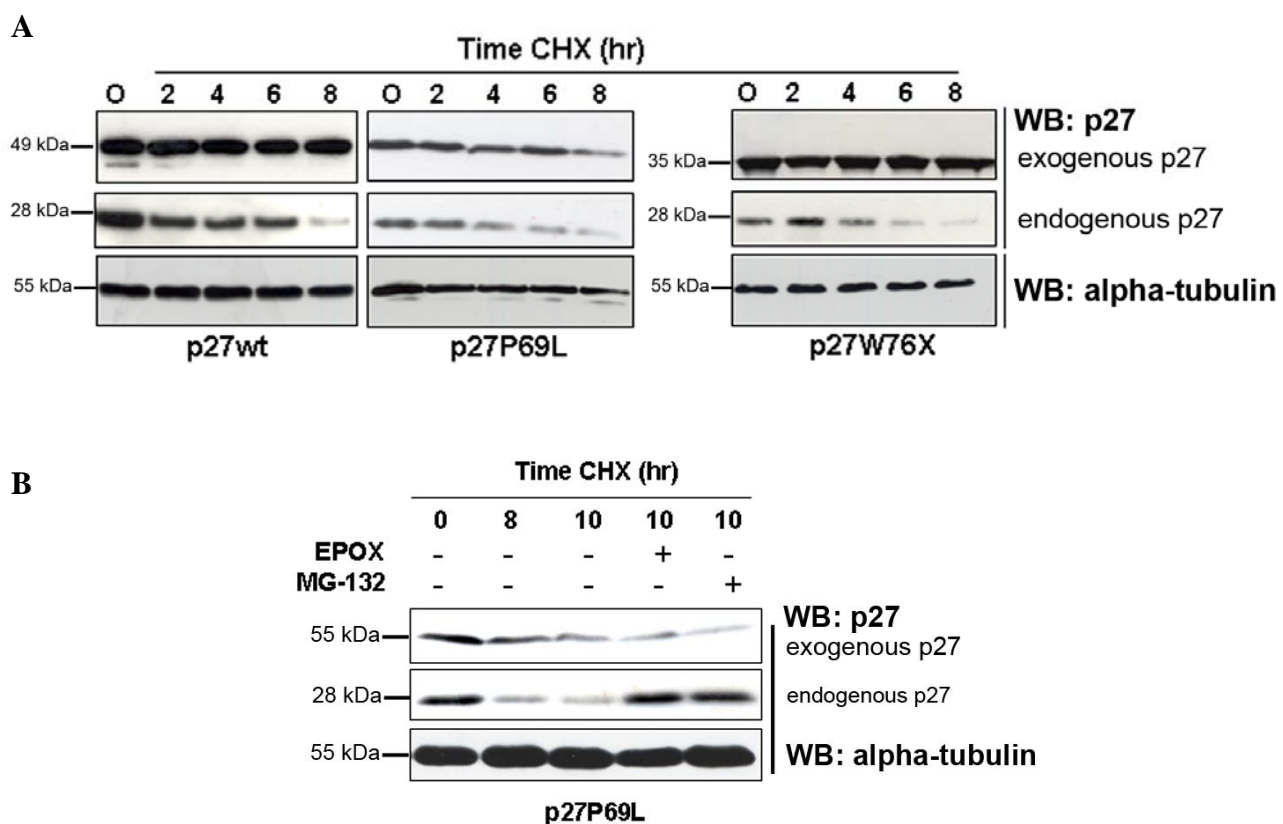


Fig.44 p27P69L is more unstable than p27wt. (A) MCF7 cells transiently transfected with p27wt, p27P69L or p27W76X plasmids were incubated with CHX for indicated times. (B) Expression of p27 was determined in p27P69L transfected MCF7 after CHX treatment with or without proteasome inhibitors, EPOX (epoxomycin) and MG132.

To attempt to inhibit the fast degradation of p27P69L, proteasome inhibitors such as epoxomycin and MG132 were used to treat MCF7 cells transfected p27P69L. However, both compounds failed to inhibit the degradation of p27P69L, while they blocked p27wt degradation (Fig.44B). This suggested that p27P69L may be degraded by a mechanism(s) other than the proteasome.

p27wt undergoes proteasome-mediated degradation following two main pathways. The first involves the ubiquitylation-promoting complex KPC1 in the cytoplasm. The second involves the SKP2 ubiquitin ligase which induces p27 poly-ubiquitylation followed by proteasome mediated degradation in the nucleus (Carrano et al., 1999; Kamura et al., 2004). To determine the pathway responsible for the fast degradation of p27P69L siRNA oligos specific for SKP2 and KPC1 were transfected in MCF7 cells to knock-down these ubiquitin ligases. siRNA oligos were transfected together with the p27P69L plasmid. KPC1 plays a role in the degradation of both p27P69L and p27W76X. In the case of p27W76X, only KPC1 knock-down was tested because of the cytoplasmic localization of the mutant protein (Fig.45A). SKP2 is involved in p27P69L degradation Co-transfection of the various p27 proteins with scrambled siRNA confirmed the specificity of the siSKP2 and siKPC1 molecules since scrambled oligos did not affect the amount of these proteins (Fig.45B).

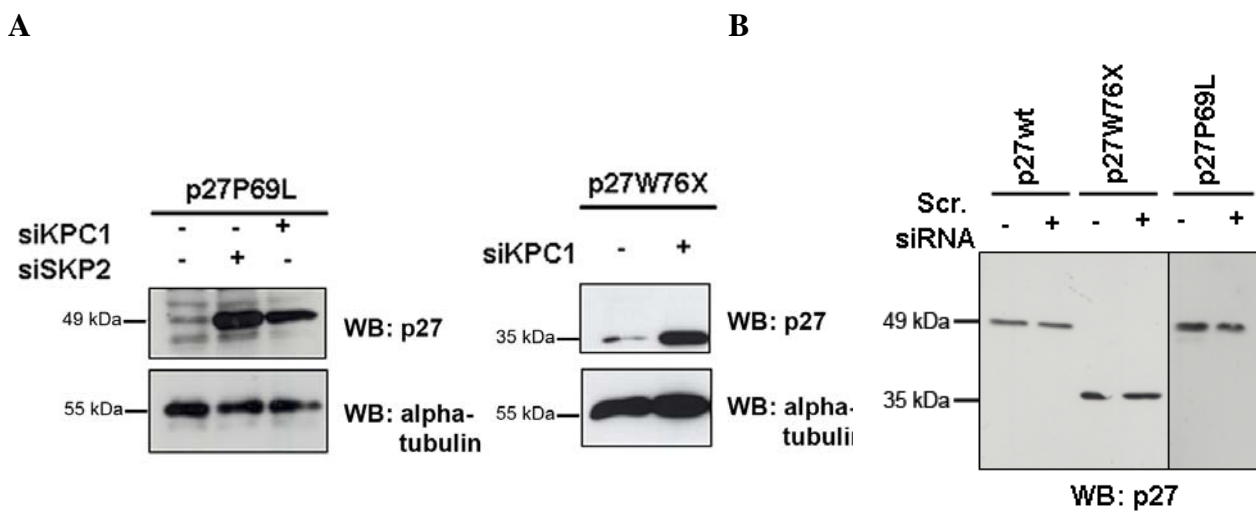


Fig.45 SKP2 and KPC1 play a role in the degradation of p27P69L and p27W76X. (A) MCF7 cells were transfected with siRNA against SKP2 or KPC1 together with expression plasmids for YFP-p27wt, -p27W76X and -p27P69L and analyzed 48 h later by western blotting for p27. Only transfected exogenous p27 proteins are shown. (B) Scrambled siRNA (Scr. siRNA) has no effect on the expression of p27 proteins. Only the transfected proteins are shown.

Considering the crystal structure of the p27-CyclinA-Cdk2 protein complex, the P69L change affects one of the six amino acids involved in the direct binding to Cdk2 (Russo et al., 1996). To verify whether this mutation indeed alters the binding of p27 to Cdk2, Cdk2 pull-down assays were performed using HeLa cells transiently-transfected with p27P69L or control p27wt. Associated p27 proteins were detected by western blotting (WB). While p27wt binds Cdk2, p27P69L does not bind to the kinase (Fig.46).

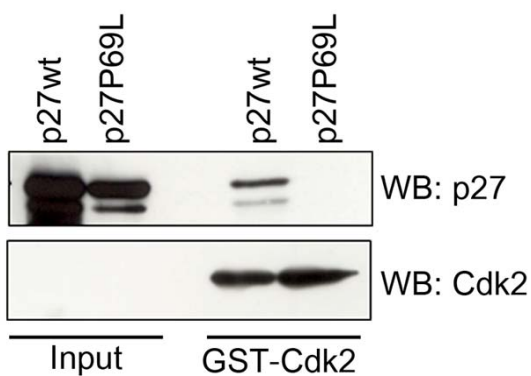


Fig.46 p27P69L does not associate with Cdk2. Lysates obtained upon transfection of HeLa cells with p27wt or p27P69L were incubated with purified GST-Cdk2 protein. Following GST pull-down, 50 µg of the original lysate (Input) and the entire pull-down (GST-Cdk2) were analyzed by Western blotting (WB) with antibodies against p27 or Cdk2.

5.4.4. p27W76X fails to inhibit cell growth

To assess the capacity of the mutated proteins to still regulate the cell cycle progression, we performed a clonogenic assay using the p27-negative GH3 pituitary adenoma cell line. p27wt, p27P69L, p27W76X and pYGFP (used as mock vector) were transfected in GH3 cells and transfected cell populations were grown in the presence of the selection drug G418. Growing cell colonies which were resistant to G418 were stained and counted approximately after 3 weeks. The results showed that p27wt inhibits the growth of these cells while p27W76X does not. p27P69L was less efficient than p27wt at suppressing cell growth (Fig.47). Since the p27W76X mutation prevents the encoded p27 protein from entering the nucleus, the cell compartment where p27 exerts its function as a cell cycle inhibitor, it makes sense that this mutant can no longer inhibit the growth of GH3 cells.

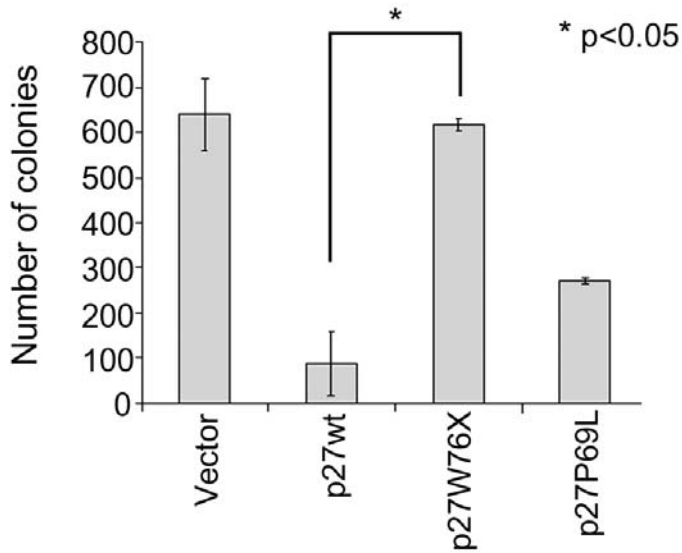


Fig.47 Ability of the variant p27 proteins to suppress cell growth. p27-negative GH3 cells were transfected with the indicated expression plasmids and then selected in G418-containing media for 3 weeks. Colonies were stained and counted. The values represent the mean of 2 independent experiments (each consisting of 6 separate plates) \pm SD.

5.4.5. Stability of p27K96Q and p27I119T and their ability to inhibit cell growth.

We then characterized the mutations in p27 associated to familial isolated pituitary adenoma (FIPA): p27K96Q and p27I119T. To assess protein stability, the rates of degradation of p27wt and mutant p27 proteins were measured in cells GH3 cells treated with cycloheximide (CHX) to block new protein synthesis. Because p27wt is degraded via the proteasome, transfected cells were also treated with MG132 a proteasome inhibitor that would normally increase p27 protein levels. p27wt and p27K96Q both had a half-life of approximately 8-10 hr, and MG132 did not affect the expression of the mutant proteins, suggesting that p27K96Q may be degraded by a mechanism(s) other than the proteasome. In striking contrast, p27I119T was quite stable after CHX treatment. p27I119T levels also were not increased following treatment with MG132 (Fig.48A).

To determine the capacity of the mutated p27 proteins to regulate cell cycle progression, a clonogenic assay was performed using the p27-negative GH3 pituitary adenoma cell line. Vectors expressing p27wt, p27K96Q or p27I119T and the pYFP vector (used as mock vector)

were transfected in GH3 cells. Transfected cell populations were grown in the presence of the selection drug G418. We counted the cell colonies resistant to G418 3 weeks after selection. p27K96Q and p27I119T-transfected GH3 cells showed a number of colony similar to p27wt-transfected cells (Fig.48B). Thus, these results clearly show that both p27 mutants retain the ability of the p27wt protein to inhibit GH3 cells growth.

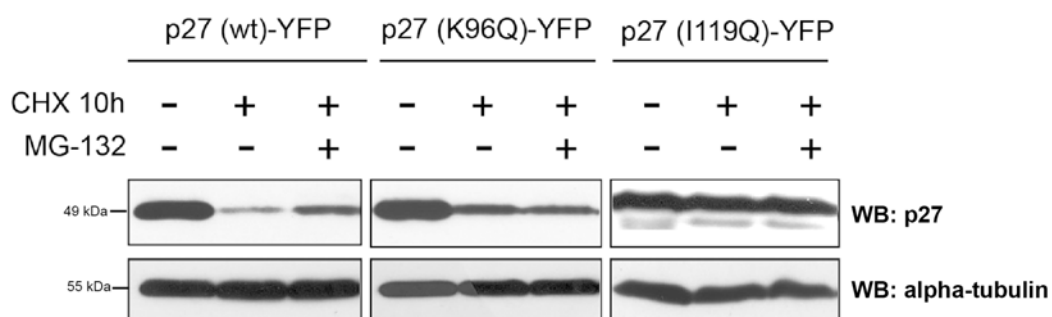
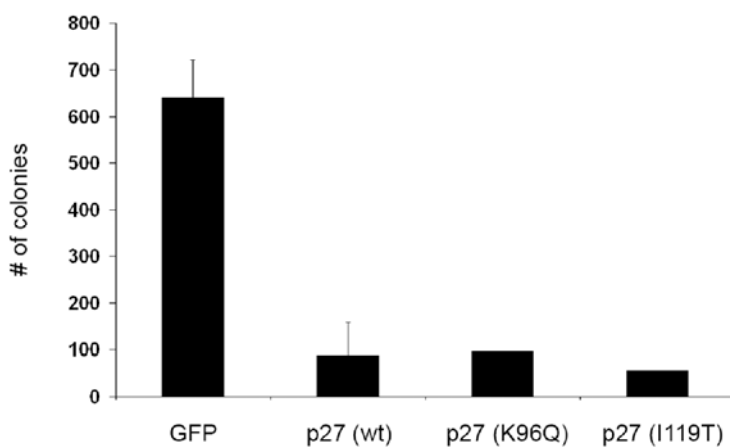
A**B**

Fig.48 Molecular characteristics of p27K96Q and p27I119T. (A) GH3 cells transiently transfected with p27wt, p27K96Q or p27I119T plasmid were incubated with CHX for 10h with or without the proteasome inhibitor, MG132. Exogenous p27 proteins were analysed by immunoblotting for p27 and alpha-tubulin. (B) p27-negative GH3 cells were transfected with the indicated expression plasmids and then selected in G418-containing media for 3 weeks. Colonies were stained and counted. The values represent the mean of 2 independent experiments (each consisting of 6 separate plates) ±SD.

5.4.6. p27K96Q has reduced Grb2 binding ability

The K96Q mutation affects the last amino acids of the Grb2 binding site thus it might influence the binding with Grb2. To assess whether p27K96Q was still able to bind Grb2, a pull down assay was performed using GST-Grb2 recombinant protein as bait. As shown in Fig.49, we pulled down a little amount of p27K96 compared to the p27wt. Thus, p27K96Q seems to have a reduced affinity for Grb2 binding.

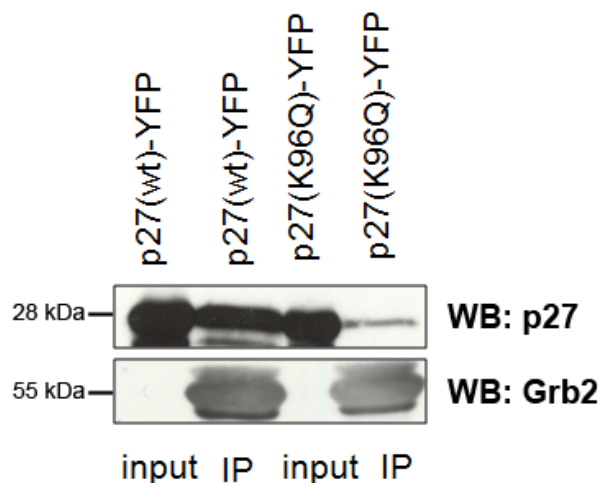


Fig.49 p27K96Q binds Grb2 with low efficiency. HeLa cells were transfected with p27wt-YFP or p27K96Q-YFP. Cell lysates (INPUT) were incubated with recombinant GST-Grb2 protein, after washing and the bound proteins (IP) were eluted. 50 µg of input and the whole IP were loaded in SDS-PAGE gels. Immunoblotting was performed with anti-p27 and subsequently with anti-Grb2 antibodies.

5.4.7. The size-shift of p27I119T does not depend on abnormal phosphorylation

As shown in Fig.36B, the p27I119T protein migrates slower than all other proteins in SDS-PAGE. To make sure that this migration shift was not an artifact of the cloning procedure, we introduced this mutation also in a vector that expresses human p27wt with an HA tag at the C-terminus. The expression of p27I119T-HA is also associated to a shift in migration. Importantly, the p27 proteins in lymphoblastoid cells established from p27I119T mutation-bearing patients also showed the same abnormal migration behaviour. Indeed, the patient, who is heterozygous for the p27I119T mutant, shows two bands following SDS-PAGE and

western blotting for p27. This indicates that the size-shift occurs also *in vivo* not only *in vitro* (Fig.50A). As p27wt is the target of many kinases that specifically phosphorylate regulatory residues, the migration behavior of p27I119T (where a Isoleucine becomes Threonin) could be caused by an altered phosphorylation pattern compared to the p27wt protein. To understand the relationship between phosphorylation and the migration shift of the mutant protein, we used a pool of inhibitors of protein kinases A, G and C. HeLa cells were transfected with p27wt-HA and p27I119T-HA and then incubated with the inhibitors. The p27wt protein contains two major phosphorylation sites: Ser 10 and Thr 187. Phosphorylation at Thr187 was used as control to monitor the efficiency of the kinase inhibitors treatment. The level of phospho-Thr187-p27 was determined after incubation of the transfected cells with pool inhibitors (staurosporin, H89 and H8) for 24 h. As seen in Fig.50B, treatment of cells expressing either p27wt or p27I119T with the inhibitors decreased the level of phospho-Thr187 compared to untreated cells. However, inhibition of protein kinase A, G and C did not affect the migration shift of p27I119T. Thus, the migration shift of p27I119T is not due to increased or altered phosphorylation of the protein.

To confirm whether the atypical migration of p27I119T in SDS-PAGE gels is linked specifically to the isoleucine 119 residue, we introduced three additional mutant proteins at this residue (Fig.50C). The p27I119A mutant that cannot be phosphorylated showed the same migration pattern as p27I119. Surprisingly, when two-phospho-mimetic amino acids (Aspartic acid=D, Glutamic acid=E) were substituted to Ile to generate two mutant proteins, p27I119D and p27I119E, the proteins shifted to a higher molecular weight even more than p27I119T (Fig.50D). Thus, Isoleucine 119 of p27 might be an important residue that affects the migration pattern of the p27 protein.

The studies performed to characterize the germline p27 mutations associated with the MEN4 syndrome showed that the ability of p27 to interact with partner proteins or its strongly are important functions of the molecule. Tumor predisposition occurs when these functions are implicated.

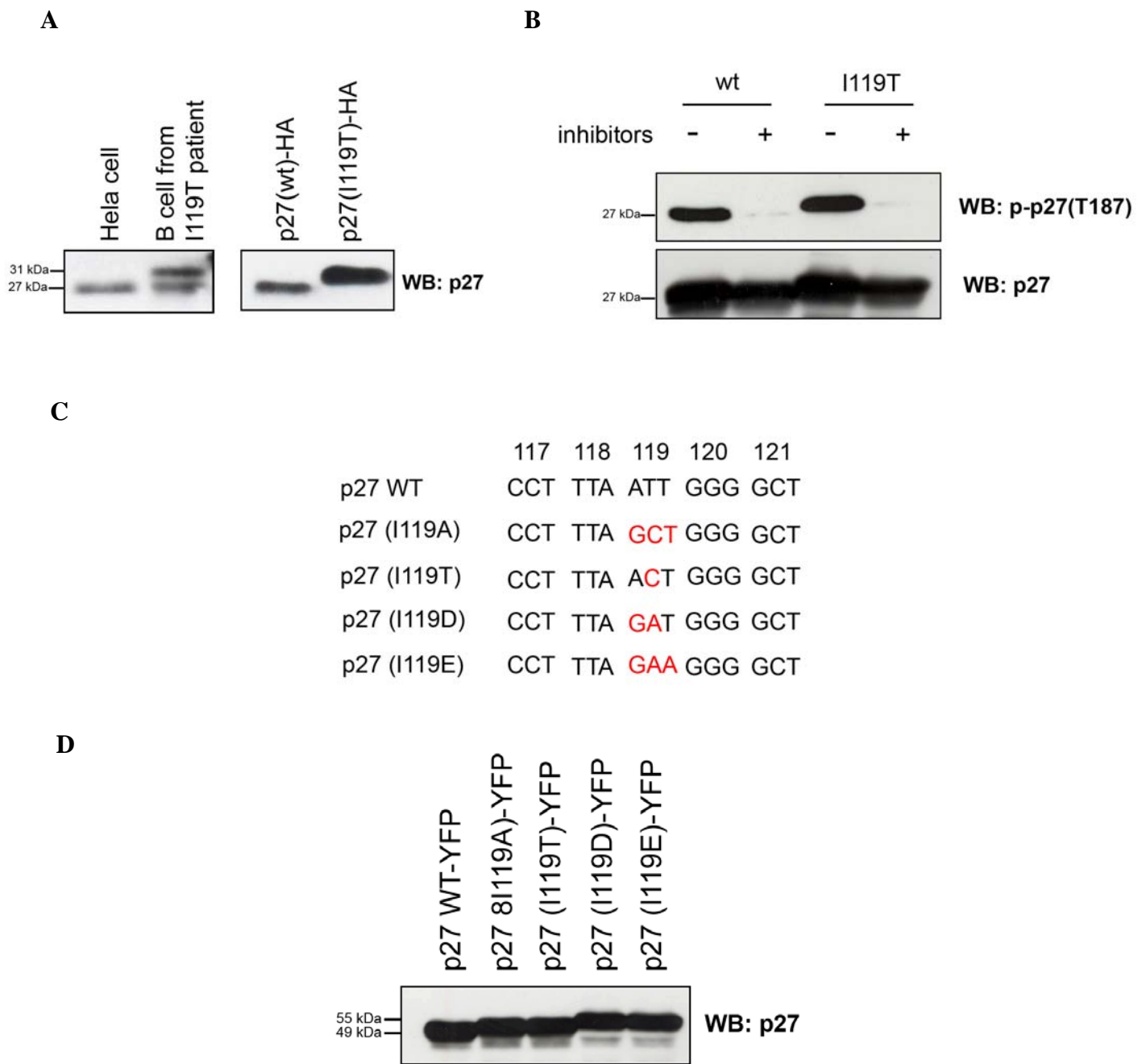


Fig.50 p27I119T is associated with abnormal SDS-PAGE migration. (A) Western blotting analysis of the whole lysates from lymphoblastoid B cell of I119T patient and p27I119T-HA transfected GH3 cells showed the same migration behavior as the patient cells. (B) Hela cells were transfected with HAp27wt and Hap27I119T constructs. After 24 hours, cells were incubated for 6 hours in a culture medium supplemented with a pool of protein kinase inhibitors (staurosporin, H89 and H8) or left untreated. (C) Scheme of the mutations introduced at the isolucine 119 residue. (D) Hela cells were transfected with YFP-p27 constructs containing p27wt, p27I119A, p27I119T, p27I119D or p27I119E mutant proteins and examined by Western blotting. The altered mobility of the 119 mutations is evident.

6. DISCUSSION

p27 is a negative key regulator of cell cycle progression. For this reason, somatic mutations of the *CDKN1B* gene have been sought by various groups in the major tumor types, but only 3 in hundreds of cases analyzed were found. Recently our group identified a *Cdkn1b* germline frameshift mutation as the cause of a recessive multiple endocrine neoplasia (MEN)-like syndrome (named MENX) in the rats (Pellegata et al., 2006). Capitalizing on this discovery, we and others identified germline mutations in *CDKN1B* in patients developing multiple endocrine tumors (MEN4 syndrome).

To understand the role of p27 in the predisposition to neuroendocrine tumors, we first identified the molecular phenotype of the rat germline mutation in *Cdkn1b* (encoding the mutant p27fs177 protein) associated with the MENX syndrome. In parallel, we also performed the functional *in vitro* analysis of four novel *CDKN1B* mutations (p27P69L, p27W76X, p27K96Q and p27I119T) found in patients with multiple endocrine tumors to compare with MENX rat.

The mutant p27 protein (p27fs177) associated with MENX is very unstable due to the p27-unrelated C-terminal domain. Its rapid degradation might be one of the reasons for the low expression of p27 in affected rat tissues, similarly to what has been observed in several of human cancers (Loda et al., 1997; Pagano et al., 1995). The fast degradation of p27fs177 is, at least in part, mediated by the Skp2-dependent ubiquitination pathway, just as p27wt. Interestingly, it has been reported that Skp2-dependent ubiquitination and subsequent degradation of p27 requires its phosphorylation at the Thr187 residue, which is then recognized and bound by the Skp2 ubiquitin ligase. Since p27fs177 lacks the Thr187 residue but its degradation is still regulated by Skp2 (as seen in siRNA knock-down experiments), we have to postulate that a Skp2-dependent but Thr187-independent mechanism for p27 degradation exists, as it had been previously hypothesized based on studies of cells (fibroblasts, thymocytes) from p27T187A (Thr substituted by Ala) knock-in mice (Malek et al., 2001). A mutant ubiquitin that inhibits ubiquitin chain elongation has no effect on the degradation of p27fs177, while it rescues p27wt degradation, indicating that p27fs177 is also degraded by mechanisms different from those modulating the level of p27wt.

The expression of p27fs177 can be recovered by proteasome-inhibition. This finding, combined with the fact that p27fs177 retains the capacity to interact with cyclins and Cdks, suggests that if the expression of this protein can be rescued inhibiting the proteasome, it might resume its anti-proliferative activity. The fact that p27fs177 retains the potential to bind

to the usual partners of p27 is highly relevant: if this protein can be re-expressed in the tumor cells, it might then resume its inhibitory effect on the cell cycle and therefore prevent or reverse tumor growth *in vivo*. This is in agreement with the finding that p27 is frequently down-regulated in human tumors and in some of them increased proteasomal degradation has been identified as the cause of the reduced p27 level (Gstaiger et al., 2001; Loda et al., 1997). Concerning the human *CDKN1B* mutations we identified in patients with multiple endocrine tumors, p27P69L associates to lower expression *in vitro*. This mutation affects an amino acid located in the Cdk2 binding domain of the protein (amino acids 52-93) and this change is predicted with a high degree of confidence to reduce by more than 55% the hydrophobicity of the region (<http://www.expasy.org/spdbv/>), thereby dramatically altering the environmental conditions necessary for binding to the kinase. Our studies demonstrated that indeed this variant does not bind to Cdk2. The CyclinE/Cdk2 complex is a very important target of p27 and this binding is crucial for p27-mediated regulation of G1 to S phase cell cycle progression (Sherr and Roberts, 1999). The lower expression level of p27P69L, together with the inability of the mutant protein to bind to Cdk2, associate with impaired growth suppression of GH3 neuroendocrine tumor cells *in vitro* upon overexpression of this mutant protein.

Similar to p27P69L, other p27 mutations loose their ability to bind molecules involved in p27-related pathways. For instance, the missense mutation p27K96Q is situated in the proline rich domain (amino acids 90-96) at the C-terminus which mediates the binding to Grb2 (Sugiyama et al., 2001). p27wt competes with the Ras-GEF Sos for binding to Grb2, thereby preventing Ras activation (Moeller et al., 2003). This mutant protein fails to bind to Grb2. Thus we speculate that this impaired binding may lead to Ras activation and consequently to increased cell proliferation, which ultimately might promote tumorigenesis in this patient.

The p27W76X mutant protein we identified lacks the nuclear localization signal and is localized in the cytoplasm. The association between cytoplasmic mislocalization of p27 and tumor formation has been studied various tumors, such as breast cancer (Liang et al., 2002), mylogenous leukemia (Min et al., 2004), colon cancer and thyroid carcinoma (Motti et al., 2005). In these tumors, cytoplasmic mislocalization of p27 has been shown to be associated with poor prognosis. The inability of p27W76X to enter the nucleus, the cell compartment where p27 exerts its function as a cell cycle inhibitor, abolishes its ability to inhibit the growth of GH3 cells both by clonogenic assay and by stable expression of this variant p27 protein. Interestingly, p27W76X has lost the pro-apoptotic function of p27wt. This finding is in agreement with previously reported data stating that cytoplasmic p27 are resistant to apoptosis, but can become sensitive upon relocation of the protein to the nucleus (Short et al., 2008).

Changes in the migration of proteins in SDS-PAGE (band-shifts) due to phosphorylation, which is one of the post-translational modification, have been reported for many proteins and kinases (Kuroda et al., 2007; MacKenzie et al., 2002). It is already known that phosphorylated p27 (e.g. at the Ser10 residue) is associated with a band that migrates more slowly in SDS-PAGE, seen in various cell lines (Ishida et al., 2000). This electrophoretic mobility shift disappears with mutation on phosphorylation site, such as p27S10A. However, in the p27I119T mutation we failed to alter the band shift using protein kinase inhibitors and the change at the I119 residue into an amino acid (Ala) that cannot be phosphorylated (I119A) also does not alter protein migration. Moreover, introducing two phospho-mimetic amino acids at residue 119, Glu (I119D) and Asp (I119E), we obtained p27 proteins that migrate slower than p27I119T or p27I119A. Therefore, the size shift associated with p27I119T does not appear to be due to phosphorylation of the novel Thr residue.

Another possible explanation for the migration shift associated with the I119T variant could be the changing in the binding affinity to other proteins. For instance, the I119T change might alter the interaction with the negative regulator of p27, p38^{jab1}, because codon 119 is located in the surface amino acids that mediate the interaction of the two proteins, surface that spans amino acid residues 97 to 151 of the p27 protein (Tomoda et al., 1999). However, whether changes in the interaction affinity cause the abnormal migration of p27 on SDS-PAGE is an intriguing question that merits further investigation.

Alternatively, since glycosylation occurs at serine, threonine or asparatic residues, the migration shift of these mutations on 119 position might be caused by glycosylation (Dennis et al., 1999). It is known that glycosylation results in protein stability (Chen et al., 2006). In agreement with this finding, p27I119T is also more stable than the p27wt following treatment with CHX that prevents new protein synthesis.

Even if the change c.356T/C (I119T) has been rarely found in prostate cancer (Chang et al., 2004), we could not identify a specific effect of this change on the protein's function except migration shift in SDS-PAGE. Ile 119 is situated in the so-called "scatter domain" of p27 (amino acids 118-158) which is responsible for actin cytoskeletal rearrangement and cell migration. Thus, this mutation could play important role in invasion *in vivo* (McAllister et al., 2003) and its further characterization seems important.

In order to use MENX rats as an animal model system of human neuroendocrine tumors, we first needed to characterize the rat tumors. We concentrated on the rat pituitary tumors. We demonstrated that these tumors express FSH β , LH β , α SU and the SF1. α SU was highly expressed in all lesions of MENX mutant animals. Only a minority of human gonadotroph adenomas produce alpha-subunit to the extent seen in our animal model. During progression most rat pituitary adenomas exhausted their ability of producing hormones and appeared morphologically similar to null cell adenomas. The cell of origin of null cell adenomas is still a matter of debate. Null cells exist in the nontumorous adenohypophysis and they may represent undifferentiated progenitors of mature hormone-synthesizing pituitary cells, or they may derive from mature adenohypophysial cells that undergo de-differentiation due to the abrogation of transcription factors and co-factors necessary for the differentiation into the various pituitary cell lineages. The studies in our animal model demonstrate that the rat tumors derive from preceding small tumor lesions made of differentiated cells expressing LH β and FSH β through molecular mechanisms leading to loss of hormone expression. The tumor cells are committed progenitors since they express the α SU, but have lost the capacity to produce hormones.

p27^{-/-} mice (129/Sv \times C57/B6J hybrids) have been generated and characterized several years ago. These mice show as sole tumour phenotype, pituitary adenoma of the intermediate lobe (IL) tumors occur with complete penetrance and are already evident at 4-6 weeks of age. In *p27* null mice the occurrence of hyperplastic nodules composed of corticotroph cells of IL precedes the formation of adenomas. Interestingly, in young *p27* nullizygous mice there was no evidence of focal lesions surrounded by normal-appearing cells but rather the entire IL is affected (Fero et al., 1996). This suggests that ablation of *p27* in mice is sufficient to cause abnormal proliferation of corticotroph cells without necessarily requiring a second genetic event.

MENX-affected rats show a pathological phenotype in the *pars distalis* of the pituitary gland at around 4 months of age, later in time compared to *p27*^{-/-} mice, while young rats (4 weeks old) show a macroscopically normal-looking gland. This suggests that the little amount of *p27* produced by the mutant *Cdkn1b* allele in the MENX-affected rats attenuates the tumorigenic process, or that a second genetic alteration needs to occur to provide the cells with the necessary selective advantage.

In drug development, the rat is often employed to demonstrate therapeutic efficacy and associated toxicity of drug compounds prior to human clinical trials. Since we demonstrated that MENX-affected rats develop gonadotroph nonfunctioning adenoma by histological

profiling, we decided to use MENX-affected rats as a preclinical model to evaluate the efficacy of various therapeutic compounds in the medical treatment of gonadotroph NFA. Thus, tumor cells were established as primary cultures *in vitro*. The advantages of this system are that it is quick, relatively inexpensive, and specific mechanisms of action can be more easily tested compared to *in vivo* studies.

First, we demonstrated that rat pituitary primary cells from MENX-affected rats display *Sstrs* and *Drd2* gene expression profiles, response rates to SRIF analogs and dopamine agonists and to mTOR inhibitors similar to human NFA. Second, we provided evidence for a potent antiproliferative effect of a dual PI3K/mTOR inhibitor, NVP-BEZ235, in these tumors. Although medical treatment of human NFA is still a matter of great debate, treatment with SRIF analogs and dopamine agonists has been attempted on the basis of somatostatin and dopamine receptor expression and on their partial effectiveness *in vitro* (Florio et al., 2008; Renner et al., 1998; Taboada et al., 2007; Zatelli et al., 2007a). However, in clinical settings these compounds did not fulfil the expectations and elicited only partial response. In keeping with these results, MENX rat pituitary tumors displayed limited response to SSA/DA. In our model octreotide inhibited rat pituitary cell viability more efficiently than either a multi-receptor ligand agent such as SOM230, or the chimeric compound BIM-23A670. A previous study reported that BIM-23A670 is more effective than SSA in reducing cell proliferation in cultured NFA, while its inhibitory effect is comparable to that of dopamine receptor agonists (Renner et al., 1998). The lower efficacy of the chimeric compound in our animal model compared to human NFA might be due to the different receptor expression pattern. Indeed, rat tumor cells show a lower relative level of *Drd2* (which mediates most of the effects of BIM-23A670) than *Sstr* genes compared to human NFA (Florio et al., 2008). The level of expression of the different *Sstr* genes was not associated with the response of each individual culture to SSA, with the exception of *Sstr5*. Indeed, response to both octreotide and SOM230 correlated with lower *Sstr5* expression, phenomenon that reached the statistical significance in the group of cultures that did not respond (nonresponders) to octreotide. Interestingly, human primary NFA cultures that respond to SOM230 virtually lack *Sstr5* expression, while this gene is present in the nonresponders group (Zatelli et al., 2007). Although studies specifically assessing the expression of *Sstr5* in NFA cells treated with octreotide are not available, acromegalic patients (GH secreting pituitary adenomas) with lower *Sstr5* expression respond better to octreotide (Taboada et al., 2007).

The stronger immunoreactivity for p-Akt in rat pituitary tumor tissues compared to normal pituitary lead us to evaluate the antiproliferative effect of PI3K/AKT/mTOR inhibitors on rat

primary tumor cells. Noteworthy, hyperactivation of the AKT/mTOR pathway has also been reported in human NFA (Musat et al., 2005). RAD001, a single mTOR inhibitor has shown significant inhibition of cell viability in a rat GH-secreting pituitary tumor cell line (GH3), in human GH-secreting and nonfunctioning pituitary tumors (Gorshtein et al., 2009; Zatelli et al., 2010). In our model, RAD001 showed limited inhibition effect of cell viability in part of cultures. It might be single mTOR inhibitors induce the activation of AKT due to a feedback loop, thereby abolishing the antitumor potential of mTOR inhibition (O'Reilly et al., 2006; Um et al., 2004). Dual inhibition of PI3K/mTOR leads to a more pronounced reduction in viable rat adenoma cells than either anti-receptor therapy or single mTOR inhibition (RAD001).

A detailed analysis of the molecular events mediating the antiproliferative activity of NVP-BEZ235 has been reported in other studies and was beyond the scope of our present study (Baumann et al., 2009; Cao et al., 2009; Maira et al., 2008; Serra et al., 2008). However, it is interesting to note that the exposure of MENX-associated NFA cells to NVP-BEZ235 promotes the same molecular events already observed in many human cancer cell lines of various origins, including neuroendocrine cell lines (i.e. reduced Akt and S6 phosphorylation) (Zitzmann et al., 2010), indicating that the germline defect in p27 does not impair upstream events in the signalling cascade. Also, NVP-BEZ235 reduced rat NFA cell viability by inducing apoptosis, since activated caspase-3 was observed in 2 tested primary cultures. In recent studies, NVP-BEZ235 is shown to induce apoptosis in cancer cell lines bearing PI3K activating mutations and/or HER2 gene amplifications (Brachmann et al., 2009; Faber et al., 2009). Since all primary cultures from MENX responded to the antiproliferative activity of NVP-BEZ235, thus the other effects of this drug are similar in all cultures. Thus, the increase in caspase-3 is suggestive of the mechanism of action of NVP-BEZ235 in pituitary primary tumor cells from MENX rats. In conclusion, based on the results here reported, we predict that NVP-BEZ235 would be highly effective in treating human NFA.

Inhibition of the PI3K signaling cascade often induces nuclear accumulation of p27 and this is believed to mediate the block of cell cycle progression observed in some tumor cell lines after treatment (Taboada et al., 2007). MENX mutant rats bear a germline frameshift *Cdkn1b* mutation which encodes an unstable p27 protein, barely detectable or undetectable in tissues/cells of the affected animals (Pellegata et al., 2006). Thus, we wondered whether the lack/reduction of p27 function in rat pituitary tumor cells had any bearing on the response to NVP-BEZ235. As previously reported for other MEF cells (Breuleux et al., 2009), these primary cultures show a low basal level of Akt phosphorylation. For this reason, we could use

various cell systems (REF cells, MEF cells and GH3 cells) having different levels of functional p27 we could verify that cells expressing higher levels of p27wt are more sensitive to NVP-BEZ235 than those expressing low level of p27wt or the unstable p27fs177. The enhanced sensitivity to NVP-BEZ235 associates with a more pronounced activation of downstream signaling pathways in cells expressing normal levels of p27. In the context of our NFA model these findings meant that we could have observed an even more pronounced reduction of cell viability had there been a higher amount of p27 in the primary cells of mutant rats. This prediction proved to be correct since using bortezomib, an established anticancer proteasome inhibitor compound, to stabilize p27 increased the response to NVP-BEZ235. A synergistic effect of both drugs (bortezomib + NVP-BEZ235) at inhibiting cell viability of rat primary pituitary tumor cells in culture was observed. Combined treatment of primary fibroblasts from mutant rats with NVP-BEZ235 and bortezomib also resulted in decreased cell viability compared with the application of each individual drug and concurrently led to a significant inhibition of Akt and S6K phosphorylation. The synergistic effect of bortezomib and PI3K/mTOR pathway inhibition is likely not only due to the stabilization of p27, since a wide array of molecular events are elicited by this compound (Wright, 2010). However, in line with our hypothesis that p27 plays a crucial role in mediating the antitumor effect of bortezomib, it was recently shown that this drug increases the efficiency of trastuzumab against Her2-positive breast cancer cells, and that the synergistic effect of both agents correlates with the ability of bortezomib to induce nuclear accumulation of p27 (Cardoso et al., 2006). Our results suggest that combination treatment with bortezomib may be used to enhance the antiproliferative effect of NVP-BEZ235 in specific cell types.

Compounds with very promising antitumor activity *in vitro* or in xenograft tumor models often give only modest objective response rates when used in patients. One key element to improve the outcome of clinical trials for novel drugs is to select among the eligible patients those having the highest chance to respond to the therapy and treat those only. Patient selection can be achieved only if biomarkers able to predict the response are available. Our studies suggest that the intracellular amount of p27 might be a predictive biomarker of the sensitivity of tumor cells to NVP-BEZ235. In line with our findings is the article by Chen and colleagues (Chen et al., 2006) reporting that the expression level of p27 is a candidate predictive biomarker for the response to rapalogs-based therapy.

Altogether, the recognition of both the MENX (rat) and the MEN4 (human) syndromes has identified *Cdkn1b/CDKN1B* as a new tumor susceptibility gene for multiple neuroendocrine tumors. These findings, together with previous analysis of animal models with defective p27 function, point to a critical role for p27-mediated cell cycle regulation in neuroendocrine cells homeostasis. The identification and functional characterization of the currently known and novel *CDKN1B* mutations will broaden our understanding of the relationship between p27 and neuroendocrine tumor predisposition. In addition, knowing the properties of the mutant p27 proteins associated to hereditary neuroendocrine tumors may facilitate the development of targeted therapeutic strategies for a more effective clinical management of the patients carrying those mutations and of their families. Moreover, our studies have shown that the MENX animal model may be exploited for preclinical therapy-response studies of NFA *in vivo* and such studies have already provided evidence that NVP-BEZ235 is a very potent inhibitor of NFA cell proliferation. Our hypothesis that p27 might be employed as a predictive biomarker for the selection of patient undergoing NVP-BEZ235 treatment warrants further validation in clinical studies since this drug is currently being employed in Phase I/II clinical trials.

7. REFERENCES

- Abraham, R.T., and Wiederrecht, G.J. (1996). Immunopharmacology of rapamycin. *Annu Rev Immunol* *14*, 483-510.
- Agarwal, S.K., Guru, S.C., Heppner, C., Erdos, M.R., Collins, R.M., Park, S.Y., Saggar, S., Chandrasekharappa, S.C., Collins, F.S., Spiegel, A.M., *et al.* (1999). Menin interacts with the AP1 transcription factor JunD and represses JunD-activated transcription. *Cell* *96*, 143-152.
- Agarwal, S.K., Kennedy, P.A., Scacheri, P.C., Novotny, E.A., Hickman, A.B., Cerrato, A., Rice, T.S., Moore, J.B., Rao, S., Ji, Y., *et al.* (2005). Menin molecular interactions: insights into normal functions and tumorigenesis. *Horm Metab Res* *37*, 369-374.
- Agarwal, S.K., Mateo, C.M., and Marx, S.J. (2009). Rare germline mutations in cyclin-dependent kinase inhibitor genes in multiple endocrine neoplasia type 1 and related states. *J Clin Endocrinol Metab* *94*, 1826-1834.
- Alessi, D.R., James, S.R., Downes, C.P., Holmes, A.B., Gaffney, P.R., Reese, C.B., and Cohen, P. (1997). Characterization of a 3-phosphoinositide-dependent protein kinase which phosphorylates and activates protein kinase Balphα. *Curr Biol* *7*, 261-269.
- Arighi, E., Borrello, M.G., and Sariola, H. (2005). RET tyrosine kinase signaling in development and cancer. *Cytokine Growth Factor Rev* *16*, 441-467.
- Asa, S.L., Bamberger, A.M., Cao, B., Wong, M., Parker, K.L., and Ezzat, S. (1996). The transcription activator steroidogenic factor-1 is preferentially expressed in the human pituitary gonadotroph. *J Clin Endocrinol Metab* *81*, 2165-2170.
- Asa, S.L., and Ezzat, S. (2002). The pathogenesis of pituitary tumours. *Nat Rev Cancer* *2*, 836-849.
- Asa, S.L., and Ezzat, S. (2009). The pathogenesis of pituitary tumors. *Annu Rev Pathol* *4*, 97-126.
- Baumann, P., Mandl-Weber, S., Oduncu, F., and Schmidmaier, R. (2009). The novel orally bioavailable inhibitor of phosphoinositol-3-kinase and mammalian target of rapamycin, NVP-BEZ235, inhibits growth and proliferation in multiple myeloma. *Exp Cell Res* *315*, 485-497.
- Ben-Jonathan, N., and Hnasko, R. (2001). Dopamine as a prolactin (PRL) inhibitor. *Endocr Rev* *22*, 724-763.
- Besson, A., Hwang, H.C., Cicero, S., Donovan, S.L., Gurian-West, M., Johnson, D., Clurman, B.E., Dyer, M.A., and Roberts, J.M. (2007). Discovery of an oncogenic activity in p27Kip1 that causes stem cell expansion and a multiple tumor phenotype. *Genes Dev* *21*, 1731-1746.
- Beuvink, I., Boulay, A., Fumagalli, S., Zilberman, F., Ruettz, S., O'Reilly, T., Natt, F., Hall, J., Lane, H.A., and Thomas, G. (2005). The mTOR inhibitor RAD001 sensitizes tumor cells to DNA-damaged induced apoptosis through inhibition of p21 translation. *Cell* *120*, 747-759.

- Bevan, J.S., Webster, J., Burke, C.W., and Scanlon, M.F. (1992). Dopamine agonists and pituitary tumor shrinkage. *Endocr Rev* 13, 220-240.
- Brachmann, S.M., Hofmann, I., Schnell, C., Fritsch, C., Wee, S., Lane, H., Wang, S., Garcia-Echeverria, C., and Maira, S.M. (2009). Specific apoptosis induction by the dual PI3K/mTor inhibitor NVP-BEZ235 in HER2 amplified and PIK3CA mutant breast cancer cells. *Proc Natl Acad Sci U S A* 106, 22299-22304.
- Brandi, M.L., Gagel, R.F., Angeli, A., Bilezikian, J.P., Beck-Peccoz, P., Bordi, C., Conte-Devolx, B., Falchetti, A., Gheri, R.G., Libroia, A., *et al.* (2001). Guidelines for diagnosis and therapy of MEN type 1 and type 2. *J Clin Endocrinol Metab* 86, 5658-5671.
- Breuleux, M., Klopfenstein, M., Stephan, C., Doughty, C.A., Barys, L., Maira, S.M., Kwiatkowski, D., and Lane, H.A. (2009). Increased AKT S473 phosphorylation after mTORC1 inhibition is rictor dependent and does not predict tumor cell response to PI3K/mTOR inhibition. *Mol Cancer Ther* 8, 742-753.
- Bruno, J.F., Xu, Y., and Berelowitz, M. (1994). Somatostatin regulates somatostatin receptor subtype mRNA expression in GH3 cells. *Biochem Biophys Res Commun* 202, 1738-1743.
- Buchfelder, M., and Schlaffer, S. (2009). Surgical treatment of pituitary tumours. *Best Pract Res Clin Endocrinol Metab* 23, 677-692.
- Cantley, L.C. (2002). The phosphoinositide 3-kinase pathway. *Science* 296, 1655-1657.
- Cao, P., Maira, S.M., Garcia-Echeverria, C., and Hedley, D.W. (2009). Activity of a novel, dual PI3-kinase/mTor inhibitor NVP-BEZ235 against primary human pancreatic cancers grown as orthotopic xenografts. *Br J Cancer* 100, 1267-1276.
- Cardoso, F., Durbecq, V., Laes, J.F., Badran, B., Lagneaux, L., Bex, F., Desmedt, C., Willard-Gallo, K., Ross, J.S., Burny, A., *et al.* (2006). Bortezomib (PS-341, Velcade) increases the efficacy of trastuzumab (Herceptin) in HER-2-positive breast cancer cells in a synergistic manner. *Mol Cancer Ther* 5, 3042-3051.
- Carrano, A.C., Eytan, E., Hershko, A., and Pagano, M. (1999). SKP2 is required for ubiquitin-mediated degradation of the CDK inhibitor p27. *Nat Cell Biol* 1, 193-199.
- Chandrasekharappa, S.C., Guru, S.C., Manickam, P., Olufemi, S.E., Collins, F.S., Emmert-Buck, M.R., Debelenko, L.V., Zhuang, Z., Lubensky, I.A., Liotta, L.A., *et al.* (1997). Positional cloning of the gene for multiple endocrine neoplasia-type 1. *Science* 276, 404-407.
- Chang, B.L., Zheng, S.L., Isaacs, S.D., Wiley, K.E., Turner, A., Li, G., Walsh, P.C., Meyers, D.A., Isaacs, W.B., and Xu, J. (2004). A polymorphism in the CDKN1B gene is associated with increased risk of hereditary prostate cancer. *Cancer Res* 64, 1997-1999.
- Chen, G., Frohlich, O., Yang, Y., Klein, J.D., and Sands, J.M. (2006). Loss of N-linked glycosylation reduces urea transporter UT-A1 response to vasopressin. *J Biol Chem* 281, 27436-27442.

- Chien, W.M., Garrison, K., Caufield, E., Orthel, J., Dill, J., and Fero, M.L. (2007). Differential gene expression of p27Kip1 and Rb knockout pituitary tumors associated with altered growth and angiogenesis. *Cell Cycle* 6, 750-757.
- Chung, J., Kuo, C.J., Crabtree, G.R., and Blenis, J. (1992). Rapamycin-FKBP specifically blocks growth-dependent activation of and signaling by the 70 kd S6 protein kinases. *Cell* 69, 1227-1236.
- Crawford, M.J., Lanctot, C., Tremblay, J.J., Jenkins, N., Gilbert, D., Copeland, N., Beatty, B., and Drouin, J. (1997). Human and murine PTX1/Ptx1 gene maps to the region for Treacher Collins syndrome. *Mamm Genome* 8, 841-845.
- Cully, M., You, H., Levine, A.J., and Mak, T.W. (2006). Beyond PTEN mutations: the PI3K pathway as an integrator of multiple inputs during tumorigenesis. *Nat Rev Cancer* 6, 184-192.
- Dasen, J.S., O'Connell, S.M., Flynn, S.E., Treier, M., Gleiberman, A.S., Szeto, D.P., Hooshmand, F., Aggarwal, A.K., and Rosenfeld, M.G. (1999). Reciprocal interactions of Pit1 and GATA2 mediate signaling gradient-induced determination of pituitary cell types. *Cell* 97, 587-598.
- Dattani, M.T., Martinez-Barbera, J.P., Thomas, P.Q., Brickman, J.M., Gupta, R., Martensson, I.L., Toresson, H., Fox, M., Wales, J.K., Hindmarsh, P.C., *et al.* (1998). Mutations in the homeobox gene HESX1/Hesx1 associated with septo-optic dysplasia in human and mouse. *Nat Genet* 19, 125-133.
- Day, R.N., Koike, S., Sakai, M., Muramatsu, M., and Maurer, R.A. (1990). Both Pit-1 and the estrogen receptor are required for estrogen responsiveness of the rat prolactin gene. *Mol Endocrinol* 4, 1964-1971.
- de Groot, J.W., Links, T.P., Plukker, J.T., Lips, C.J., and Hofstra, R.M. (2006). RET as a diagnostic and therapeutic target in sporadic and hereditary endocrine tumors. *Endocr Rev* 27, 535-560.
- Dennis, J.W., Granovsky, M., and Warren, C.E. (1999). Protein glycosylation in development and disease. *Bioessays* 21, 412-421.
- Dijkers, P.F., Medema, R.H., Pals, C., Banerji, L., Thomas, N.S., Lam, E.W., Burgering, B.M., Raaijmakers, J.A., Lammers, J.W., Koenderman, L., *et al.* (2000). Forkhead transcription factor FKHR-L1 modulates cytokine-dependent transcriptional regulation of p27(KIP1). *Mol Cell Biol* 20, 9138-9148.
- Drolet, D.W., Scully, K.M., Simmons, D.M., Wegner, M., Chu, K.T., Swanson, L.W., and Rosenfeld, M.G. (1991). TEF, a transcription factor expressed specifically in the anterior pituitary during embryogenesis, defines a new class of leucine zipper proteins. *Genes Dev* 5, 1739-1753.
- Ezzat, S., Snyder, P.J., Young, W.F., Boyajy, L.D., Newman, C., Klibanski, A., Molitch, M.E., Boyd, A.E., Sheeler, L., Cook, D.M., *et al.* (1992). Octreotide treatment of acromegaly. A randomized, multicenter study. *Ann Intern Med* 117, 711-718.

- Faber, A.C., Li, D., Song, Y., Liang, M.C., Yeap, B.Y., Bronson, R.T., Lifshits, E., Chen, Z., Maira, S.M., Garcia-Echeverria, C., *et al.* (2009). Differential induction of apoptosis in HER2 and EGFR addicted cancers following PI3K inhibition. *Proc Natl Acad Sci U S A* *106*, 19503-19508.
- Fedele, M., Battista, S., Kenyon, L., Baldassarre, G., Fidanza, V., Klein-Szanto, A.J., Parlow, A.F., Visone, R., Pierantoni, G.M., Outwater, E., *et al.* (2002). Overexpression of the HMGA2 gene in transgenic mice leads to the onset of pituitary adenomas. *Oncogene* *21*, 3190-3198.
- Fedele, M., Pentimalli, F., Baldassarre, G., Battista, S., Klein-Szanto, A.J., Kenyon, L., Visone, R., De Martino, I., Ciarmiello, A., Arra, C., *et al.* (2005). Transgenic mice overexpressing the wild-type form of the HMGA1 gene develop mixed growth hormone/prolactin cell pituitary adenomas and natural killer cell lymphomas. *Oncogene* *24*, 3427-3435.
- Fero, M.L., Rivkin, M., Tasch, M., Porter, P., Carow, C.E., Firpo, E., Polyak, K., Tsai, L.H., Broudy, V., Perlmutter, R.M., *et al.* (1996). A syndrome of multiorgan hyperplasia with features of gigantism, tumorigenesis, and female sterility in p27(Kip1)-deficient mice. *Cell* *85*, 733-744.
- Ferrante, E., Ferraroni, M., Castrignano, T., Menicatti, L., Anagni, M., Reimondo, G., Del Monte, P., Bernasconi, D., Loli, P., Faustini-Fustini, M., *et al.* (2006). Non-functioning pituitary adenoma database: a useful resource to improve the clinical management of pituitary tumors. *Eur J Endocrinol* *155*, 823-829.
- Filtz, T.M., Guan, W., Artymyshyn, R.P., Facheo, M., Ford, C., and Molinoff, P.B. (1994). Mechanisms of up-regulation of D2L dopamine receptors by agonists and antagonists in transfected HEK-293 cells. *J Pharmacol Exp Ther* *271*, 1574-1582.
- Florio, T., Barbieri, F., Spaziante, R., Zona, G., Hofland, L.J., van Koetsveld, P.M., Feelders, R.A., Stalla, G.K., Theodoropoulou, M., Culler, M.D., *et al.* (2008). Efficacy of a dopamine-somatostatin chimeric molecule, BIM-23A760, in the control of cell growth from primary cultures of human non-functioning pituitary adenomas: a multi-center study. *Endocr Relat Cancer* *15*, 583-596.
- Franklin, D.S., Godfrey, V.L., Lee, H., Kovalev, G.I., Schoonhoven, R., Chen-Kiang, S., Su, L., and Xiong, Y. (1998). CDK inhibitors p18(INK4c) and p27(Kip1) mediate two separate pathways to collaboratively suppress pituitary tumorigenesis. *Genes Dev* *12*, 2899-2911.
- Franklin, D.S., Godfrey, V.L., O'Brien, D.A., Deng, C., and Xiong, Y. (2000). Functional collaboration between different cyclin-dependent kinase inhibitors suppresses tumor growth with distinct tissue specificity. *Mol Cell Biol* *20*, 6147-6158.
- Fritz, A., Walch, A., Piotrowska, K., Rosemann, M., Schaffer, E., Weber, K., Timper, A., Wildner, G., Graw, J., Hofler, H., *et al.* (2002). Recessive transmission of a multiple endocrine neoplasia syndrome in the rat. *Cancer Res* *62*, 3048-3051.
- Fusco, A., Gunz, G., Jaquet, P., Dufour, H., Germanetti, A.L., Culler, M.D., Barlier, A., and Saveanu, A. (2008). Somatostatinergic ligands in dopamine-sensitive and -resistant prolactinomas. *Eur J Endocrinol* *158*, 595-603.

- Gage, P.J., and Camper, S.A. (1997). Pituitary homeobox 2, a novel member of the bicoid-related family of homeobox genes, is a potential regulator of anterior structure formation. *Hum Mol Genet* 6, 457-464.
- Georgitsi, M., Raitila, A., Karhu, A., van der Luijt, R.B., Aalfs, C.M., Sane, T., Vierimaa, O., Makinen, M.J., Tuppurainen, K., Paschke, R., *et al.* (2007). Germline CDKN1B/p27Kip1 mutation in multiple endocrine neoplasia. *J Clin Endocrinol Metab* 92, 3321-3325.
- Gilbert, W., and Maxam, A. (1973). The nucleotide sequence of the lac operator. *Proc Natl Acad Sci U S A* 70, 3581-3584.
- Gorshtain, A., Rubinfeld, H., Kendler, E., Theodoropoulou, M., Cerovac, V., Stalla, G.K., Cohen, Z.R., Hadani, M., and Shimon, I. (2009). Mammalian target of rapamycin inhibitors rapamycin and RAD001 (everolimus) induce anti-proliferative effects in GH-secreting pituitary tumor cells in vitro. *Endocr Relat Cancer* 16, 1017-1027.
- Griffin, K.J., Kirschner, L.S., Matyakhina, L., Stergiopoulos, S.G., Robinson-White, A., Lenherr, S.M., Weinberg, F.D., Clafin, E.S., Batista, D., Bourdeau, I., *et al.* (2004). A transgenic mouse bearing an antisense construct of regulatory subunit type 1A of protein kinase A develops endocrine and other tumours: comparison with Carney complex and other PRKAR1A induced lesions. *J Med Genet* 41, 923-931.
- Gstaiger, M., Jordan, R., Lim, M., Catzavelos, C., Mestan, J., Slingerland, J., and Krek, W. (2001). Skp2 is oncogenic and overexpressed in human cancers. *Proc Natl Acad Sci U S A* 98, 5043-5048.
- Guillemin, R. (2005). Hypothalamic hormones a.k.a. hypothalamic releasing factors. *J Endocrinol* 184, 11-28.
- Hara, K., Yonezawa, K., Weng, Q.P., Kozlowski, M.T., Belham, C., and Avruch, J. (1998). Amino acid sufficiency and mTOR regulate p70 S6 kinase and eIF-4E BP1 through a common effector mechanism. *J Biol Chem* 273, 14484-14494.
- Hasty, P. (2010). Rapamycin: the cure for all that ails. *J Mol Cell Biol* 2, 17-19.
- Heinonen, H., Nieminen, A., Saarela, M., Kallioniemi, A., Klefstrom, J., Hautaniemi, S., and Monni, O. (2008). Deciphering downstream gene targets of PI3K/mTOR/p70S6K pathway in breast cancer. *BMC Genomics* 9, 348.
- Hermesz, E., Mackem, S., and Mahon, K.A. (1996). Rpx: a novel anterior-restricted homeobox gene progressively activated in the prechordal plate, anterior neural plate and Rathke's pouch of the mouse embryo. *Development* 122, 41-52.
- Hofler, H., Walter, G.F., and Denk, H. (1984). Immunohistochemistry of folliculo-stellate cells in normal human adenohypophyses and in pituitary adenomas. *Acta Neuropathol* 65, 35-40.
- Hubina, E., Nanzer, A.M., Hanson, M.R., Ciccarelli, E., Losa, M., Gaia, D., Papotti, M., Terreni, M.R., Khalaf, S., Jordan, S., *et al.* (2006). Somatostatin analogues stimulate p27 expression and inhibit the MAP kinase pathway in pituitary tumours. *Eur J Endocrinol* 155, 371-379.

- Hudes, G., Carducci, M., Tomczak, P., Dutcher, J., Figlin, R., Kapoor, A., Staroslawska, E., Sosman, J., McDermott, D., Bodrogi, I., *et al.* (2007). Temsirolimus, interferon alfa, or both for advanced renal-cell carcinoma. *N Engl J Med* 356, 2271-2281.
- Hukovic, N., Rocheville, M., Kumar, U., Sasi, R., Khare, S., and Patel, Y.C. (1999). Agonist-dependent up-regulation of human somatostatin receptor type 1 requires molecular signals in the cytoplasmic C-tail. *J Biol Chem* 274, 24550-24558.
- Ishida, N., Hara, T., Kamura, T., Yoshida, M., Nakayama, K., and Nakayama, K.I. (2002). Phosphorylation of p27Kip1 on serine 10 is required for its binding to CRM1 and nuclear export. *J Biol Chem* 277, 14355-14358.
- Ishida, N., Kitagawa, M., Hatakeyama, S., and Nakayama, K. (2000). Phosphorylation at serine 10, a major phosphorylation site of p27(Kip1), increases its protein stability. *J Biol Chem* 275, 25146-25154.
- Jacks, T., Fazeli, A., Schmitt, E.M., Bronson, R.T., Goodell, M.A., and Weinberg, R.A. (1992). Effects of an Rb mutation in the mouse. *Nature* 359, 295-300.
- Jaquet, P., Gunz, G., Saveanu, A., Barlier, A., Dufour, H., Taylor, J., Dong, J., Kim, S., Moreau, J.P., and Culler, M.D. (2005a). BIM-23A760, a chimeric molecule directed towards somatostatin and dopamine receptors, vs universal somatostatin receptors ligands in GH-secreting pituitary adenomas partial responders to octreotide. *J Endocrinol Invest* 28, 21-27.
- Jaquet, P., Gunz, G., Saveanu, A., Dufour, H., Taylor, J., Dong, J., Kim, S., Moreau, J.P., Enjalbert, A., and Culler, M.D. (2005b). Efficacy of chimeric molecules directed towards multiple somatostatin and dopamine receptors on inhibition of GH and prolactin secretion from GH-secreting pituitary adenomas classified as partially responsive to somatostatin analog therapy. *Eur J Endocrinol* 153, 135-141.
- Kamura, T., Hara, T., Matsumoto, M., Ishida, N., Okumura, F., Hatakeyama, S., Yoshida, M., Nakayama, K., and Nakayama, K.I. (2004). Cytoplasmic ubiquitin ligase KPC regulates proteolysis of p27(Kip1) at G1 phase. *Nat Cell Biol* 6, 1229-1235.
- Kawamata, S., Sakaida, H., Hori, T., Maeda, M., and Uchiyama, T. (1998). The upregulation of p27Kip1 by rapamycin results in G1 arrest in exponentially growing T-cell lines. *Blood* 91, 561-569.
- Kim, D.H., Sarbassov, D.D., Ali, S.M., King, J.E., Latek, R.R., Erdjument-Bromage, H., Tempst, P., and Sabatini, D.M. (2002). mTOR interacts with raptor to form a nutrient-sensitive complex that signals to the cell growth machinery. *Cell* 110, 163-175.
- Koch, C.A. (2005). Molecular pathogenesis of MEN2-associated tumors. *Fam Cancer* 4, 3-7.
- Kong, D., and Yamori, T. (2009). Advances in development of phosphatidylinositol 3-kinase inhibitors. *Curr Med Chem* 16, 2839-2854.
- Kouki, T., Imai, H., Aoto, K., Eto, K., Shioda, S., Kawamura, K., and Kikuyama, S. (2001). Developmental origin of the rat adenohypophysis prior to the formation of Rathke's pouch. *Development* 128, 959-963.

- Kovacs, K., Horvath, E., and Vidal, S. (2001). Classification of pituitary adenomas. *J Neurooncol* 54, 121-127.
- Kuroda, F., Moss, J., and Vaughan, M. (2007). Regulation of brefeldin A-inhibited guanine nucleotide-exchange protein 1 (BIG1) and BIG2 activity via PKA and protein phosphatase 1gamma. *Proc Natl Acad Sci U S A* 104, 3201-3206.
- Lairmore, T.C., Piersall, L.D., DeBenedetti, M.K., Dilley, W.G., Mutch, M.G., Whelan, A.J., and Zehnbauer, B. (2004). Clinical genetic testing and early surgical intervention in patients with multiple endocrine neoplasia type 1 (MEN 1). *Ann Surg* 239, 637-645; discussion 645-637.
- Lamberts, S.W., Krenning, E.P., and Reubi, J.C. (1991). The role of somatostatin and its analogs in the diagnosis and treatment of tumors. *Endocr Rev* 12, 450-482.
- Lee, E.Y., Cam, H., Ziebold, U., Rayman, J.B., Lees, J.A., and Dynlacht, B.D. (2002). E2F4 loss suppresses tumorigenesis in Rb mutant mice. *Cancer Cell* 2, 463-472.
- Lemos, M.C., and Thakker, R.V. (2008). Multiple endocrine neoplasia type 1 (MEN1): analysis of 1336 mutations reported in the first decade following identification of the gene. *Hum Mutat* 29, 22-32.
- LeRoith, D., and Roberts, C.T., Jr. (2003). The insulin-like growth factor system and cancer. *Cancer Lett* 195, 127-137.
- Liang, J., Zubovitz, J., Petrocelli, T., Kotchetkov, R., Connor, M.K., Han, K., Lee, J.H., Ciarallo, S., Catzavelos, C., Beniston, R., *et al.* (2002). PKB/Akt phosphorylates p27, impairs nuclear import of p27 and opposes p27-mediated G1 arrest. *Nat Med* 8, 1153-1160.
- Liu, T.J., Koul, D., LaFortune, T., Tiao, N., Shen, R.J., Maira, S.M., Garcia-Echeverria, C., and Yung, W.K. (2009). NVP-BEZ235, a novel dual phosphatidylinositol 3-kinase/mammalian target of rapamycin inhibitor, elicits multifaceted antitumor activities in human gliomas. *Mol Cancer Ther* 8, 2204-2210.
- Lloyd, R.V. (2004). Advances in pituitary pathology: use of novel techniques. *Front Horm Res* 32, 146-174.
- Loda, M., Cukor, B., Tam, S.W., Lavin, P., Fiorentino, M., Draetta, G.F., Jessup, J.M., and Pagano, M. (1997). Increased proteasome-dependent degradation of the cyclin-dependent kinase inhibitor p27 in aggressive colorectal carcinomas. *Nat Med* 3, 231-234.
- MacKenzie, S.J., Baillie, G.S., McPhee, I., MacKenzie, C., Seamons, R., McSorley, T., Millen, J., Beard, M.B., van Heeke, G., and Houslay, M.D. (2002). Long PDE4 cAMP specific phosphodiesterases are activated by protein kinase A-mediated phosphorylation of a single serine residue in Upstream Conserved Region 1 (UCR1). *Br J Pharmacol* 136, 421-433.
- Maira, S.M., Stauffer, F., Brueggen, J., Furet, P., Schnell, C., Fritsch, C., Brachmann, S., Chene, P., De Pover, A., Schoemaker, K., *et al.* (2008). Identification and characterization of NVP-BEZ235, a new orally available dual phosphatidylinositol 3-kinase/mammalian target of rapamycin inhibitor with potent in vivo antitumor activity. *Mol Cancer Ther* 7, 1851-1863.

- Malek, N.P., Sundberg, H., McGrew, S., Nakayama, K., Kyriakides, T.R., and Roberts, J.M. (2001). A mouse knock-in model exposes sequential proteolytic pathways that regulate p27Kip1 in G1 and S phase. *Nature* 413, 323-327.
- Malumbres, M., and Barbacid, M. (2009). Cell cycle, CDKs and cancer: a changing paradigm. *Nat Rev Cancer* 9, 153-166.
- Marini, F., Falchetti, A., Del Monte, F., Carbonell Sala, S., Tognarini, I., Luzi, E., and Brandi, M.L. (2006). Multiple endocrine neoplasia type 2. *Orphanet J Rare Dis* 1, 45.
- Marinoni, I., and Pellegata, N.S. (2010). p27kip1: A New Multiple Endocrine Neoplasia Gene? *Neuroendocrinology*.
- McAllister, S.S., Becker-Hapak, M., Pintucci, G., Pagano, M., and Dowdy, S.F. (2003). Novel p27(kip1) C-terminal scatter domain mediates Rac-dependent cell migration independent of cell cycle arrest functions. *Mol Cell Biol* 23, 216-228.
- McDonald, P.C., Oloumi, A., Mills, J., Dobreva, I., Maidan, M., Gray, V., Wederell, E.D., Bally, M.B., Foster, L.J., and Dedhar, S. (2008). Rictor and integrin-linked kinase interact and regulate Akt phosphorylation and cancer cell survival. *Cancer Res* 68, 1618-1624.
- Meng, L., Mohan, R., Kwok, B.H., Elofsson, M., Sin, N., and Crews, C.M. (1999). Epoxomicin, a potent and selective proteasome inhibitor, exhibits in vivo antiinflammatory activity. *Proc Natl Acad Sci U S A* 96, 10403-10408.
- Millard, S.S., Yan, J.S., Nguyen, H., Pagano, M., Kiyokawa, H., and Koff, A. (1997). Enhanced ribosomal association of p27(Kip1) mRNA is a mechanism contributing to accumulation during growth arrest. *J Biol Chem* 272, 7093-7098.
- Min, Y.H., Cheong, J.W., Lee, M.H., Kim, J.Y., Lee, S.T., Hahn, J.S., and Ko, Y.W. (2004). Elevated S-phase kinase-associated protein 2 protein expression in acute myelogenous leukemia: its association with constitutive phosphorylation of phosphatase and tensin homologue protein and poor prognosis. *Clin Cancer Res* 10, 5123-5130.
- Moeller, S.J., Head, E.D., and Sheaff, R.J. (2003). p27Kip1 inhibition of GRB2-SOS formation can regulate Ras activation. *Mol Cell Biol* 23, 3735-3752.
- Molatore, S., Marinoni, I., Lee, M., Pulz, E., Ambrosio, M.R., degli Uberti, E.C., Zatelli, M.C., and Pellegata, N.S. (2010a). A novel germline CDKN1B mutation causing multiple endocrine tumors: clinical, genetic and functional characterization. *Hum Mutat* 31, E1825-1835.
- Molatore, S., and Pellegata, N.S. (2010b). The MENX syndrome and p27: relationships with multiple endocrine neoplasia. *Prog Brain Res* 182, 295-320.
- Morgan, D.O. (1997). Cyclin-dependent kinases: engines, clocks, and microprocessors. *Annu Rev Cell Dev Biol* 13, 261-291.

- Motti, M.L., Califano, D., Troncone, G., De Marco, C., Migliaccio, I., Palmieri, E., Pezzullo, L., Palombini, L., Fusco, A., and Viglietto, G. (2005). Complex regulation of the cyclin-dependent kinase inhibitor p27kip1 in thyroid cancer cells by the PI3K/AKT pathway: regulation of p27kip1 expression and localization. *Am J Pathol* *166*, 737-749.
- Mulligan, L.M., Kwok, J.B., Healey, C.S., Elsdon, M.J., Eng, C., Gardner, E., Love, D.R., Mole, S.E., Moore, J.K., Papi, L., *et al.* (1993). Germ-line mutations of the RET proto-oncogene in multiple endocrine neoplasia type 2A. *Nature* *363*, 458-460.
- Musat, M., Korbonits, M., Kola, B., Borboli, N., Hanson, M.R., Nanzer, A.M., Grigson, J., Jordan, S., Morris, D.G., Gueorguiev, M., *et al.* (2005). Enhanced protein kinase B/Akt signalling in pituitary tumours. *Endocr Relat Cancer* *12*, 423-433.
- Newman, C.B., Melmed, S., Snyder, P.J., Young, W.F., Boyajy, L.D., Levy, R., Stewart, W.N., Klibanski, A., Molitch, M.E., and Gagel, R.F. (1995). Safety and efficacy of long-term octreotide therapy of acromegaly: results of a multicenter trial in 103 patients--a clinical research center study. *J Clin Endocrinol Metab* *80*, 2768-2775.
- O'Reilly, K.E., Rojo, F., She, Q.B., Solit, D., Mills, G.B., Smith, D., Lane, H., Hofmann, F., Hicklin, D.J., Ludwig, D.L., *et al.* (2006). mTOR inhibition induces upstream receptor tyrosine kinase signaling and activates Akt. *Cancer Res* *66*, 1500-1508.
- Osamura, R.Y., Kajiya, H., Takei, M., Egashira, N., Tobita, M., Takekoshi, S., and Teramoto, A. (2008). Pathology of the human pituitary adenomas. *Histochem Cell Biol* *130*, 495-507.
- Osumi-Yamashita, N., Ninomiya, Y., Doi, H., and Eto, K. (1994). The contribution of both forebrain and midbrain crest cells to the mesenchyme in the frontonasal mass of mouse embryos. *Dev Biol* *164*, 409-419.
- Pagano, M., Tam, S.W., Theodoras, A.M., Beer-Romero, P., Del Sal, G., Chau, V., Yew, P.R., Draetta, G.F., and Rolfe, M. (1995). Role of the ubiquitin-proteasome pathway in regulating abundance of the cyclin-dependent kinase inhibitor p27. *Science* *269*, 682-685.
- Panetta, R., and Patel, Y.C. (1995). Expression of mRNA for all five human somatostatin receptors (hSSTR1-5) in pituitary tumors. *Life Sci* *56*, 333-342.
- Panwalkar, A., Verstovsek, S., and Giles, F.J. (2004). Mammalian target of rapamycin inhibition as therapy for hematologic malignancies. *Cancer* *100*, 657-666.
- Park, M.S., Rosai, J., Nguyen, H.T., Capodieci, P., Cordon-Cardo, C., and Koff, A. (1999). p27 and Rb are on overlapping pathways suppressing tumorigenesis in mice. *Proc Natl Acad Sci U S A* *96*, 6382-6387.
- Patel, Y.C. (1999). Somatostatin and its receptor family. *Front Neuroendocrinol* *20*, 157-198.
- Pellegata, N.S., Quintanilla-Martinez, L., Siggelkow, H., Samson, E., Bink, K., Hofler, H., Fend, F., Graw, J., and Atkinson, M.J. (2006). Germ-line mutations in p27Kip1 cause a multiple endocrine neoplasia syndrome in rats and humans. *Proc Natl Acad Sci U S A* *103*, 15558-15563.

- Pivonello, R., Ferone, D., de Herder, W.W., de Krijger, R.R., Waaijers, M., Mooij, D.M., van Koetsveld, P.M., Barreca, A., De Caro, M.L., Lombardi, G., *et al.* (2004). Dopamine receptor expression and function in human normal adrenal gland and adrenal tumors. *J Clin Endocrinol Metab* 89, 4493-4502.
- Platta, C.S., Mackay, C., and Welsh, J.S. (2010). Pituitary adenoma: a radiotherapeutic perspective. *Am J Clin Oncol* 33, 408-419.
- Qian, X., Jin, L., Kulig, E., and Lloyd, R.V. (1998). DNA methylation regulates p27kip1 expression in rodent pituitary cell lines. *Am J Pathol* 153, 1475-1482.
- Quereda, V., and Malumbres, M. (2009). Cell cycle control of pituitary development and disease. *J Mol Endocrinol* 42, 75-86.
- Ramsey, M.R., Krishnamurthy, J., Pei, X.H., Torrice, C., Lin, W., Carrasco, D.R., Ligon, K.L., Xiong, Y., and Sharpless, N.E. (2007). Expression of p16Ink4a compensates for p18Ink4c loss in cyclin-dependent kinase 4/6-dependent tumors and tissues. *Cancer Res* 67, 4732-4741.
- Renner, U., Arzberger, T., Pagotto, U., Leimgruber, S., Uhl, E., Muller, A., Lange, M., Weindl, A., and Stalla, G.K. (1998). Heterogeneous dopamine D2 receptor subtype messenger ribonucleic acid expression in clinically nonfunctioning pituitary adenomas. *J Clin Endocrinol Metab* 83, 1368-1375.
- Russo, A.A., Jeffrey, P.D., Patten, A.K., Massague, J., and Pavletich, N.P. (1996). Crystal structure of the p27Kip1 cyclin-dependent-kinase inhibitor bound to the cyclin A-Cdk2 complex. *Nature* 382, 325-331.
- Sabatini, D.M. (2006). mTOR and cancer: insights into a complex relationship. *Nat Rev Cancer* 6, 729-734.
- Samuels, Y., Diaz, L.A., Jr., Schmidt-Kittler, O., Cummins, J.M., Delong, L., Cheong, I., Rago, C., Huso, D.L., Lengauer, C., Kinzler, K.W., *et al.* (2005). Mutant PIK3CA promotes cell growth and invasion of human cancer cells. *Cancer Cell* 7, 561-573.
- Sanger, F., and Coulson, A.R. (1975). A rapid method for determining sequences in DNA by primed synthesis with DNA polymerase. *J Mol Biol* 94, 441-448.
- Sarbassov, D.D., Guertin, D.A., Ali, S.M., and Sabatini, D.M. (2005). Phosphorylation and regulation of Akt/PKB by the rictor-mTOR complex. *Science* 307, 1098-1101.
- Saveanu, A., and Jaquet, P. (2009). Somatostatin-dopamine ligands in the treatment of pituitary adenomas. *Rev Endocr Metab Disord* 10, 83-90.
- Scully, K.M., and Rosenfeld, M.G. (2002). Pituitary development: regulatory codes in mammalian organogenesis. *Science* 295, 2231-2235.
- Sehgal, S.N., Baker, H., and Vezina, C. (1975). Rapamycin (AY-22,989), a new antifungal antibiotic. II. Fermentation, isolation and characterization. *J Antibiot (Tokyo)* 28, 727-732.

- Serra, V., Markman, B., Scaltriti, M., Eichhorn, P.J., Valero, V., Guzman, M., Botero, M.L., Llonch, E., Atzori, F., Di Cosimo, S., *et al.* (2008). NVP-BEZ235, a dual PI3K/mTOR inhibitor, prevents PI3K signaling and inhibits the growth of cancer cells with activating PI3K mutations. *Cancer Res* 68, 8022-8030.
- Servant, M.J., Coulombe, P., Turgeon, B., and Meloche, S. (2000). Differential regulation of p27(Kip1) expression by mitogenic and hypertrophic factors: Involvement of transcriptional and posttranscriptional mechanisms. *J Cell Biol* 148, 543-556.
- Sheaff, R.J., Groudine, M., Gordon, M., Roberts, J.M., and Clurman, B.E. (1997). Cyclin E-CDK2 is a regulator of p27Kip1. *Genes Dev* 11, 1464-1478.
- Sheng, H.Z., Zhadanov, A.B., Mosinger, B., Jr., Fujii, T., Bertuzzi, S., Grinberg, A., Lee, E.J., Huang, S.P., Mahon, K.A., and Westphal, H. (1996). Specification of pituitary cell lineages by the LIM homeobox gene Lhx3. *Science* 272, 1004-1007.
- Sherr, C.J. (1994). G1 phase progression: cycling on cue. *Cell* 79, 551-555.
- Sherr, C.J., and Roberts, J.M. (1995). Inhibitors of mammalian G1 cyclin-dependent kinases. *Genes Dev* 9, 1149-1163.
- Sherr, C.J., and Roberts, J.M. (1999). CDK inhibitors: positive and negative regulators of G1-phase progression. *Genes Dev* 13, 1501-1512.
- Short, J.D., Houston, K.D., Dere, R., Cai, S.L., Kim, J., Johnson, C.L., Broaddus, R.R., Shen, J., Miyamoto, S., Tamanoi, F., *et al.* (2008). AMP-activated protein kinase signaling results in cytoplasmic sequestration of p27. *Cancer Res* 68, 6496-6506.
- Smith, P.K., Krohn, R.I., Hermanson, G.T., Mallia, A.K., Gartner, F.H., Provenzano, M.D., Fujimoto, E.K., Goedeke, N.M., Olson, B.J., and Klenk, D.C. (1985). Measurement of protein using bicinchoninic acid. *Anal Biochem* 150, 76-85.
- Snyder, P.J., Bashey, H.M., Phillips, J.L., and Gennarelli, T.A. (1985). Comparison of hormonal secretory behavior of gonadotroph cell adenomas in vivo and in culture. *J Clin Endocrinol Metab* 61, 1061-1065.
- Sordillo, L.M., Oliver, S.P., and Akers, R.M. (1988). Culture of bovine mammary epithelial cells in D-valine modified medium: selective removal of contaminating fibroblasts. *Cell Biol Int Rep* 12, 355-364.
- Sornson, M.W., Wu, W., Dasen, J.S., Flynn, S.E., Norman, D.J., O'Connell, S.M., Gukovsky, I., Carriere, C., Ryan, A.K., Miller, A.P., *et al.* (1996). Pituitary lineage determination by the Prophet of Pit-1 homeodomain factor defective in Ames dwarfism. *Nature* 384, 327-333.
- Stefaneanu, L., Kovacs, K., Horvath, E., Buchfelder, M., Fahrbusch, R., and Lancranjan, L. (2001). Dopamine D2 receptor gene expression in human adenohypophysial adenomas. *Endocrine* 14, 329-336.
- Stokoe, D., Stephens, L.R., Copeland, T., Gaffney, P.R., Reese, C.B., Painter, G.F., Holmes, A.B., McCormick, F., and Hawkins, P.T. (1997). Dual role of phosphatidylinositol-3,4,5-trisphosphate in the activation of protein kinase B. *Science* 277, 567-570.

- Sugiyama, Y., Tomoda, K., Tanaka, T., Arata, Y., Yoneda-Kato, N., and Kato, J. (2001). Direct binding of the signal-transducing adaptor Grb2 facilitates down-regulation of the cyclin-dependent kinase inhibitor p27Kip1. *J Biol Chem* *276*, 12084-12090.
- Taboada, G.F., Luque, R.M., Bastos, W., Guimaraes, R.F., Marcondes, J.B., Chimelli, L.M., Fontes, R., Mata, P.J., Filho, P.N., Carvalho, D.P., *et al.* (2007). Quantitative analysis of somatostatin receptor subtype (SSTR1-5) gene expression levels in somatotropinomas and non-functioning pituitary adenomas. *Eur J Endocrinol* *156*, 65-74.
- Thapar, K., Kovacs, K., Scheithauer, B.W., Stefanescu, L., Horvath, E., Pernicone, P.J., Murray, D., and Laws, E.R., Jr. (1996). Proliferative activity and invasiveness among pituitary adenomas and carcinomas: an analysis using the MIB-1 antibody. *Neurosurgery* *38*, 99-106; discussion 106-107.
- Tomoda, K., Kubota, Y., and Kato, J. (1999). Degradation of the cyclin-dependent-kinase inhibitor p27Kip1 is instigated by Jab1. *Nature* *398*, 160-165.
- Um, S.H., Frigerio, F., Watanabe, M., Picard, F., Joaquin, M., Sticker, M., Fumagalli, S., Allegrini, P.R., Kozma, S.C., Auwerx, J., *et al.* (2004). Absence of S6K1 protects against age- and diet-induced obesity while enhancing insulin sensitivity. *Nature* *431*, 200-205.
- van der Hoek, J., Lamberts, S.W., and Hofland, L.J. (2004). The role of somatostatin analogs in Cushing's disease. *Pituitary* *7*, 257-264.
- Vance, M.L., and Harris, A.G. (1991). Long-term treatment of 189 acromegalic patients with the somatostatin analog octreotide. Results of the International Multicenter Acromegaly Study Group. *Arch Intern Med* *151*, 1573-1578.
- Verges, B., Boureille, F., Goudet, P., Murat, A., Beckers, A., Sassolas, G., Cougard, P., Chambe, B., Montvernay, C., and Calender, A. (2002). Pituitary disease in MEN type 1 (MEN1): data from the France-Belgium MEN1 multicenter study. *J Clin Endocrinol Metab* *87*, 457-465.
- Veugelers, M., Wilkes, D., Burton, K., McDermott, D.A., Song, Y., Goldstein, M.M., La Perle, K., Vaughan, C.J., O'Hagan, A., Bennett, K.R., *et al.* (2004). Comparative PRKAR1A genotype-phenotype analyses in humans with Carney complex and prkar1a haploinsufficient mice. *Proc Natl Acad Sci U S A* *101*, 14222-14227.
- Vierimaa, O., Georgitsi, M., Lehtonen, R., Vahteristo, P., Kokko, A., Raitila, A., Tuppurainen, K., Ebeling, T.M., Salmela, P.I., Paschke, R., *et al.* (2006). Pituitary adenoma predisposition caused by germline mutations in the AIP gene. *Science* *312*, 1228-1230.
- Williams, B.O., Schmitt, E.M., Remington, L., Bronson, R.T., Albert, D.M., Weinberg, R.A., and Jacks, T. (1994). Extensive contribution of Rb-deficient cells to adult chimeric mice with limited histopathological consequences. *EMBO J* *13*, 4251-4259.
- Wright, J.J. (2010). Combination therapy of bortezomib with novel targeted agents: an emerging treatment strategy. *Clin Cancer Res* *16*, 4094-4104.
- Wullschleger, S., Loewith, R., and Hall, M.N. (2006). TOR signaling in growth and metabolism. *Cell* *124*, 471-484.

- Yamasaki, L., Bronson, R., Williams, B.O., Dyson, N.J., Harlow, E., and Jacks, T. (1998). Loss of E2F-1 reduces tumorigenesis and extends the lifespan of Rb1(+-)mice. *Nat Genet* 18, 360-364.
- Yang, Y., and Hua, X. (2007). In search of tumor suppressing functions of menin. *Mol Cell Endocrinol* 265-266, 34-41.
- Yen, R.S., Allen, B., Ott, R., and Brodsky, M. (1992). The syndrome of right atrial myxoma, spotty skin pigmentation, and acromegaly. *Am Heart J* 123, 243-244.
- Zatelli, M.C., Ambrosio, M.R., Bondanelli, M., and Uberti, E.C. (2007a). Control of pituitary adenoma cell proliferation by somatostatin analogs, dopamine agonists and novel chimeric compounds. *Eur J Endocrinol* 156 Suppl 1, S29-35.
- Zatelli, M.C., Minoia, M., Martini, C., Tagliati, F., Ambrosio, M.R., Schiavon, M., Buratto, M., Calabrese, F., Gentilin, E., Cavallesco, G., *et al.* (2010). Everolimus as a new potential antiproliferative agent in aggressive human bronchial carcinoids. *Endocr Relat Cancer* 17, 719-729.
- Zatelli, M.C., Piccin, D., Vignali, C., Tagliati, F., Ambrosio, M.R., Bondanelli, M., Cimino, V., Bianchi, A., Schmid, H.A., Scanarini, M., *et al.* (2007b). Pasireotide, a multiple somatostatin receptor subtypes ligand, reduces cell viability in non-functioning pituitary adenomas by inhibiting vascular endothelial growth factor secretion. *Endocr Relat Cancer* 14, 91-102.
- Zhang, L.J., Lachowicz, J.E., and Sibley, D.R. (1994). The D2S and D2L dopamine receptor isoforms are differentially regulated in Chinese hamster ovary cells. *Mol Pharmacol* 45, 878-889.
- Zitzmann, K., Ruden, J., Brand, S., Goke, B., Lichtl, J., Spottl, G., and Auernhammer, C.J. (2010). Compensatory activation of Akt in response to mTOR and Raf inhibitors - a rationale for dual-targeted therapy approaches in neuroendocrine tumor disease. *Cancer Lett* 295, 100-109.

Publikationen

1. **Lee M**, Theodoropoulou M, Graw J, Roncaroli F, Zatelli M, Pellegata NS. Levels of p27 sensitize to dual PI3K/mTOR inhibition. *Mol Cancer Ther* (2011) in press
2. **Lee M**, Reubi JC, Pellegata NS. Secretin receptor is overexpressed in rat models of pheochromocytoma and stimulates tumor cell proliferation. (in preparation)
3. Marinoni I, **Lee M**, Perren A, Bravi I, Feuchtinger A, Syed N, Roncaroli F ,Pellegata NS, Pituitary adenomas in MENX rat model show features of aggressive gonadotroph tumors. (submitted)
4. Molatore S, Kiermaier E, Jung CB, **Lee M**, Pulz E, Höfler H, Atkinson MJ, Pellegata NS. Characterization of a naturally-occurring p27 mutation predisposing to multiple endocrine tumors. *Mol Cancer*;2010 May; 21:116
5. Molatore S, Marinoni I, **Lee M**, Pulz E, Ambrosio MR, degli Uberti EC, Zatelli MC, Pellegata NS. A novel germline CDKN1B mutation causing multiple endocrine tumors: clinical, genetic and functional characterization. *Hum Mutat*. 2010 Nov; 31:1825-35.
6. Park CS, **Lee MS**, Oh HJ, Chun JS, Song WK Modulation of β -catenin by cyclin-dependent kinase 6 in Wnt-stimulated cells. *European Journal of Cell Biology* ;2007 Feb; 86:111-23.
7. Kim K, **Lee MS**, Park H, Kim JH, Kim SH, Chung HS, Choi GW, Kwon IC Cell-Permeable and Biocompatible Polymeric Nanoparticles for Apoptosis Imaging. *J. Am. Chem. Soc.*; 2006 ;128:3490-91
8. Kim SI, Park CS, **Lee MS**, Kwon MS, Jho EH, Song WK Cyclin-dependent kinase 2 regulates the interaction of Axin with beta-catenin. *Biochem Biophys Res Commun*. 2004 Apr 30; 317: 478-83.
9. Park CS, Kim SI, **Lee MS**, Youn CY, Kim DJ, Jho EH, Song WK Modulation of beta-catenin phosphorylation/degradation by cyclin-dependent kinase. *J Biol Chem*. 2004 May ; 279:19592-99

Posterpräsentationen

1. **Lee MS**, Marinoni I, Theodoropoulou M and Pellegata NS MENX (multiple endocrine neoplasia syndrome) as a preclinical model to evaluate compounds with therapeutic activity against pituitary tumors. ENEA Congress 2010, Liège, Belgien, September 22-25, 2010

2. Lee MS, Culler MD and Pellegata NS

MENX as a preclinical model to evaluate compounds with therapeutic activity against neuroendocrine tumors. The 21st Korean society for molecular and cellular biology meeting, Seoul, Korea, Oktober 15-17, 2009

3. Lee MS, Culler MD and Pellegata NS

MENX as a preclinical model to evaluate compounds with therapeutic activity against neuroendocrine tumors. The 6th Annual ENETS conference for the Diagnosis and Treatment of Neuroendocrine Tumor Disease, Granada, Spanien, März 05-07, 2009

4. Lee DS, Park SJ, Lee MS, Nam JH and Byun Y

Polyethylene glycol(PEG) conjugation with ameliorated cyclosporine for prolongation of pancreatic islet survival. The 7th International Congress of the Cell Transplant Society, Boston, Massachusetts, USA, November 17-19, 2004

5. Lee DS, Park SJ, Lee MS, Nam JH and Byun Y

Expression of hemeoxygenase-1 and poly(ethyleneglycol) conjugation for long term immunoprotection of transplanted islet. The 7th International Congress of the Cell Transplant Society, Boston, Massachusetts, USA, November 17-19, 2004

Vortrag

Novartis Research Day, Nürnberg, Deutschland, Mai 04-05, 2010

MENX (multiple endocrine neoplasia syndrome) as a preclinical model to evaluate compounds with therapeutic activity against neuroendocrine tumors.